Masters by Research (M. Res) Thesis

Durham University, Department of Biosciences, Durham DH1 3LE, United Kingdom.

Development of methods to monitor maturation and trafficking of Carboxypeptidase Y (CPY) and its G255R mutant (CPY*)

Student: Mr Yeshurun A. Tanna

Supervisor: Dr Martin Schroeder

Thursday 31st March 2022

1.0 Abstract

Protein folding is a vital biological process which underpins many cellular functions in both eukaryotic and prokaryotic cells. This mechanism is a prime example of macromolecular self-assembly which leads to important biological function, such as molecular trafficking to specific cellular parts and cellular differentiation. However, whilst for the majority of cases proteins fold into their correct 3D structure with long-term stability, there is a propensity for proteins to misfold due to insufficient molecular interactions between the amino acids within the polypeptide chain. Once formed, these misfolded proteins have the potential to aggregate and cause pathological or even neurological diseases. Thus, it is of importance to probe the mechanism(s) of protein misfolding to uncover its molecular origins.

The yeast species known as baker's yeast (*S. Cerevisiae*) is a model organism to probe this mechanism, and carboxypeptidase Y (CPY) has been proposed as a suitable model protein, due to its high abundance within the yeast endoplasmic reticulum (ER), to understand this process. Literature has shown that CPY is a widely used model protein in understanding protein sorting events within the ER of *S. Cerevisiae*. The advantages, and subsequent choice of this protein, are based upon its structure and role. It plays a part in the C-terminal chemistry of polypeptides, and thus may inform on mis-interactions which contribute to misfolding. Furthermore, CPY trafficking from the ER to the Golgi to the vacuole has provided information on sorting signal events which are like mammalian cellular signals, and thus share similar features with other organisms. It is also a preferable model protein due to its unique catalytic triad (active site). Although classified as a serine protease, it has a much greater pH and temperature range than other proteases, and can thus maintain high activity across environmental changes. Its mutated analogue, carboxypeptidase Y* (CPY*), has also been chosen as a model protein to compare its molecular sorting mechanism with CPY. It is characterised by a glycine-arginine mutation at the 255 amino acid position.

The purpose of this project is to uncover the molecular mechanisms of misfolding, namely, post trafficking of CPY & CPY*, whether these misfolded proteins renature and continue trafficking or whether they are degraded by cellular machinery. Alternatively, whether there is evidence of competition between these processes. This would also shed light on the kinetics of these processes and the likelihood of clearance of these misfolded proteins from the ER. To probe these processes, the maturation of pre-cursor forms of both CPY and CPY* have been studied, as they undergo cellular trafficking across the secretory pathway from the ER to the Golgi to the vacuole.

The initial experiments have been used to test whether CPY/CPY* can be detected in a western blot through SDS-PAGE gels, and whether CPY/CPY* can be detected in an immunoprecipitate. The final experiment was used to assess whether the dose-dependent cell-cycle regulator 2 (DCR2) plays a role in ER-induced stress, by specifically affecting CPY* degradation. All such experiments employ classical molecular biology techniques. These findings could shed light on whether degradation, by means of disulphide bond breaking and thus slower migration on SDS-PAGE gels, or renaturation, by means of cellular mechanisms, is the dominant mechanism within the ER.

TABLE OF CONTENTS

2.0 Figures, Tables & Graphs

2.1 Figures

2.2 Tables

Table 1. – Solutions

Table 2. – Buffers

Table 3. – Plasmids

Table 4. – Commercially available kits

Table 5. – Media composition for cell cultures: SD agar

Table 6. – Media composition for cell cultures: SD media

Table 7. – Media composition for cell cultures: PSP2 agar

Table 8. – Media composition for cell cultures: SD Galactose/Raffinose (2% (w/v)/1% (w/v)) media

Table 9. – *E. coli* & *S. cerevisiae* strain information

Table 10. – Antibody information

Table 11. – Master mix preparation for single digest of pAC595 & pAC667 plasmids

Table 12. – Master mix preparation for double digest of pAC595 & pAC667 plasmids

Table 13. – Tabulated western blot data: CPY detection with α-CPY (1:1,000, 1:20,000) with ECL2

Table 14. – Tabulated western blot data: CPY detection with α-CPY (1:5,000, 1:50,000) with ECL2

Table 15. – Tabulated western blot data: CPY detection with α-CPY (1:1,000, 1:20,000) with Luminol.

Table 16. – Tabulated western blot data: Ratios for CPY detection with α-CPY across all CPY detection experiments.

Table 17. – Tabulated western blot data: Ratios and Western Blot data for CPY* Cu^{2+} induction with α-CPY, ECL2 across all Cu^{2+} experiments: pRS423

Table 18. – Tabulated western blot data: Ratios and Western Blot data for CPY* Cu^{2+} induction with α-CPY, Luminol across all Cu^{2+} experiments: pRS423

Table 19. – Tabulated western blot data: Ratios and Western Blot data for CPY* Cu^{2+} induction with α-CPY, ECL2 across all Cu^{2+} experiments: pRS423–$P_{GAL1,\ 10}$ –DCR2– HA (-His)

Table 20. – Tabulated western blot data: Ratios and Western Blot data for CPY* Cu^{2+} induction with α-CPY, ECL2 across all Cu^{2+} experiments: pRS423–$P_{GAL1,\ 10}$ –H338A-DCR2–HA (-His)

Table 21. – List and composition of buffers used in CPY detection

2.2 Graphs

Graph 1. – α-CPY ratios plotted for all three CPY detection experiments

Graph 2. – α-CPY ratios plotted for the 1st strain in the Cu^{2+} induction experiment, ECL2

Graph 3. – α-CPY ratios plotted for the 1st strain in the Cu^{2+} induction experiment, Luminol

Graph 4. – α-CPY ratios plotted for the 2nd strain in the Cu^{2+} induction experiment, ECL2

Graph 5. – α-CPY ratios plotted for the 3rd strain in the Cu^{2+} induction experiment, ECL2

3.0 Commonly used abbreviations

CPY – Carboxypeptidase Y

CPY* - Carboxypeptidase Y*

ER – Endoplasmic reticulum

ERAD – Endoplasmic reticulum associated degradation

WT – Wild type

prc1Δ – Mutant type

m-CPY – Mature form of CPY

p-CPY – Precursor form of CPY

PDI – Protein disulphide isomerase

DCR2 – Dosage dependent cell-cycle regulator 2

4.0 Acknowledgements

I would personally like to thank Dr Martin Schroeder for his continual support and help throughout my Masters' project. I would also like to thank the other Masters' student in our research group, Adam Read, for his encouragement, as well as the other PhD students in our research group, Hanan Sagini & Amnah Obidan.

Further, I would like to additionally acknowledge support from staff members within the Biosciences department. Special thanks to Dr Martin Schroeder for his provision of plasmids used in my project.

5.0 Statement of Copyright

6.0 Introduction

In this project there are two questions to investigate and probe in detail, namely whether misfolded proteins renature and continue protein trafficking through the secretory pathway, or whether they are degraded, subsequently whether competition exists between these two processes. Secondly, to address the kinetics of renaturation relative to denaturation of misfolded proteins, and ultimately the fate of aggregation or clearance of these molecules from the endoplasmic reticulum.

6.1 Protein Structure & Stability

Firstly, I will address the mechanism by which proteins fold, and consequently the propensity for protein misfolding. Both the sequence of amino acids within the polypeptide chain and the extrinsic cellular conditions impact the folding process. This mechanism is crucial for biological function and self-assembly, and only the correct three-dimensional conformation will result in protein stability within appropriate physiological conditions (Dobson, 2003). In my project, I utilised the Carboxypeptidase Y 'reporter' protein to study the cellular trafficking of this vacuolar protease across the secretory pathway. Protein stability relies upon favourable bioenergetics, as can be seen in the native state on a so called 'energy landscape' (Fig. 1). At a molecular level, this process is intrinsically statistical (stochastic) and requires the analysis of small proteins with limited residues (80-100), to further dissect the folding mechanism from unfolded states to native states. This has been found to favour a lower Gibbs free energy, and subsequently represents an absolute minimum in the energy landscape, which results in the formation of a stable protein structure (Dobson, 2003).

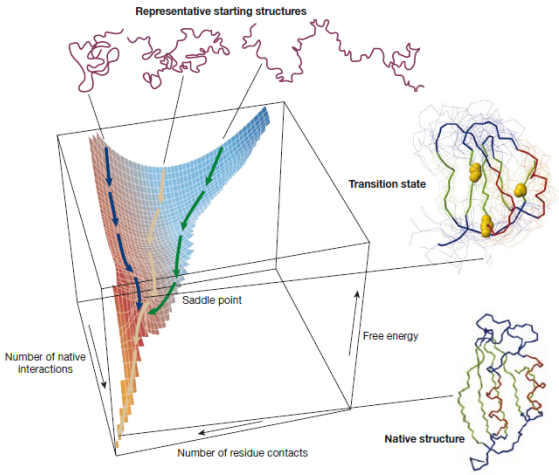

Figure 1. *An energy landscape diagram for the process of protein folding. Of importance is the saddle point which represents a pre-requisite state, which most protein molecules must cross, to achieve their respective native states (Dobson, 2003).*

Molecular simulation methods have found that amino acid interactions in the same polypeptide chain are minimised when the polypeptide is linear. The linear conformation is unfolded and leads to a higher Gibbs free energy than the folded conformation (Shrivastava, 2017). Importantly, there is a great difference between the standard Gibbs free energy in a folded/native state compared with an unfolded/non-native one, and this may be caused by an equilibrium existing between such states (Shrivastava, 2017). If $\Delta G^0 > 0$ for the folding reaction, this may also result in protein misfolding.

The secondary structure contributes to stability during protein folding. The α helices and β pleated sheets (Fig. 2), present within the native protein structures, undergo hydrogen bonding of their side chains to water molecules, thus partially favouring the folding process (Dill, 1990). Both these sub-structures aid in appropriate folding due to extensive hydrogen bonding within the secondary structure which provides additional conformational stability. However, given that most protein structures have far greater than one hundred residues, the chemical and physical properties of these residues also affect the folding mechanism. Evidence for stochasticity, mentioned earlier, has been shown by the strong relationship between protein folding rates and the folding complexity. This complexity is a measure of the separation of different residues, which chemically bind to each other, present in the native structure. This experimental evidence has led scientists to believe that most of the functional proteins fold within so called 'modules' (Dobson, 2003). Evolution by natural selection has shown that proteins have evolved to maximise the frequency distribution of the number of domains where proteins fold, to ensure a valid three dimensional structure. This is advantageous to survival, as multi-complex proteins can be formed with high functionality and specificity (Lipman and Wilbur, 1991).

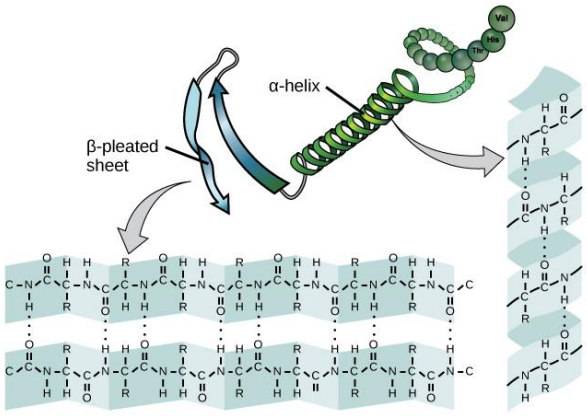

Figure 2. *A ribbon representation of the alpha helix and beta sheets present in the secondary structure of proteins (Khan Academy).*

6.2 Hydrophobic Effect

Further, the hydrophobic effect is a vital process of the folding mechanism, as this ensures that the hydrophobic side chains form a complex aggregate, hydrophilicity is accounted, which results in favourable native interactions to form the ideal 3D conformation (Dobson, 2003). Cooperativity ensures a stable, folded conformation. Primarily, due to the presence of partially folded states within a single protein, there is a small amount of conformational strain which contributes to the overall cooperativity and folding, but also due to the entropic decrease of the fully solvated protein due to stable interactions present in the folded state (Shrivastava, 2017), (Fig. 3).

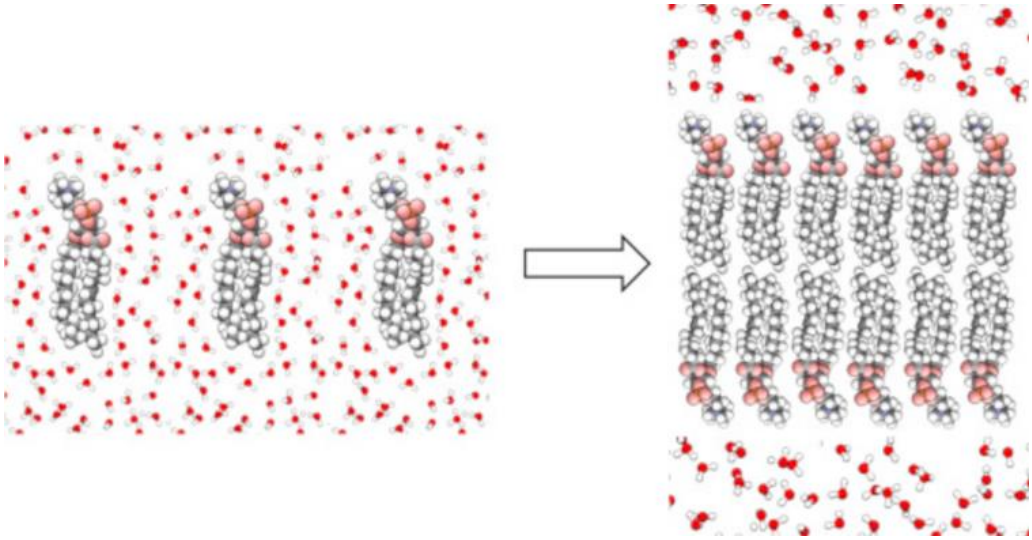

Figure 3. *Maximising of hydrogen bonding between the water molecules. Hydrophobic tails of the lipid molecules are aligned with the hydrogen atoms of the water molecules. The first image, with lipids scattered amongst water molecules, is more ordered (lower entropy). The second image, with lipid aggregation amidst water molecules, is less ordered (Shrivastava, 2017).*

6.3 Protein Folding & Misfolding

Protein folding in the cell takes place in a variety of places. All polypeptide chains are assembled in the ribosome, exit the ribosomes via the ribosome channel, and finally initiate folding. However, for protein structures to maintain their specific functionality post-synthesis, there must be a specific mechanism which sustains and controls the conformational shape, namely using chaperones and proteases. Chaperones are biomolecules which assist the protein in correct folding, and further limit the propensity for aggregation and subsequently protein misfolding. They cause the formation of intra-molecular interactions between the hydrophobic contacts on the buried protein core, thus reducing aggregation of proteins and assist the protein in reaching its native state (Wickner et al., 1999) (Fig. 4).

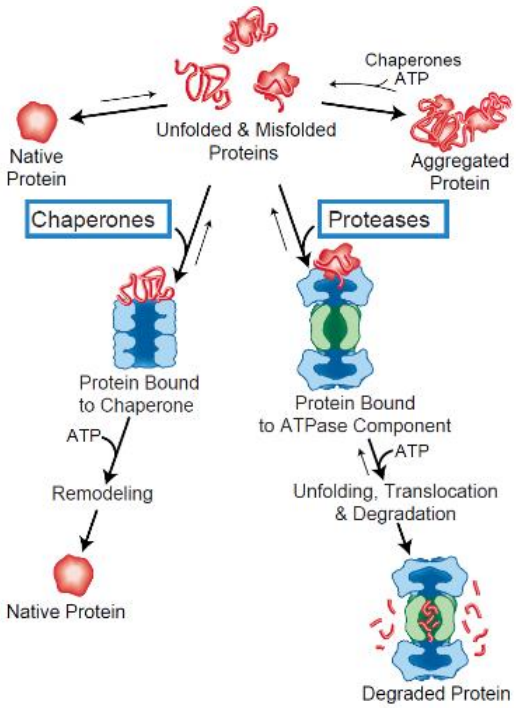

Figure 4. *Different protein states for quality control. Hydrophobic residues of proteins are exposed and bind via chaperones or proteases. The binding of intermediates by the action of chaperones can lead to a native state, whilst proteases help to distinguish non-native protein states from native ones (Wickner et al., 1999).*

Research has found that chaperones work synergistically with cellular ATP energy. The Hsp70 protein is an example of a chaperone which acts during translation (Fig. 5). The mechanism of action of Hsp70 is critical, as they not only assist in protein folding, but also recognise misfolded proteins as unfolded. Its purpose is to promote intra-molecular interactions of the hydrophobic regions present in the unfolded proteins which initiates stabilisation of this chain into a fully formed, native, stable protein (Hartl, 1996).

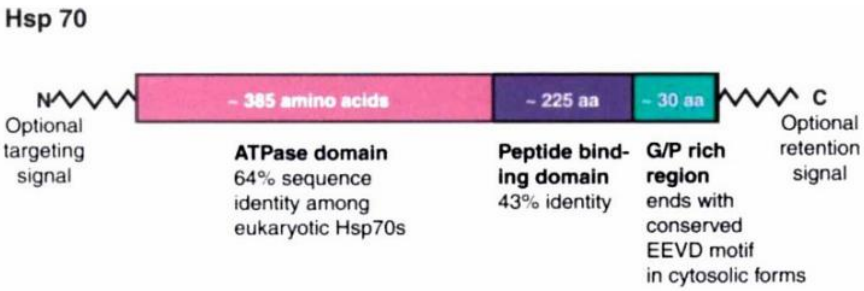

Figure 5. *Domain structure of the Hsp70. The N-terminal optional targeting signal is for the ER & mitochondria, whist the C-terminal optional (ER) retention signal is present in many eukaryotic organisms. The function of the conserved EEVD motif is to control regulation of the ATPase domain (Hartl, 1996).*

However, there is a high propensity for a protein to misfold if it is incapable of reaching its native state. The intrinsic amino acids of the protein are susceptible to sequence alteration and the extrinsic external factors, such as pH/temperature/solvent, may also contribute to this process (Dobson, 2003). Within the native, correctly folded state, the intra-molecular interactions between the α-helices, which provide structure, are broken and thus cause structure destabilisation. This occurs alongside the formation of certain β-sheets, which collectively cause protein aggregation. This is similar to amyloid formation (Fig. 6), which is promoted by additional hydrogen bonds which form across the fibril within the β-sheets, essentially as a result of stacking of hydrophobic amino acid side chains. At a chemical level, this leads to supra-molecular assembly of the protein aggregates, which can trigger protein misfolding within tissues (Makin et al., 2005).

Current research has found that amyloid fibrils are composed of stacks of beta-sheets, due to an equilibrium between soluble oligomeric molecules and insoluble protein aggregates. Many external factors, such as protein concentration, inter and intracellular interactions and temperature influence aggregation (Aguzzi and O'Connor, 2010).

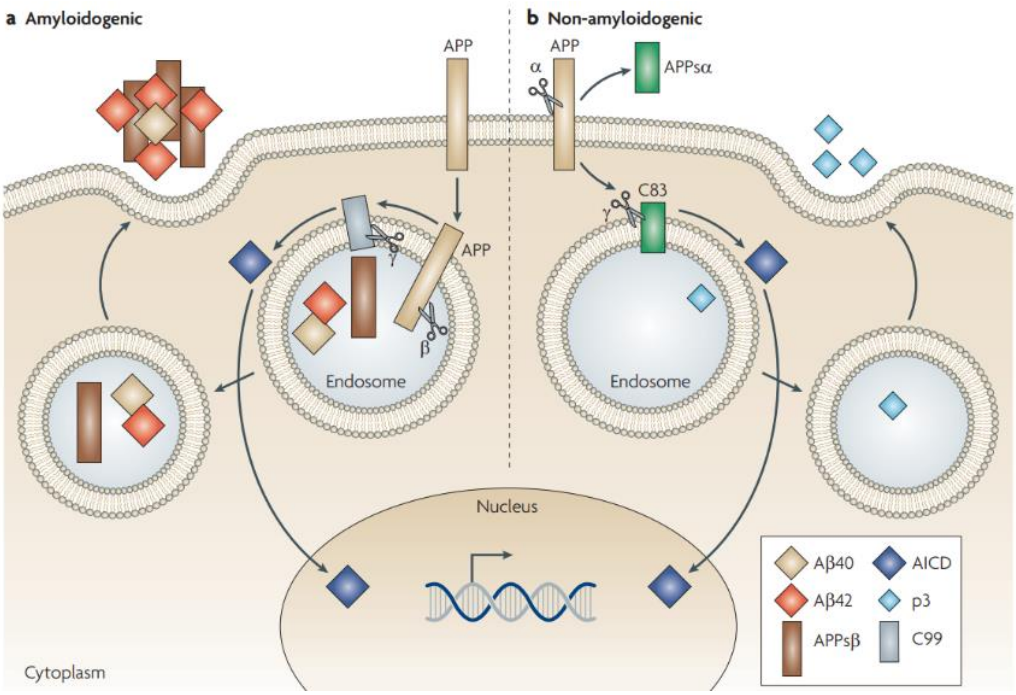

Figure 6. *The mechanism of amyloid-β formation. APP (amyloid precursor protein) is responsible for the breakdown of specific protein fragments within cell neurons which leads to the accumulation of amyloid-β plaques (Aguzzi and O'Connor, 2010).*

A temperature rise, pH change and reduction in cellular energy (ATP) all contribute to partial folding or unfolding of the protein, which implies a reduced chance of the protein folding into its native state. Temperature plays the greatest role in destabilisation of the protein structure, as the negative enthalpic value reduces the hydrogen bonding, electrostatics, and Van der Waals interactions which exist between the side chain moieties on the amino acids. Further, pH may affect the protein stability due to an equilibrium shift in the protonation exchange within amino acids. Again, contributing to protein destabilising and causing unfolded proteins to emerge (O'Brien et al., 2012). Within cellular processes, it is vital to initiate the renaturation of the protein back into its native state or cause protein degradation of any unfolded protein (Fig. 7). The evasion of such processes would cause protein aggregation, further accumulation of misfolded protein, and eventually cell death (Lins and Brasseur, 1995). As mentioned earlier, change of the amino acid sequence is one way in which aggregates form, another is due to intermolecular forces which form between hydrophobic parts of the 'modules' which exist within unfolded/partially folded protein structures. The net result is prevention of the protein ever reaching its native state (Calloni et al., 2005; Lins and Brasseur, 1995).

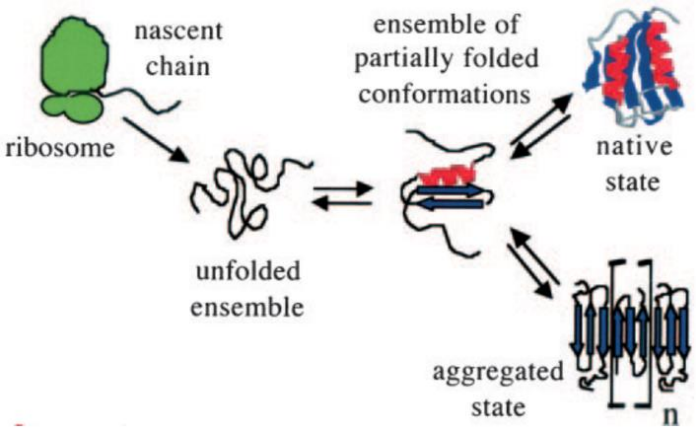

Figure 7. *An equilibrium diagram which represents the different protein states. Once the folded protein assumes an unfolded state, it can change to a partially folded state and then form either a native or aggregated state. The formation of these is dependent upon its system thermodynamics (Calloni et al., 2005).*

A further complication of aggregation may be caused by cellular oxidative stress. This is induced by reactive, short-lived, electron deficient species known as radicals. During the final stage of respiratory metabolism, known as oxidative phosphorylation, if reduction of molecular oxygen to water is incomplete, oxygen radicals can form and thus cause protein

destabilisation. Further, these highly reactive species cause high levels of oxidation which can perturb non-covalent interactions and lead to protein aggregation (Uttara et al., 2009).

6.4 Degradation Mechanisms of Misfolded Proteins

Fortunately, the cell is capable of efficient degradation of misfolded proteins, through a series of biochemical mechanisms. Complexity of this process arises due to the vast number of genetic materials which are utilised in degradation. Evolution has selected for a quality-control system which disposes of misfolded proteins, thus protecting the functionality of correctly folded proteins in cellular systems. The protein degradation process is dependent upon ATP molecules from respiratory metabolism and glycolysis. This biochemical discovery has prompted an understanding of both the 26S proteasome and the ubiquitin conjugation – both being coupled processes which underpin this protein degradation (Goldberg, 2003), (Fig. 8). Misfolded proteins in the ER are usually attached to ubiquitin (Kostova and Wolf, 2003).

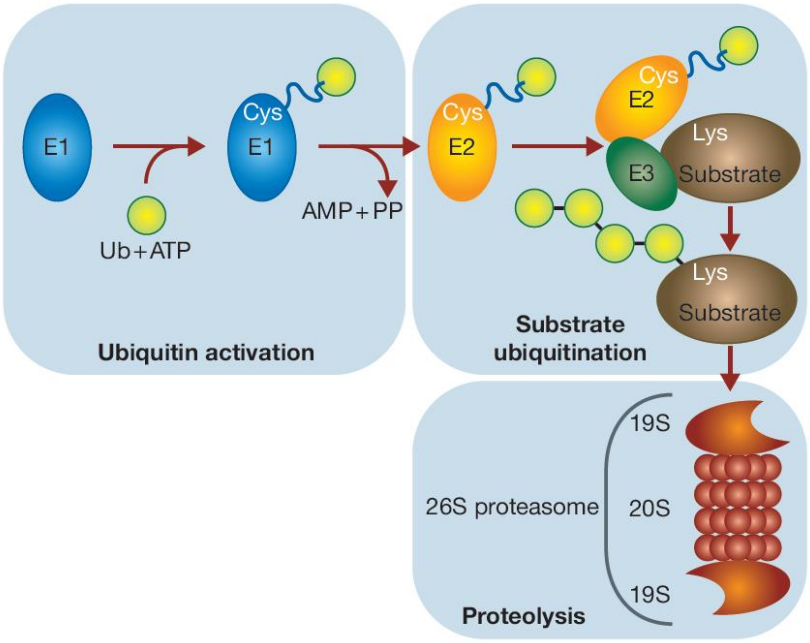

Figure 8. *Mechanism of the Ubiquitin-Proteasome system (UPS) (Meusser et al., 2005).*

Three enzymes are utilised in the attachment of this biomolecule to misfolded proteins. Firstly, the E1 (ubiquitin activating) enzyme activates this protein in an ATP-dependent process. Secondly, the E2 enzyme influences this protein through a conjugate addition mechanism which forms the thiol-ester between the C-terminus of ubiquitin and an active site cysteine of the E2. Tertiary, the E3 (ubiquitin) ligase causes these activated proteins, which are taken from the E2, to bind with multiple lysine residues, which correlates with the site of

degradation at the N-terminus of the protein (Kikkert et al., 2004). The ultimate role of E3s is to optimise ubiquitination through binding of the E2 and enzymatic substrate. To grow this sequence of activated proteins, more and more activated ubiquitin binds to the lysine residues which leads to the formation of a polyubiquitin molecule. Such chains are identified through the machinery of the 26S proteasome (Meusser et al., 2005), (Fig. 9).

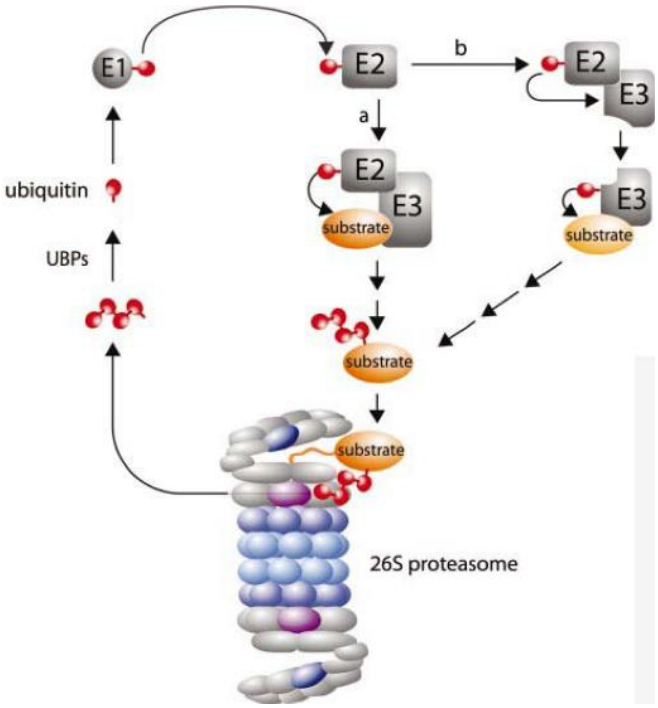

Figure 9. *Mechanism of the 26S proteasome and Ubiquitylation pathway (Kostova and Wolf, 2003).*

The mechanism of proteasomal degradation requires the formation of the polyubiquitin substrate. The 26S proteasome essentially attaches itself to this substrate, unfolds this substrate, and then causes degradation. The 26S proteasome consists of the 20S core and the 19S regulatory protein (Fig. 10). The 20S core possesses rotational symmetry and is formed by four uniform stacked rings. Each ring possesses seven unique α or β sub-units, with a molecular geometrical shape of ‘α7β7β7α7’ (Hirsch and Ploegh, 2000).

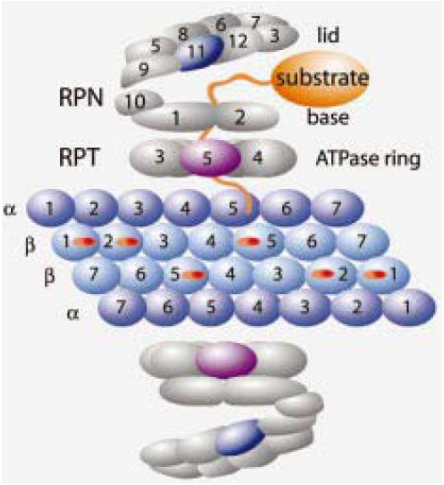

Figure 10. *Components of the 26S proteasome (Kostova and Wolf, 2003).*

Only three of the seven β sub-units collectively are proteases. Whilst the lid of the 19S subunit controls entry of recently degraded proteins, post interaction in the proteasomal system, α sub-unit rings provide space as a scaffold for the attachment of β sub-units to the 19S cap. The 19S subunit precedes the 20S subunit in the pathway of protein degradation. It regulates the proteasomal binding and unfolding of recently ubiquitylated misfolded proteins and initiates the action of the 20S subunit. The 19S subunit consists of both a base and a lid, segregated into two unique compartments (Meusser et al., 2005). The base is made of multiple ATPases (six), which bind to α sub-unit rings, and fewer non ATPase sub-units (three). One of the ATPases, namely Rpt5, regulates substrate binding; and a second ATPase, namely Rpt2, regulates protein entry across the 20S system. One of the non-ATPase sub-units, namely Rpn1, plays a critical role in the process of transfer of post-ubiquitylated material to the proteasome. It achieves this through the attachment of itself to two proteins which possess specific domains for ubiquitin-like proteins, namely Rad23 and Dsk2. However, the lid is made from eight units, each with designated biochemical nomenclature. The most important sub-unit, Rpn11, acts as a metalloprotease for the purpose of substrate proteolysis and thus reversible protein ubiquitylation. Omission of such a process may result in a clog of excessive substrate material within the proteasome. The entire process is cyclical, in that after the misfolded protein is degraded, the polyubiquitin hydrolyses to form ubiquitin, for recently synthesised misfolded proteins to be degraded (Kostova and Wolf, 2003). This demonstrates that the polyubiquitin chain must be removed before entry into the 20S subunit because of space constraints. Hence, there is a continual degradation process, by the reformation of ubiquitin from polyubiquitin.

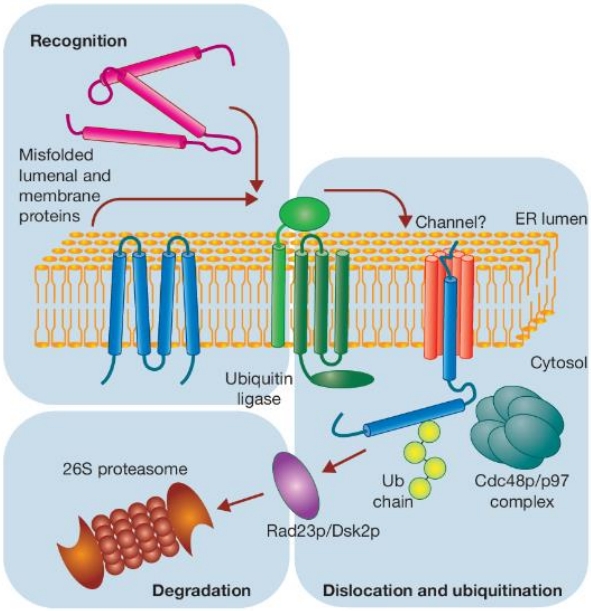

Figure 11. *Proteasomal degradation (ERAD) of selected protein targets (Meusser et al., 2005).*

The cytoplasmic ubiquitin-proteasomal pathway is a key step in ERAD – endoplasmic reticulum associated degradation of misfolded proteins (Fig. 11). This is a quality-control mechanism which exists within the ER lumen to efficiently cause degradation of misfolded proteins (Trombetta and Parodi, 2003). The ER regulates most proteins which enter the secretory pathway (Meusser et al., 2005). Initially, these proteins adopt an unfolded state as they transit across the ER membrane by the Sec61 complex. This complex also enables misfolded proteins to transit across the ER to the cytosol for degradation. The Sec61 protein complex acts as a pore-forming channel, to allow protein translocation across the ER (Kostova and Wolf, 2003). The structure of the Sec61 complex present in the *S. cerevisiae* yeast species, consists of both Sec61 (hydrophobic TM protein) and two units, namely Sbh1 and Sss1. Due to the continual attachment of the Sec61 to the translocation protein site, it plays a fundamental role in this translocation process. Within *S. cerevisiae*, and potentially other yeast species, additional gene products were found to contribute to the protein translocation across the ER, namely Sec62 and Sec63; again, being characterised as hydrophobic TM proteins. Such proteins are bound to other proteins, namely Sec71 and Sec72, to form a more complex protein structure. Whilst in the ER, a pre-secretory protein is released and binds to the Sec63 complex, this in turn transits across the Sec61. This pore-forming channel can only be activated by a signalling molecule. Channel opening inhibition may result in protein aggregation within the ER, thus leading to accumulation of misfolded protein in the ER (Pilon et al., 1997).

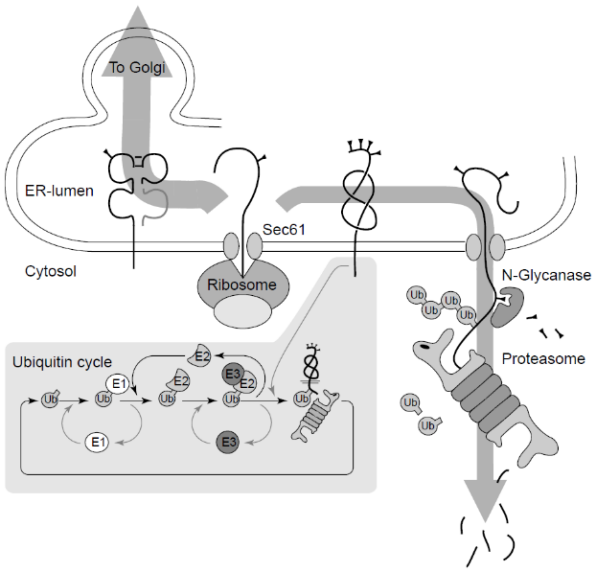

Figure 12. *A schematic of the Ubiquitin cycle (Hirsch and Ploegh, 2000).*

If a protein fails to reach its native state due to misfolding, the cell machinery may activate proteases which aid in degradation of these proteins, specifically within the proteasome. This degradation is less likely to occur within the ER lumen, due to the lower abundance of proteases, but far more likely within the proteasome, due to the higher abundance (Hirsch and Ploegh, 2000). Cellular proteins can distinguish between misfolded and partially folded proteins, based upon molecular recognition of the chaperones mentioned earlier. Such molecules induce retro-translocation of misfolded proteins to the cytosol, where ubiquitylated proteins are present and thus degradation is more achievable (Peter and Candido, 1997). Research has found that both Ubc7 and Ubc6 are important for misfolded protein degradation, within the ubiquitin-proteasome pathway (Hirsch and Ploegh, 2000), (Fig. 12).

6.5 Carboxypeptidase Y: Tool for Protein Misfolding

Carboxypeptidase Y (Fig. 13), my reporter protein for this project, is a protease with high abundance present in the ER of *S. cerevisiae* which undertakes a series of steps from its initial precursor forms (p1-CPY/p2-CPY) to its mature form (m-CPY); from the ER to the vacuole across the secretory pathway (Makino et al., 2019). CPY has been chosen as a model to study protein misfolding within this species of yeast due to its ability to distinguish between the different forms of CPY by running positions in SDS-PAGE gels, which would shed light on the cellular localisation of each form. Further, its ability to tolerate a wide range of environmental conditions, such as temperature and pH, make it a suitable model vacuolar protein. An example of this property is its ability to tolerate acidic pH levels, whilst

maintaining good selectivity for protein degradation (Jung et al., 1999). CPY is characteristic of a serine protease due to the presence of a histidine-397, Serine-146, and Asp-102 residues, present in the catalytic triad of this macromolecule. The 3D structure of this vacuolar protease contains a classic 'α/β hydrolase fold pattern' with a couple of central domains, namely a 'core' and 'insertion' domain. The catalytic triad, composed of the named residues, apart from Aspartic acid-102, are present in the core domain. Whilst the core domain regulates biochemical activity, the insertion domain controls the protein folding/topology by a series of covalent attachments of the helices to the core domain. Within the latter domain, there exists the 'V-shaped helix' which is composed of parallel α-helices which encapsulates the active site of the catalytic triad. This protease possesses four intramolecular disulphide bonds at different positions within the amino acid sequence. The structure also contains cysteine residues; thus, the first disulphide bond is found at cysteine-193 to cysteine-207, whilst the second is found at the far side of the protein at cysteine-262 to cysteine-268; both within the V-shaped helix. The other two are involved in covalent attachment to the α-helices which stabilise the V-shaped helix, namely present at cysteine-217 to cysteine-240 and cysteine-224 to cysteine-233 (Makino et al., 2019). Thus, the action of reducing agents upon this protease could shed light on how the pre-cursor form of CPY undergoes maturation to the mature form of CPY, potentially due to the breaking of disulphide bonds.

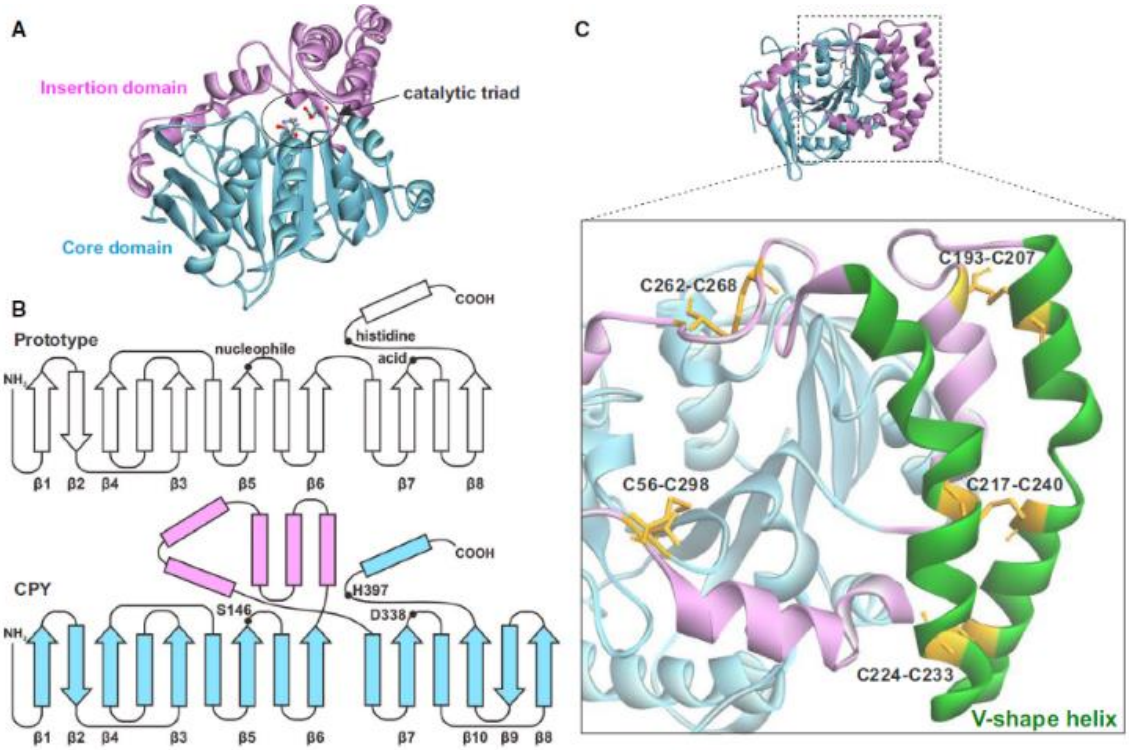

Figure 13. *Biomolecular ribbon representation of m-CPY. A) Insertion domain is coloured pink, whilst the core domain is coloured blue. Catalytic triad is found within the active site of the core domain. B) α/β hydrolase fold pattern, arrows correspond to β-strands, whilst rectangles correspond to α-helices. C) V-shaped helix & intramolecular disulphide bonds in CPY. V-shape helix is composed of 2 helices (green) which are integral to the insertion domain. Cysteine residues are coloured yellow (Makino et al., 2019).*

CPY, initially present as pre-pro-CPY after direct ribosomal synthesis, has a molecular weight of 61kDa. It undergoes transit within the secretory pathway from the ER to the Golgi (carbohydrate modification) to the vacuole and is then either degraded or re-purposed (Fig. 14). Unlike the m-CPY, the pro-CPY contains an additional 91 residues in its prosequence and thus is at a higher molecular weight than m-CPY. Further, this additional propeptide segment is critical to the folding process within the secretory pathway, and may uncover the degradation/renaturation rate for this vacuolar protease (Kato et al., 2003).

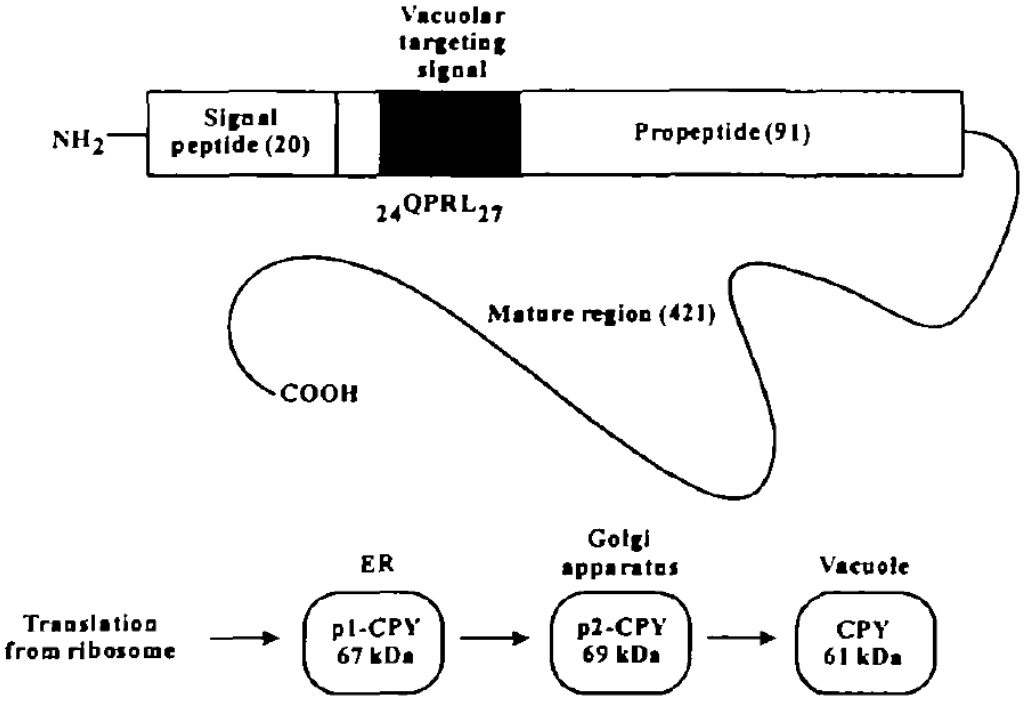

Figure 14. *A diagram of both the sequence structure of CPY and CPY processing from the precursor to its mature form, as it passes through the secretory pathway from the ER to the vacuole (Jung et al., 1999).*

Secretion can be constitutive, and thus independent of signalling, but is shared with all eukaryotic cells. Therefore, CPY is trafficked in a similar way to plasma membrane receptors. An example has been shown with lysosomes. Analysis of the passage of these

organelles across the secretory pathway are related to the attachment of oligosaccharide chains on these molecules. After covalent attachment of these carbohydrates to the lysosomes, these molecules are able to be trafficked and secreted past the vacuole, in a similar way to CPY (Stevens et al., 1982), (Fig. 15).

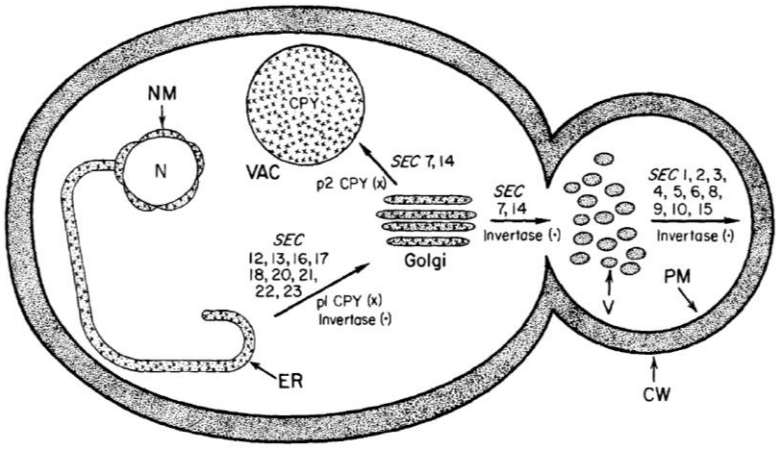

Figure 15. *Mechanism of protein transport (both secretory & vacuolar) within S. cerevisiae (Stevens et al., 1982).*

CPY is coded by the *PRC1* gene (Fig. 16), and initially forms a pre-pro structure which constitutes a propeptide, signal peptide and mature region, being 20, 91 and 421 amino acids in length respectively (Jung et al., 1999). The CPY sorting events from the ER to the vacuole are dependent upon a receptor. Thus, the likelihood of CPY secretion versus CPY vacuolar delivery would be higher in protein domains where point mutations of the *PRC1* encoded gene are present (Valls et al., 1987).

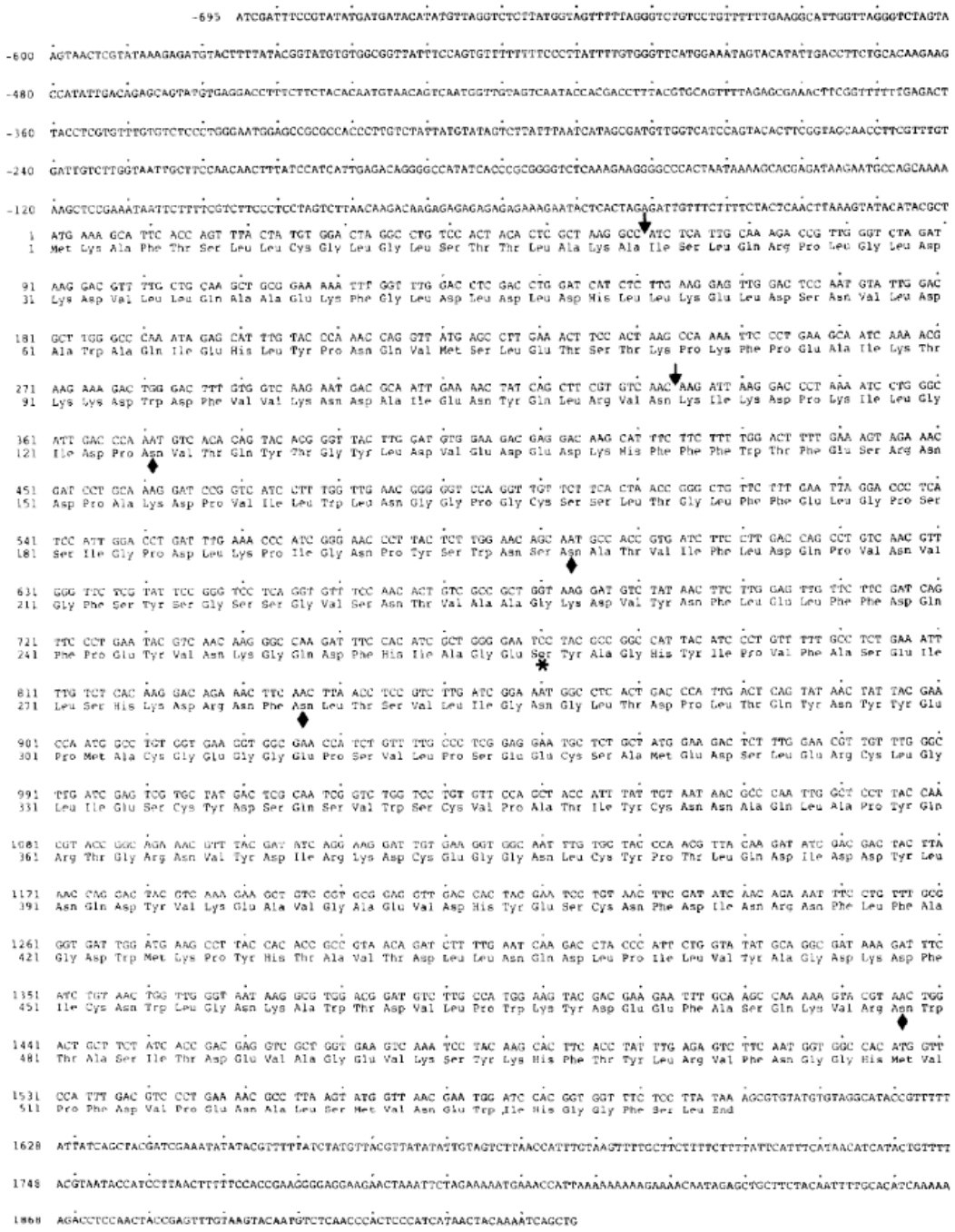

Figure 16. *Triplet codon and amino acid sequence of the PRC1 gene, arrow corresponds with a signal sequence cleavage and subsequent transition to the m-CPY, star corresponds with the serine residue within the active site cavity and the diamond corresponds with the site of N-glycosylation (Valls et al., 1987).*

Translocation of this proenzyme across the ER membrane results in the cleavage of the 20-amino acid length signal peptide by an ER-bound peptidase. Also, glycosylation and folding of the proenzyme occurs which increases the molecular weight of CPY from 61kDa to 67kDa; identified as p1-CPY (first pre-cursor form). As p1-CPY transits across the ER to the Golgi, further glycosylation occurs which increases the molecular weight of CPY from 67kDa to 69kDa; being the p2-CPY (second pre-cursor form) (Valls et al., 1990). Non-glycosylated CPY will remain as the pre-cursor form in the ER, due to its inability to fold correctly. This propeptide part of CPY achieves appropriate folding within the ER and is thus vital in the overall folding of CPY. Post glycosylation events in the Golgi, the pro-CPY can be converted into the mature form of CPY (Fig. 17). The motion of pro-CPY across the pathway from the Golgi to the vacuole requires a sorting signal to divert CPY into the vacuole and prevent its secretion. This signal is composed of four different amino acids, namely glutamine, arginine, proline and leucine found sandwiched between the signal peptide and the propeptide; but closer to the amino terminal of CPY (Jung et al., 1999).

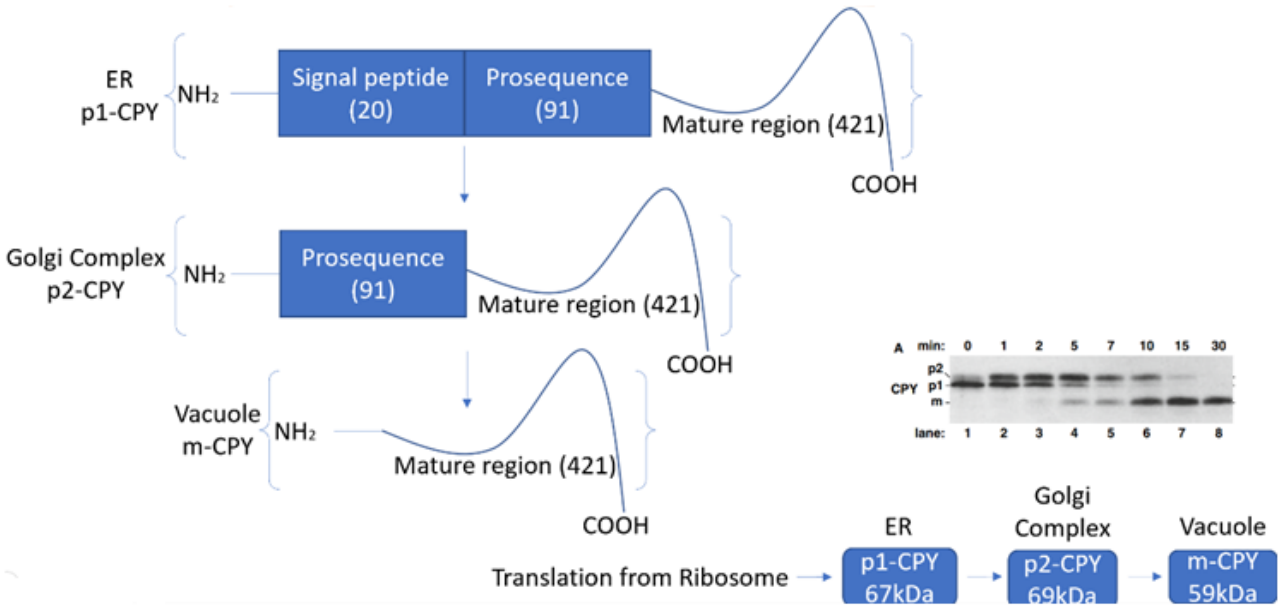

Figure 17. *Summary of the events of CPY.*

6.6 Carboxypeptidase Y: Role of Vacuolar Proteases

Whilst vacuolar activation is contingent on a signal sequence, this entire process occurs by the *PEP4* gene product. A mutation in this gene is both recessive and pleiotropic; coded as the *pep4-3* mutant allele. Although this mutation naturally supresses CPY expression, it has been found to regulate the production of a vast array of vacuolar proteases found within *S. cerevisiae*. The *prc1-1* mutant of *PRC1* and the *pep4-3* mutant of *PEP4* have been found to undergo independent segregation during meiosis. This genetic phenomenon is key to understanding the role that the *PEP4* gene plays in the maturation of the proenzyme to the mature form of CPY (Fig. 18); with a molecular weight of 59kDa (Jones et al., 1982).

As CPY is colloquially known as Proteinase C, another vacuolar protease, namely Proteinase B which is coded for by the *PRB1* gene, has been investigated into its role, alongside the *PEP4* gene, for the conversion of the pro-CPY to m-CPY. Although *PEP4* supresses the vacuolar protease expression levels, *PRC1*, not *PEP4*, is the structural genetic basis for CPY, and thus the recessive mutation at the loci of *PEP4* and *PRC1* may in fact lead to greater levels of maturation within CPY, due to posttranslational modifications of this protein (Hemmings et al., 1981).

Yet another vacuolar proteinase, namely Proteinase A, has been found to play a part in the maturation of pro-CPY, as well as activate the inactive precursors present in both PrB and CPY. PrA, like PrB, is an endoproteinase which is coded for by the *PEP4* gene. PrA is distinct from PrB and CPY, in that it is categorised as an aspartyl proteinase. Its disulphide bonds are formed intramolecularly between four cysteine residues, found within the catalytic active site of the protein. PrA contributes to one of the proteolytic cleavage reactions, namely

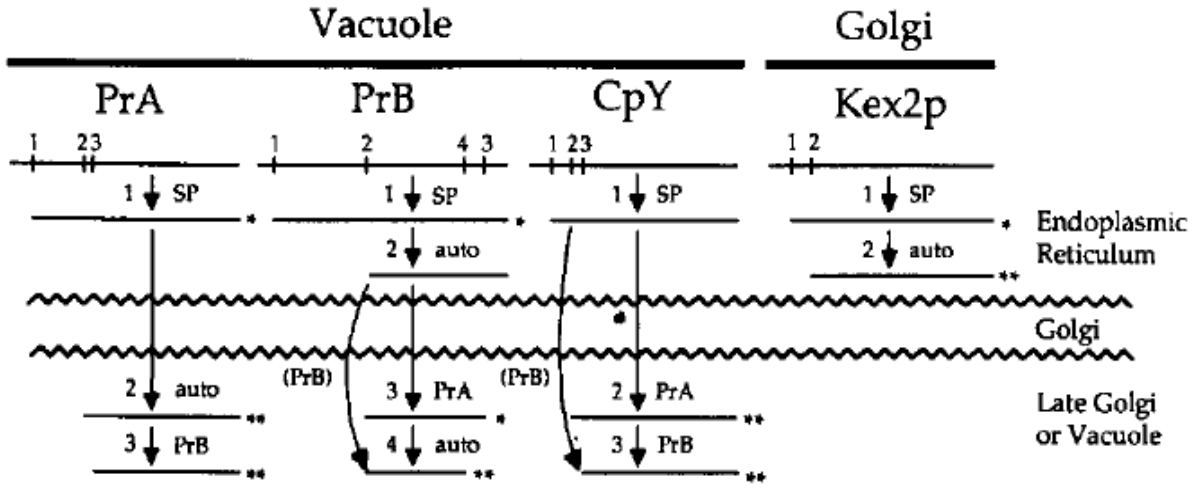

the removal of an amino-terminal peptide within the vacuole, which is the main mechanism of maturation of CPY (Jones, 1991).

Figure 18. *Mechanisms of maturation of specific vacuolar proteases within S. cerevisiae. SP corresponds to signal peptidase, auto corresponds with autocatalytic and Kex2p corresponds with Kex2 endoproteinase (Jones, 1991).*

From further analysis, four-point mutations were found to be present in PrA, namely *pra1-1*, *pra1-2*, *pra1-3* and *pra1-4*. *Pra1-1* and *pra1-4* were relevant to the maturation process due to their lack of antigenic material. The similarity between the former and latter mutant are their shared lack of PrA activity, but their difference was apparent in that the former mutants possessed PrB and CPY activity, whilst this was lacking in *pep4-3*. Experimental evidence has shown that hybridisation of the *pep4-3* with *PEP4* genes can lead to a WT strain present in both PrA and CPY. Therefore, evidence points to *pra1-1* and *pra1-4* processing but not assisting in CPY maturation. However, whilst PrA may lead to activation of the pre-cursor form of CPY, this alone may not be sufficient to produce high levels of expression of CPY (Mechler, 1987). Through an SDS-PAGE experiment of the combination of PrA and PrB (double mutants) added to pro-CPY, distinct bands appear, these are likely attributed to degradation products of CPY and not the mature form. Thus, the intermediary stage of CPY maturation must be through PrB, if *pra1-1* mutant is utilised in the process and vice versa for the *prb1-1* mutant. This highlights the relevance of both mutants working in concert. As shown earlier with *pep4-3*, the significance of CPY maturation will depend upon the difference in PrB processing with *pep4-3* compared with PrA (Germany, 1982), (Fig. 19). Although, an additional component is required for the complete maturation of CPY, at the expected ~59kDa band in the SDS-PAGE experiment. Evidence has been found which supports the theory that the inclusion of a vacuolar salt compound could potentially contribute to full activation and maturation of CPY. Either sodium chloride or sodium polyphosphate have been proposed as a potential species for this process. However, it is hard to quantifiably establish the difference in effect of PrA/PrB (vacuolar hydrolases) versus the salt species on the maturation of pro-CPY (Mechler, 1987).

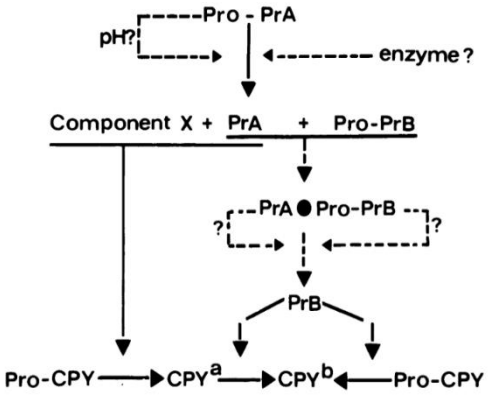

Figure 19. *A series of maturation pathways which results in the formation of CPY. Straight arrows correspond with results obtained from experimental data, whilst the dotted arrows correspond with proposed theoretical predictions. Ultimately the formation of CPY from pro-CPY is crucial (Mechler, 1987).*

6.7 Carboxypeptidase Y: Tool for understanding the effect of its overexpression on ER-induced stress*

Carboxypeptidase Y*, a mutant of CPY, has been studied to understand the renaturation and degradation of this 'mutant' reporter protein relative to CPY. CPY* is known as a G255R mutant of CPY, meaning that it possesses a point mutation, as the glycine codon has mutated to an arginine codon, at position 255. Unlike regular CPY, the precursor form of CPY* (p1-CPY*) is processed to neither p2-CPY* nor m-CPY* but is instead degraded by ER machinery (Mancini et al., 2003). It undergoes both retro-translocation and degradation by ERAD; utilising the ubiquitin-proteasomal system as mentioned earlier. CPY* degradation has been found to rely heavily upon α1,2-mannosidase activity within the ER. This mechanism is multi-faceted, with the establishment of a unique oligosaccharide structure being key to CPY* degradation. Evidence has shown that the degradation rate is greater with the appropriate oligosaccharide structure, namely $Man_8GlcNAc_2$ (Fig. 20). A positive correlation has been found between a reduction in the number of mannose-residues attached to the oligosaccharide structure and a reduced CPY* degradation rate (Byrd et al., 1982). Interestingly, the enzymatic kinetics of α1,2-mannosidase are critical to discovering the kinetics of CPY* degradation, by calculation of the time it takes for oligosaccharide formation of the optimal structure; $Man_8GlcNAc_2$. Coincidentally, the time required for correct folding of CPY and complete degradation of misfolded CPY* are very similar, suggesting shared kinetics (Jakob et al., 1998).

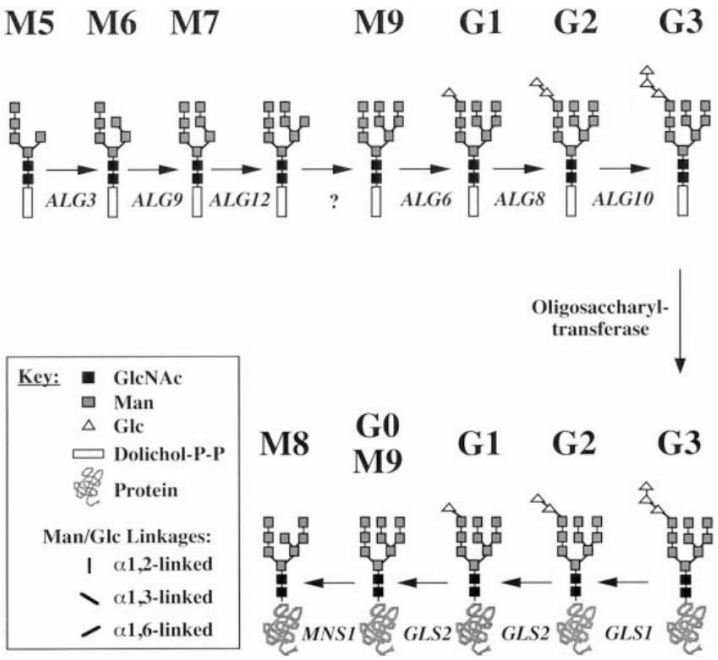

Figure 20. *Modification and biosynthesis of N-linked oligosaccharides within the ER lumen of S. cerevisiae. The purpose of this mechanism is to synthesise* $Man_8GlcNAc_2$ *oligosaccharide (Jakob et al., 1998).*

Further, a comparison of un-glycosylated CPY* to glycosylated CPY* is useful to study, to understand whether there is accumulation and subsequent degradation of one form over the other. Un-glycosylated CPY* is biosynthesised from genes which code for both CPY* (*prc1-1* allele) and un-glycosylated CPY, although CPY being coded by a different allele to CPY*. Western blot analysis showed two bands with similar intensities which corresponded to almost equal amounts of protein present for both un-glycosylated CPY and un-glycosylated CPY* (Fig. 21). However, the biosynthesis of (un-glycosylated) CPY* is independent of PrA, and thus possesses a different molecular weight to CPY, so will appear at a different position in the SDS-PAGE (Knop et al., 1996). As the coding sequence for CPY has been removed from the genome of Y10885 (prc1Δ strain), there would be no accumulation of CPY/CPY* in the vacuole.

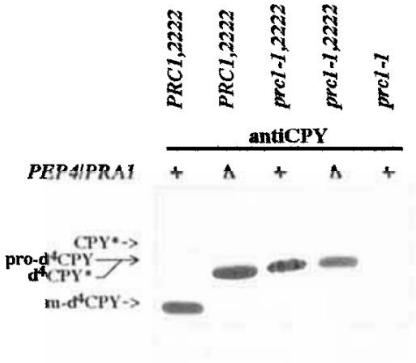

Figure 21. *Western blot data for the detection of d^4-CPY, d^4-CPY* and CPY*. Both pre and mature forms of CPY are present, and the unglycosylated form of CPY* is stable (Knop et al., 1996).*

The western blot results from a pulse-chase experiment have provided conclusive evidence that un-glycosylated CPY* does indeed accumulate in the cell due to its additional stability. Further, the amount of this mutant protein remains at a similar volume with increasing chase time; implying that stability contributes to un-glycosylated CPY* long-term retention in the ER. Also, evidence has shed light on the inability of the ER to cause CPY* degradation in an efficient manner, most likely since CPY* has no glycosyl residues (Knop et al., 1996).

A protein has been identified which provides additional confirmation of the retention of un-glycosylated CPY* in the ER. Alongside vacuolar hydrolases, *S. cerevisiae* possesses BiP, an ER-resident protein which is coded by the *KAR2* gene (Fig. 22). This protein belongs to the 'stress-70 heat shock' family of proteins and is responsible in part for the correct folding of proteins which transit across the secretory pathway from the ER to the vacuole. External factors, such as temperature/pH etc., which induce stress within all classes of proteins, may well contribute to the accumulation of misfolded/unfolded protein, such an un-glycosylated CPY*, within the ER (Mori et al., 1992).

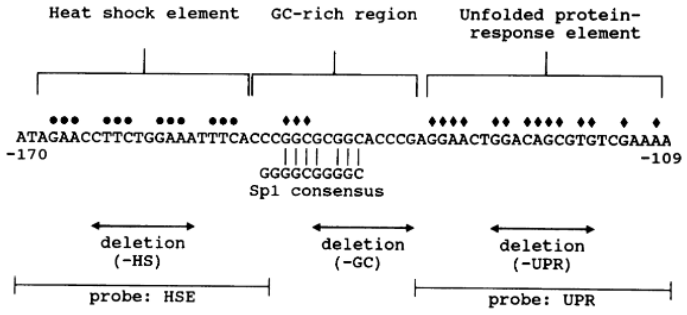

Figure 22. *Mutants, the filled circles, within the heat shock element, correspond with the 20 bp sequence composed of the named triplets. The Sp1 consensus is in alignment with the GC-rich region of the nucleotide sequence. The diamonds, within the unfolded protein-response element, indicate specific bases present in the promoter region of BiP (Mori et al., 1992).*

A means of probing CPY* degradation has been found. A comparison of yeast mutants can be helpful in determining the ability of some strains, over others, to lead to CPY* degradation by ERAD. There was a range of 'Der' mutants which were compared by their degradation ability (Hitt and Wolf, 2004).

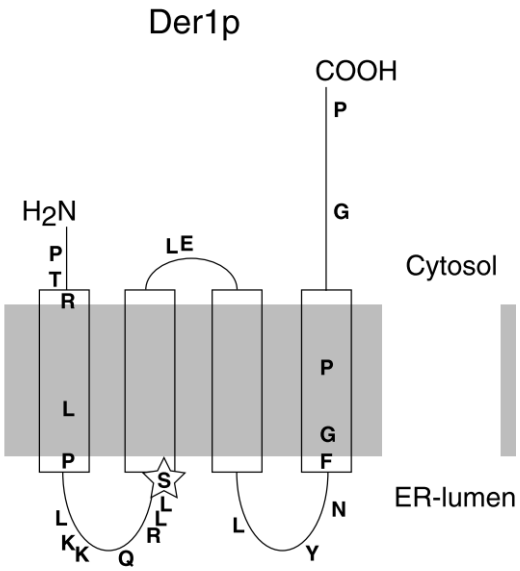

Figure 23. *Diagram of the structure of Der1p. The star corresponds with an amino acid substitution, which takes place within the der 1-2 allele (Hitt and Wolf, 2004).*

A single mutant, namely *der1-2* allele, underwent genetic cloning to identify the Der1 protein (Fig. 23). This specific protein causes high levels of CPY* degradation and is highly abundant within some compartments of the ER. The former process utilised a biochemical assay to measure the antigenic level of CPY*, due to its accumulation in the ER. Such mutant cells were grown in a carbon-rich medium and transferred onto starvation media. Following this, the cells were grown in the same media with the added effect of cycloheximide which inhibited CPY* synthesis but allowed CPY* degradation to continue. Thus, CPY* expression levels could be measured. Further probing of these mutant colonies by pulse-chase experiments, followed by western blots, revealed that there was a strong correlation between the greater volume of CPY* antigenic material present on the blot, and the stability of CPY*; with the stability being at a much higher level compared with the wild-type colonies (Knop, Finger et al., 1996).

Interestingly though, the *der1-2* mutant strain led to a higher CPY* expression level than with the *der1-1* mutant and an even higher level than with the *der2-1* mutant. Der2, the Ubc7p protein which is equivalent to the E2 enzyme, also leads to CPY* retention in the ER (Knop, Finger et al., 1996). Further, a single mutant, namely the *der2-1* allele, underwent genetic cloning to form the Der2 protein; in the same mechanistic way as Der1. This gene codes for Ubc7p, mentioned earlier, which contributes to CPY* degradation. Within *S. cerevisiae*, Ubc7p, which has an initiating (E2) activity within the ubiquitin-proteasomal

pathway, leads to the covalent attachment of ubiquitin with so called 'MATα2', a protein which undergoes degradation in a similar way to the proteasomal degradation of CPY*. CPY* immunoprecipitation, coupled with western blotting of the specific antibodies, pointed to the fact that a deletion within the Ubc7 protein corresponded with a similar effect as with the *der2-1* mutant, namely a reduction in the rate of CPY* degradation within the ER (Peter and Candido, 1997).

The active site of Ubc7 contains a cysteine residue, at 89 amino acids from the N-terminal, which accounts for its catalytic activity (Jungmann et al., 1993). There is evidence that this cysteine residue is fundamental to CPY* degradation, as it behaves in a different way to the WT strain. Ultimately, the ER possesses machinery which can degrade misfolded CPY* which has accumulated in the ER. Therefore, from my results, there should be a clear, distinct western blot band for the presence of CPY and an absent band for CPY*. The exact MW of the CPY band should be ~ 69kDa for the precursor forms of CPY and ~ 59kDa for the mature form of CPY, as mentioned earlier.

6.8 PDI: Enzymatic tool to understand its role in disulphide bond formation/breaking within misfolded proteins of the S. cerevisiae yeast species

I now turn to an exploration of the oxidative protein folding mechanism within the ER of *S. cerevisiae*, as a means of further understanding the role that disulphide bond formation plays on structure and stability of CPY/CPY*. Protein disulphide isomerase, an enzyme which catalyses the formation of disulphide bonds (Fig. 24), has been found to control the rate of formation of disulphide bonds in CPY/CPY*. PDI has been found to have a high abundance in the ER. Experimental evidence has shown that inhibition of PDI in the ER may contribute to the inability of CPY to form disulphide bonds as it transits across the secretory pathway and localises to the vacuole (Dunn et al., 1995). Within the sub-cellular compartments of the ER, the PDI works in concert with mM concentrations of both oxidised and reduced glutathione; up to three parts oxidised to one part reduced species. Whilst glutathione is a tripeptide, its central amino acid is cysteine. This cysteine exists in either its reduced form, as a thiol, or its oxidised form. A greater presence of oxidised glutathione contributes to favourable thermodynamics which leads to greater disulphide bond formation in CPY (Frand and Kaiser, 1999).

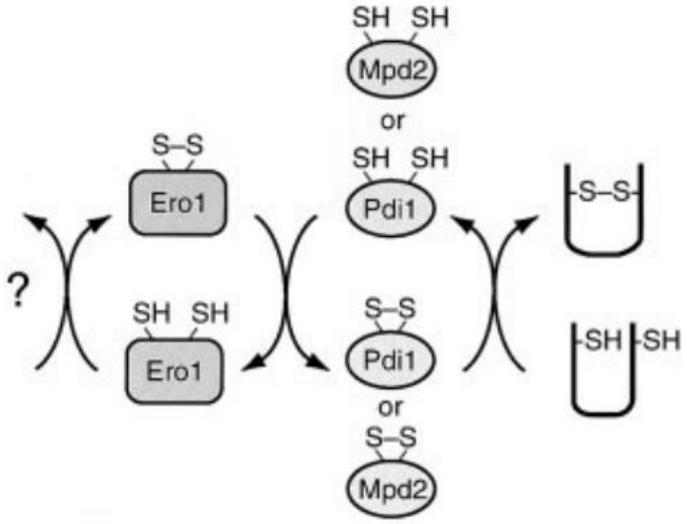

Figure 24. *Diagram of disulphide bond formation in the ER lumen of S. cerevisiae. The protein disulphide isomerase undergoes oxidation by both disulphide and dithiol catalytic exchange, attached to Ero1p. This in turn activates protein oxidation within the ER by the same mechanism but with PDI (Frand and Kaiser, 1999).*

Edman sequencing has shown that PDI possess multiple cysteine residues which contribute to its overall activity, found at the active site (Fig. 25). Further, the protein domains which constitute PDI act alongside the cysteine residues in its catalytic activity. The first protein domain active site in the 3D structure of PDI contains a proline residue which resides at the amino terminal of the enzyme, free to covalently attach with other molecules. This is in stark contrast to the enclosed leucine residue, found at the active site at the carboxy terminal which is far more sterically hindered. This experimental evidence points to the ability of disulphide bridges to form between catalytically active cysteine residues, present within the protein. Further, PDI resides in the ER, under control by a regulatory system of the -COOH terminal tetrapeptide motif. However, there is a tendency for the ER to become excessively abundant with PDI, if overexpression in *S. cerevisiae* leads to distribution across various parts of the secretory pathway (Freedman et al., 1994).

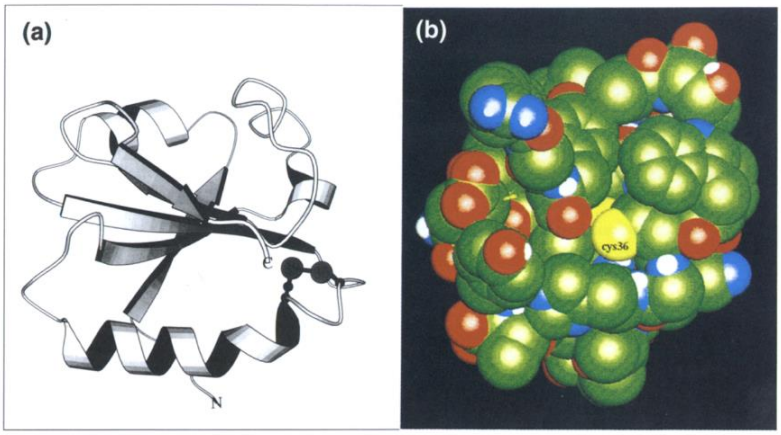

Figure 25. *The active site of PDI, a) Biomolecular ribbon representation of one of the domains with the disulphide residue, b) space-filled representation which highlights one active site cysteine residue (Freedman et al., 1994).*

The lumen of the ER, as mentioned earlier, is critical to the folding mechanism of newly synthesised proteins, such as CPY, and CPY is only allowed to move along the secretory pathway if it reaches its native, optimally folded, state. Binding affinity data of PDI to Ca^{2+} ions within the ER lumen has been found to be high, and thus important to its function (Braakman et al., 1992). Although this molecule is important in metabolic function, they bear no weight on PDI activity. The cellular role of PDI within *S. cerevisiae* has also been found to be important in understanding disulphide bond formation/breaking. There is evidence that PDI1 inhibition may lead to a problem with CPY transmission across the secretory pathway, ultimately due to an inability to form the necessary disulphide bonds (Freedman et al., 1994).

Experimental evidence has shown that the role of PDI within *S. cerevisiae* has a much greater bias towards folding of newly synthesised CPY, than as a proponent of disulphide bond formation. This effect would cause accumulation of p1-CPY, with a much greater lifetime than the strain possessing a fully intact PDI1 gene. This would suggest that the PDI1 gene, indirectly, plays a role in the trafficking of CPY from the ER to the vacuole. This behaviour was tested by the comparison of the WT cells to the mutant strain, and thus the ability to control the transit of CPY across the secretory pathway. A ^{35}S atom was chased for specific time intervals with non-labelled sulphur. The subsequent CPY labelled protein extracts were immunoprecipitated and analysed in a western blot via SDS-PAGE and autoradiography. The result was a clear, distinct difference in the processing rate of CPY for the wild type compared with the mutant strain. A reduction in protein band intensity for p1-CPY in the mutant suggested that there was an increased transport rate for CPY (LaMantia and Lennarz, 1993), (Fig. 26). This is indicative of faster transport of CPY from the ER to vacuole, and thus quicker maturation of CPY.

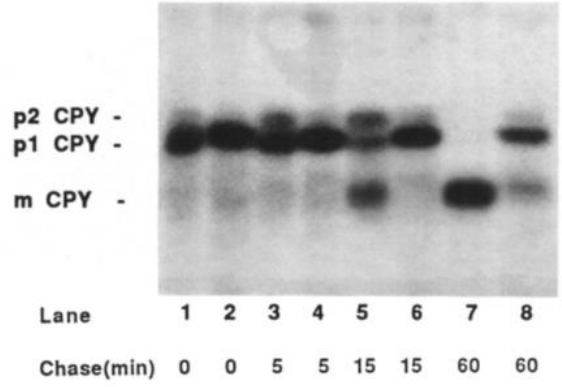

Figure 26. *Delayed transit of CPY across the secretory pathway in S. cerevisiae. Western blot results show successful CPY immunoprecipitation, with the metabolic labelling time limited to 10 min and the chase time extended to 60 min. WT (odd) and mutant (even) strains present (LaMantia and Lennarz, 1993).*

Alongside PDI, there are a variety of other ER-abundant enzymes such as Eug1 (Fig. 27) and Mpd2. Thus, there may be an additional contribution of either of these proteins to the transport, and subsequent disulphide bond formation/inhibition, of p1-CPY across the secretory pathway (Frand and Kaiser, 1999). Analysis of the amino acid sequence of Eug1 has revealed that it constitutes a total of 517 amino acids with 43% of the total sequence being identical to PDI. However, unlike PDI, each active site in Eug1 possesses only a single cysteine residue. Experimental data from a series of western blots and pulse-chase experiments confirmed that WT cells caused p1-CPY accumulation at a similar rate to natural accumulation of p1-CPY in the ER. Further analysis showed that the WT cells had an accumulation of p1-CPY in the ER at a similar abundance, due to the additive effect of overexpressed Eug1 (Tachibana and Stevens, 1992). Therefore, the logical conclusion from this mechanism is that although a lack of PDI1 gene causes a reduction in transit of CPY across the ER, Eug1 compensates by causing a greater transit of CPY, whilst not supressing the accumulation of the pre-cursor form in the ER.

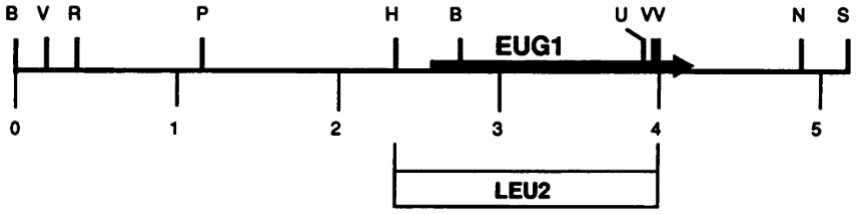

Figure 27. *Linear plasmid map of the fragment containing the EUG1 gene. This plasmid also contains an open reading frame, indicated by the right-handed arrow, and a deletion region within the EUG1 gene (Tachibana and Stevens, 1992).*

Secondly, Mpd2 (Fig. 28) plays a similar role to Eug1 in the compensation of the effect of a PDI deletion within *S. cerevisiae* cells. This enzyme is expressed by the MPD2 gene, but with a considerably different molecular structure to PDI. Mpd2 has a structure composed of 277 amino acids in length resembling its paralogue, Mpd1, encoded by the *MPD1* gene. The clear difference in structure is due to the sequence at the C-terminus of the protein, which indicated no similarity to either Eug1 or Mpd1. Mpd2, once utilised in a western blot, showed elevated

signs of expression in cells which lacked the *PDI1* gene. These results showed that there was a reduction in the maturation rate of pro-CPY to m-CPY, and thus a greater accumulation of p1-CPY in the ER, for WT cells without the *PDI1* gene and which had overexpressed levels of Mpd2 compared with regular WT cells with normal functionality. This may show that Mpd2 has a similar role to PDI. To discover whether this phenomenon is underpinned by the isomerase activity of Mdp2, it would be necessary to substitute the cysteine residues in the catalytic active site with a few serine residues. However, once WT cells were induced with serine active Mdp2, all subsequent cell growth and accumulation was halted, and the effect of PDI1 inhibition was not supressed. Thus, the presence of cysteine residues, as opposed to other types of amino acid residues, is vital to the functioning of the Mdp2 in suppression of the effect of PDI (Tachikawa et al., 1997).

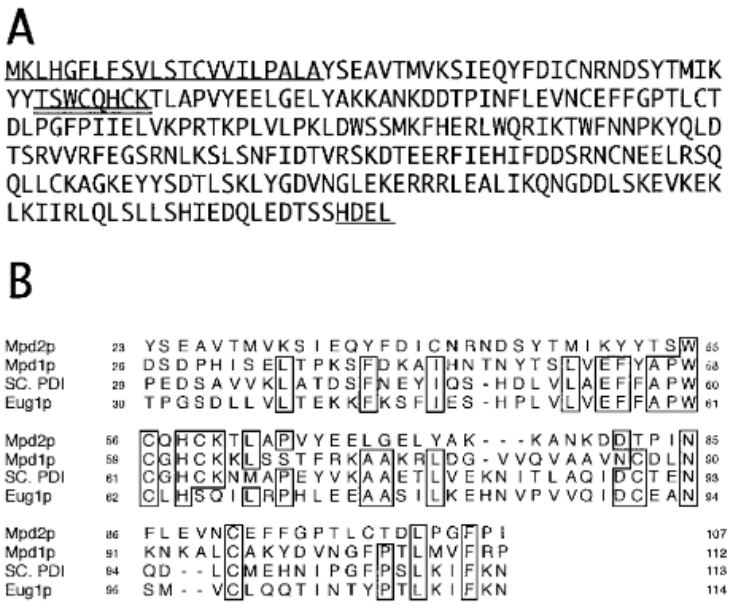

Figure 28. *The complete amino acid sequence of Mdp2 and sequence homology with respect to PDI of S. cerevisiae, a) N-terminal signal peptide and C-terminal ER retention motif are underlined, whilst the active site of Mdp2 is double-underlined, b) respective sequences for the (previously mentioned) genes (Tachikawa et al., 1997).*

6.9 Interaction of Ire1 with DCR2: Role of this phosphatase in ER-induced stress

As previously stated, excessive accumulation of unfolded protein in the ER of *S. Cerevisiae* can activate a series of events called the Unfolded Protein Response (UPR). This action is triggered if CPY/CPY* synthesis in the yeast ribosome is greater than the folding capability of proteins within the yeast cell. An ER-TM protein, known as Inositol requirement 1 (Ire1), can detect unfolded proteins by its biochemical action. Upon UPR activation, Ire1 can self-dimerise and lead to self-phosphorylation on 2 of its serine residues, namely 840 and 841. In turn this promotes its endonuclease activity to act upon Atf/Creb1 messenger RNA, being structurally characteristic to *HAC1* mRNA. For signal activation of the UPR, both serine residues must undergo auto-phosphorylation. The composite *HAC1* mRNA is formed once Ire1 removes the non-coding intron from the two splice sites of *HAC1*, which enables the coding exons to be ligated by RNA ligase, thus forming the product (Fig. 29). The *HAC1* gene is crucial to the UPR, as it controls the transcription rate of many hundreds of UPR target genes (Jinbai Guo and Michael Polymenis, 2006).

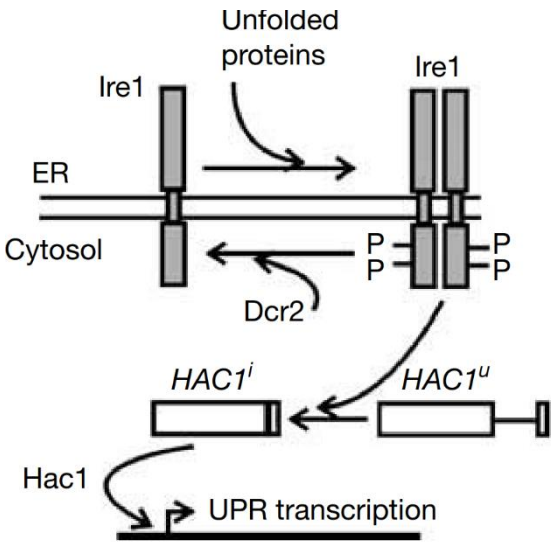

Figure 29. *Diagram which represents the suppressive action of DCR2 on the UPR, interaction of DCR2 with Ire1 which downregulates the UPR (Jinbai Guo and Michael Polymenis, 2006).*

However, the UPR inhibits mitosis within *S. Cerevisiae* cells, and thus can delay cell-cycle progression (by controlled division). Therefore, the dose-dependent cell-cycle regulator 2 phosphatase (DCR2) exists to deactivate the UPR once cell division is affected. DCR2 is a gene which, when overexpressed, promotes faster DNA replication in yeast cells. Conversely, mutant yeast cells which do not possess the DCR2 gene have been found to have a slower DNA replication rate. Within baker's yeast, its cellular functioning is consistently maintained

in its late growth phase (G_1) known as START, preceding its genetic synthesis phase (S). Once this process is activated, DNA replication follows until cell division is complete. Ultimately either overexpression or suppression of DCR2 acts to initiate or suppress START, which has a long-term implication in cellular cycle progression (Pathak et al., 2004).

Evidence points to the impact of DCR2 on acting against the UPR. Molecular splicing of the *HAC1* mRNA gene product seems to correlate well with activation of the Ire1 gene. If DCR2 acts against the UPR, there would be a difference in expression of spliced *HAC1* mRNA versus un-spliced *HAC1* mRNA gene products, in DCR2 expressed cells. Molecular techniques, such as reverse transcription-PCR and RNA blotting, were employed to measure *HAC1* mRNA splicing levels (Pathak et al., 2007). Upon the addition of tunicamycin (ER-induced stress agent), such expression levels were stopped in cells overexpressing DCR2, but continued in catalytically inactive DCR2-cells. Thus, this evidence shows that suppression of the UPR signal by DCR2 occurs before mRNA splicing. Furthermore, dephosphorylation of Ire1 by DCR2 has also been proposed as an alternative process which inhibits the UPR signal. A potential hypothesis to address this is whether DCR2, extracted from *E. Coli* bacteria, can de-phosphorylate Ire1. To achieve this, cytosolic Ire1 was expressed in *E. Coli*, with its subsequent protein being purified and its serine residues being phosphorylated. SDS-PAGE experiments show de-phosphorylation of Ire1 when exposed to DCR2, but only if the DCR2 phosphatase is active (Fig. 30). This de-phosphorylation pathway is important, as it provides a means of regulating the UPR signal and turning off its mechanism when not needed (Jinbai Guo and Michael Polymenis, 2006).

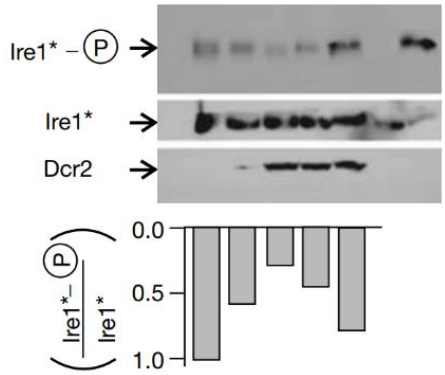

Figure 30. *Western blot results which provide band intensity comparison of phosphorylated Ire1 vs non-phosphorylated Ire1, upon interaction of DCR2 with Ire1 (Jinbai Guo and Michael Polymenis, 2006).*

6.10 Aims & Objectives

The initial aim of this project, through genetic cloning, is to construct the *prc1-1* allele in order to detect CPY and CPY*. This would lead to high expression levels of CPY/CPY* which could be validated by antibodies against CPY/CPY* in both an immunoprecipitate and western blot experiment. The first objective would be to substitute a genetic fragment of the pAC595 plasmid with a genetic fragment of pAC677 plasmid, to obtain the repaired pAC595R plasmid, thus confirming the genetic expression of CPY. Once detected, an additional aim would be to confirm the repair of this plasmid through protein molecular weight confirmation by a western blot. The objective would be to affirm that the α-CPY antibody can detect CPY, through visual evidence of a protein band at ~59kDa in an SDS-PAGE. Once fully validated, another aim would be to optimise lysis conditions for maximal detection of CPY, by the success of the α-CPY antibody to immunoprecipitate CPY. This objective would lead to protein bands which could be quantified and lead to insights into the maturation mechanism of p1-CPY to m-CPY. The final aim of this project is to improve our understanding of CPY* degradation kinetics in WT cells, cells overexpressing DCR2 and cells with catalytically inactive DCR2. This would comparatively shed light on CPY* maturation in ER-stressed cells. This objective would involve comparison of protein band intensities across a range of WT and mutant cells with different Cu^{2+} concentrations, to probe the maturation kinetics of p1-CPY*.

7.0 Materials and Methods

7.1 Materials

7.1.1.1 Solutions

Table 1. All solutions, alongside composition, used in this project.

Solution (Composition)	Quantity	Formation
10% (w/v) SDS	500ml	• Add 50g SDS to ~450ml H_2O until complete dissolution • Add H_2O to 500ml
10% (v/v) Tween 20	50ml	• Add 5.55g of Tween 20 to ~40ml autoclaved H_2O until complete dissolution • Add H_2O to 50ml • Filter sterilisation of solution
30% (w/v) Glycerol	50ml	• Add 18.9g Glycerol to ~40ml H_2O and fully mix • Add H_2O to 50ml • Autoclave solution
1M LiOAc	250ml	• Add 25.50g of $LiOAc{\cdot}2H_2O$ to ~200ml H_2O until complete dissolution • Add H_2O to 250ml • Filter sterilisation of solution
50% (w/v) PEG 4000	250ml	• Add 125g of PEG 4000 to ~100ml H_2O and fully mix • Add H_2O to 225ml until complete dissolution • Add H_2O to 250ml with mixing • Filter sterilisation of solution
10 x SDS-PAGE Buffer (1.92M Glycine, 0.248M Tris, 10g/l SDS)	11	• 144.13g Glycine • 30.03g Tris • 10.00g SDS • Add H_2O to ~900ml until complete dissolution • Add H_2O to 11
6 x SDS-PAGE Sample Buffer (350mM Tris·HCl pH 6.8, 30% (w/v) glycerol, 10% (w/v) SDS, 0.5g/l bromophenol blue, 2% (w/v) β-mercaptoethanol	1ml	• 0.35ml 1M Tris·HCl pH 6.8 • 0.378g Glycerol • 0.1g SDS • 0.125ml of 4.0g/l bromophenol blue • 20µl β-mercaptoethanol • Add H_2O to ~0.9ml until complete dissolution • Add H_2O to 1ml

Semi-dry transfer buffer (0.1M Tris, 0.192M Glycine, 5% (w/v) MeOH)	11	• 12.11g Tris • 14.41g Glycine • 50ml MeOH • Add H_2O to ~900ml until complete dissolution • Add H_2O to 11
30% (w/v) acrylamide, 0.8% (w/v) methylene bisacrylamide	500ml	• 150g acrylamide • 4g methylene bisacrylamide • Complete dissolution in ~450ml H_2O • Add H_2O to 500ml • Add 25g Dower MR-3 mixed bed ion exchanger, stir at RT for 1 hour • Filter over a 0.22µm filter and store in fridge (-4^oC) in the dark
50mg/ml ampicillin	1ml	• Add 0.05g ampicillin, Na^+ salt to ~0.8ml H_2O until complete dissolution • Add H_2O to 1ml • Filter sterilisation of solution • Store in freezer (-20^oC)
10 x DNA gel electrophoresis sample loading buffer (20% (w/v) Ficoll 400, 0.1M EDTA, 1% (w/v) SDS, 2.5g/l bromophenol blue)	250ml	• 50g Ficoll 400 • 625mg bromophenol blue • 50ml 0.5M EDTA pH 8.0 • Add H_2O to ~175ml until complete dissolution • Add H_2O to 225ml • Autoclave solution • Add 25ml of 10% (w/v) SDS
10.0 mg/ml ethidium bromide	50ml	• 250mg ethidium bromide • Add compound to ~40ml H_2O (pre-sterilised) until complete dissolution • Add sterile H_2O to 50ml • Store in fridge (-4^oC) in dark
BCA Protein Assay (Reagent A: 10g/l bicinchoninic acid disodium salt, 20g/l $Na_2CO_3 \cdot H_2O$, 1.6g/l disodium tartrate, 4.0g/l NaOH, 9.5g/l $NaHCO_3$. Adjusted to pH11.25 with 10M NaOH. Reagent B: 40g/l $CuSO_4 \cdot 5H_2O$)	15ml	• Add 1 vol. of B to 50 vol. of A • N.B: Compound may form a white precipitate, however, completely dissolves when reagents are fully mixed

10 x TBST (200mM Tris·HCl pH7.6, 1.37M NaCl, 1% (w/v) Tween 20)	11	• 24.2g Tris • 80g NaCl • 10.6g Tween 20 • Add to ~900ml H_2O until complete dissolution • Adjust pH to pH 7.6 with conc. HCl • Add H_2O to 11 • N.B: Solution was diluted 10-fold when used in washing
1M Tris·HCl pH6.8	11	• 121.14g Tris • Add to ~800ml H_2O until complete dissolution • Adjust pH to pH 6.8 with conc. HCl • Add H_2O to 11 • Autoclave solution
1M Tris·HCl pH8.9	11	• 121.14g Tris • Add to ~800ml H_2O until complete dissolution • Adjust pH to pH 8.9 with conc. HCl • Add H_2O to 11 • Autoclave solution

7.1.1.2 Buffers

Table 2. All buffers, alongside composition, used in this project.

Buffer (Composition)	Quantity	Formation
50 x TAE (2M Tris·HOAc, 0.1M EDTA pH ~ 8.5)	11	• 242g Tris • 57.1ml HOAc • 37.2g $Na_2EDTA·2H_2O$ • Add H_2O to 11
1 x TAE (40mM Tris·HOAc, 2mM EDTA pH ~ 8.5)	11	• 20ml of 50 x TAE • Add H_2O to 11
10 x TE pH 8.0 (100mM Tris·HCl pH 8.0, 10mM EDTA)	41	• 400ml 1M Tris·HCl pH 8.0 • 80ml 0.5M EDTA • Add H_2O to 41 • Autoclave solution

7.1.2 Plasmids

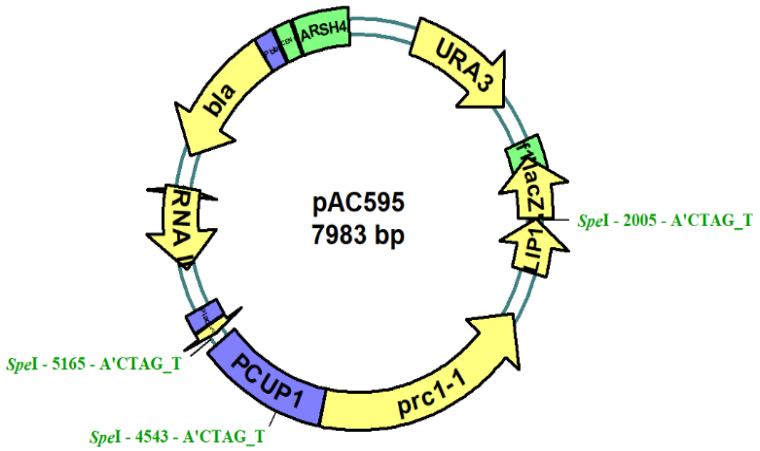

Fig. 31 *pAC595 with URA3 and under control by the PCUP1 promoter and prc1-1 ORF*

Fig. 32 *pAC667 with URA3 and under control by the PCUP1 promoter and PRC1 ORF*

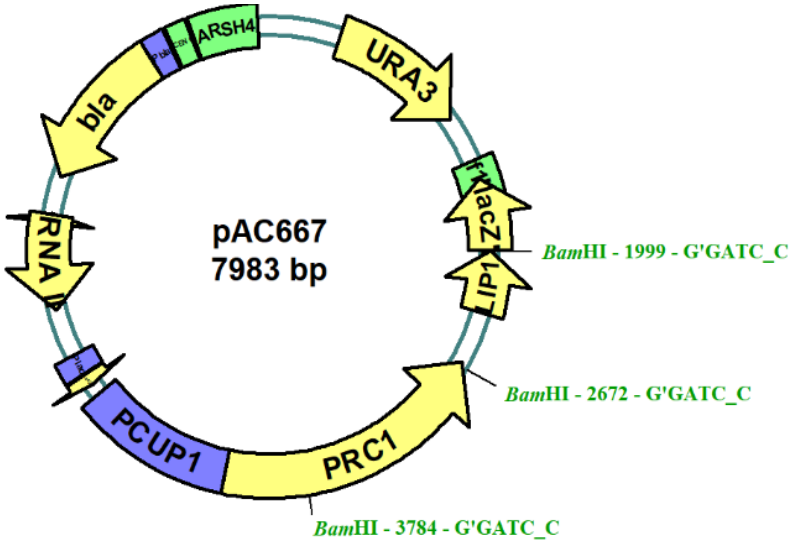

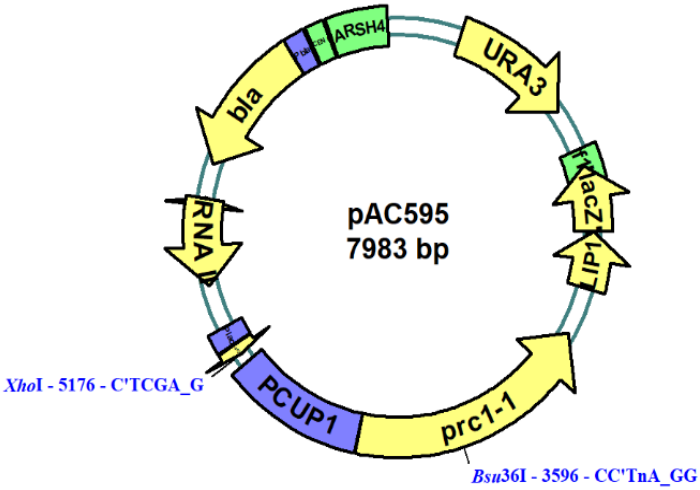

Fig. 33 *pAC595 with URA3 and under control by the PCUP1 promoter and prc1-1 ORF*

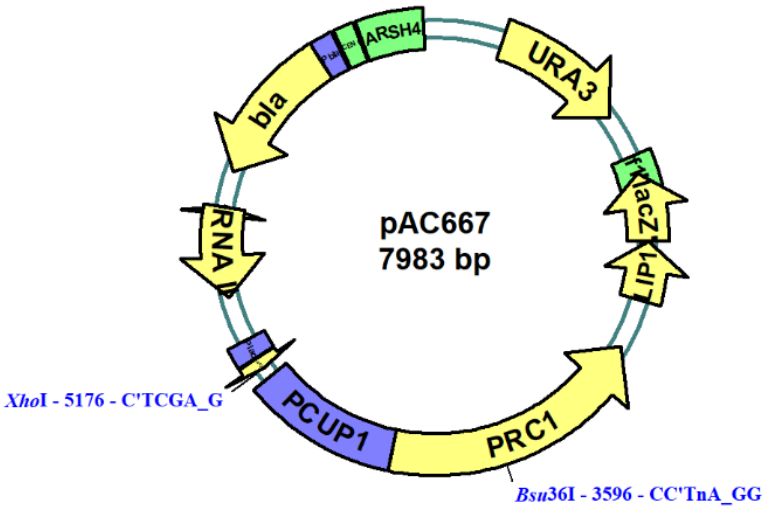

Fig. 34 *pAC667 with URA3 and under control by the PCUP1 promoter and PRC1 ORF*

Table 3. All plasmids used in this project.

Name	Source	Reference	Origin/Derivation
pAC595	A. A. Cooper, University of Missouri, Kansas City	C. M. Haynes, E. A. Titus, A. A. Cooper, Mol. Cell 15 (2004) 767-776	A. A. Cooper
pAC667	A. A. Cooper, University of Missouri, Kansas City	C. M. Haynes, E. A. Titus, A. A. Cooper, Mol. Cell 15 (2004) 767-776	A. A. Cooper
pAC595R	Produced by Y. Tanna	None	Replacement of 1,580 bp *XhoI* - *Bsu36I* fragment of pAC595 with the 1,580 bp *XhoI* - *Bsu36I* fragment of pAC667
pRS423 (-His)	Schroeder group plasmid collection	T. W. Christianson, R. S. Sikorski, M. Dante, J. H. Shero, P. Hieter, Gene 110 (1992) 119-122	M. Schroeder
pRS423 – $P_{GAL1,10}$ –DCR2 – HA(-His)	Produced by M. Schroeder	Schroeder, unpubl.	3,023 bp Cfr42I-PdiI fragment of pRSII422-PGAL1,10-DCR2-HA-ZZ was ligated to the 5,374 bp Cfr42I-PdiI fragment of pRS423
pRS423 – $P_{GAL1,10}$ –H338A - DCR2 - HA (-His)	Produced by M. Schroeder	Schroeder, unpubl.	3,023 bp Cfr42I-PdiI fragment of pRSII422-PGAL1,10-H338A-DCR2-HA-ZZ was ligated to the 5,374 bp Cfr42I-PdiI fragment of pRS423

7.1.3 Commercially available kits

Table 4. List of commercial kits, including catalogue number, supplier and biological use.

Name of Kit	Supplier	Use	Catalogue No.
Perfectprep kit midi	Eppendorf	Plasmid extraction	Discontinued
Pierce ECL Western Blotting Substrate	Thermofisher scientific	Chemiluminescent detection	32106
Pierce ECL Plus Western Blotting Substrate	Thermofisher scientific	Chemiluminescent detection	32132

7.1.4 Media composition for cell cultures

Table 5. The composition of synthetic dextrose agar, alongside the concentration of each component, lacking both uracil and leucine for cell culture. L-Asp & L-Thr were both added after autoclaving.

Component	Concentration	Mass/g, Volume/ml for 600ml	Present/Y or N	Modified mass or volume
YNB w/o aa	-	4.0	Y	3.3g
D-glucose	-	12.0	Y	10.00g
Agar	-	12.0	Y	10.00g
L-Tyr	-	0.018	Y	15.0mg
Uracil	2.4g/l	5.0	N	0.00ml
L-Arg.HCl	2.4g/l	5.0	Y	4.2ml
L-His.HCl	2.4g/l	5.0	Y	4.2ml
L-Met	2.4g/l	5.0	Y	4.2ml
L-Trp	2.4g/l	5.0	Y	4.2ml
L-Ile	3.6g/l	5.0	Y	4.2ml
L-Lys.HCl	3.6g/l	5.0	Y	4.2ml
L-Val	18g/l	5.0	Y	4.2ml
L-Ser	45g/l	5.0	Y	4.2ml
Adenine sulfate	1.2g/l	10.0	N	0.00ml
L-Phe	3.0g/l	10.0	Y	8.3ml
L-Glu	6.0g/l	10.0	Y	8.3ml
L-Leu	3.6g/l	16.7	N	0.00ml
H_2O	-	488.0	Y	433ml
Add After Autoclaving	-	-	-	-
L-Asp	4.0g/l	15.0	Y	12.5ml
L-Thr	24g/l	5.0	Y	4.2ml

Table 6. The composition of synthetic dextrose media, alongside the concentration of each component, lacking uracil for cell culture. L-Asp & L-Thr were both added after autoclaving.

Component	**Concentration**	**Mass/g, Volume/ml for 600ml**	**Present/Y or N**	**Modified mass or volume**
YNB w/o aa	-	4.0	Y	3.3g
D-glucose	-	12.0	Y	10.0g
L-Tyr	-	0.018	Y	15.0mg
Uracil	2.4g/l	5.0	N	0.0ml
L-Arg.HCl	2.4g/l	5.0	Y	4.2ml
L-His.HCl	2.4g/l	5.0	Y	4.2ml
L-Met	2.4g/l	5.0	Y	4.2ml
L-Trp	2.4g/l	5.0	Y	4.2ml
L-Ile	3.6g/l	5.0	Y	4.2ml
L-Lys.HCl	3.6g/l	5.0	Y	4.2ml
L-Val	18g/l	5.0	Y	4.2ml
L-Ser	45g/l	5.0	Y	4.2ml
Adenine sulfate	1.2g/l	10.0	N	0.0ml
L-Phe	3.0g/l	10.0	Y	8.3ml
L-Glu	6.0g/l	10.0	Y	8.3ml
L-Leu	3.6g/l	16.7	Y	13.9ml
Add After Autoclaving	-	-	-	-
L-Asp	4g/l	15.0	Y	12.5ml
L-Thr	24g/l	5.0	Y	4.2ml
Add H_2O to:	-	-	-	483.3ml

Table 7. The composition of Presporulation medium 2 agar, alongside the concentration of each component, lacking both uracil and leucine for cell culture. L-Asp & L-Thr were both added after autoclaving.

Component	**Concentration**	**Mass/g, Volume/ml for 600ml**	**Present/Y or N**	**Modified mass or volume**
K-phthalate	-	6.1	Y	10.2g
Dissolve in H_2O	-	-	-	800ml
Add H_2O to:	-	488.0	-	866.7ml
YNB w/o aa	-	4.0	Y	6.7g
Yeast extract	-	0.6	Y	1.0g
KOAc	-	6.0	Y	10.0g
Agar	-	12.0	Y	20.0g
L-Tyr	-	0.018	Y	30.0mg
Uracil	2.4g/l	5.0	N	0.0ml
L-Arg.HCl	2.4g/l	5.0	Y	8.3ml
L-His.HCl	2.4g/l	5.0	Y	8.3ml
L-Met	2.4g/l	5.0	Y	8.3ml
L-Trp	2.4g/l	5.0	Y	8.3ml
L-Ile	3.6g/l	5.0	Y	8.3ml
L-Lys.HCl	3.6g/l	5.0	Y	8.3ml
L-Val	18g/l	5.0	Y	8.3ml
L-Ser	45g/l	5.0	Y	8.3ml
Adenine sulfate	1.2g/l	10.0	N	0.0ml
L-Phe	3.0g/l	10.0	Y	16.7ml
L-Glu	6.0g/l	10.0	Y	16.7ml
L-Leu	3.6g/l	16.7	N	0.0ml
Add After Autoclaving	-	-	-	-
L-Asp	4.0g/l	15.0	Y	25ml
L-Thr	24g/l	5.0	Y	8.3ml

Table 8. The composition of Synthetic galactose/raffinose media, alongside the concentration of each component, lacking both uracil and histidine for cell culture.

Component	Concentration	Mass/g, Volume/ml for 600ml	Present/Y or N	Modified mass or volume
YNB w/o aa	-	4.0	Y	3.33g
D-galactose	-	12.0	Y	10.0g
D-raffinose	-	6.0	Y	5.0g
L-Tyr	-	0.018	Y	15.0mg
uracil	2.4g/l	5.0	N	0.00ml
L-Arg.HCl	2.4g/l	5.0	Y	4.17ml
L-His.HCl	2.4g/l	5.0	N	0.00ml
L-Met	2.4g/l	5.0	Y	4.17ml
L-Trp	2.4g/l	5.0	Y	4.17ml
L-Ile	3.6g/l	5.0	Y	4.17ml
L-Lys.HCl	3.6g/l	5.0	Y	4.17ml
L-Val	18g/l	5.0	Y	4.17ml
L-Ser	45g/l	5.0	Y	4.17ml
Adenine sulfate	1.2g/l	10.0	Y	8.33ml
L-Phe	3.0g/l	10.0	Y	8.33ml
L-Glu	6.0g/l	10.0	Y	8.33ml
L-Leu	3.6g/l	16.7	Y	13.92ml
L-Asp	4.0g/l	15.0	Y	12.50ml
L-Thr	24g/l	5.0	Y	4.17ml
Add H_2O to:	-	-	Y	483.3ml

7.1.5 Strain Information

Table 9. *E. coli* & *S. cerevisiae* strain information

Species	Strain	Genotype	Source
S. cerevisiae (Yeast)	BY 4742	S288C MATα his3Δ1 leu2Δ0 lys2Δ0 ura3Δ0	Scientific Research and Development GmbH, Oberursel, Germany
S. cerevisiae (Yeast)	Y10885	BY 4742 prc1Δ::kanMX4	Scientific Research and Development GmbH, Oberursel, Germany
E. coli (Bacteria)	DH5α	F^- ϕ80*lac*ZΔM15 Δ(*lac*ZYA-*arg*F) U169 *rec*A1 *end*A1 *hsd*R17(r_k^-, m_k^+) *pho*A *sup*E44 *thi*-1 *gyr*A96 *rel*A1 λ^-	Invitrogen Life technologies
E. coli (Bacteria)	XL10-GOLD	Tet^rΔ(*mcrA*)183 Δ(*mcrCB-hsdSMR-mrr*)*173 endA1 supE44 thi-1 recA1 gyrA96 relA1 lac* Hte [F´ *proAB lacI*^{q}ZΔ*M15* Tn*10* (Tet^r) Amy Cam^r]	Stratagene

7.1.6 Antibodies

Table 10. All antibodies used in both western blotting and chemiluminescent detection.

Antibody	Subtype	Species	Clonality	Supplier	Cat. No.	Dilution factor
anti-CPY	IgG_{2a}	Mouse	Monoclonal	Thermo-fisher scientific	A-6428	1000
anti-CPY	IgG_1	Mouse	Monoclonal	Abcam	Ab113685	1000
anti-Mouse IgG (H+L)-peroxidase	IgG	Goat	Polyclonal	Invitrogen	31432	2000
anti-β-actin	IgG_{2b}	Mouse	Monoclonal	Abcam	Ab170325	1000

7.2 Methods

7.2.1 Transformation of E. coli

- Preparation of competent cells

Once having acquired a set of LB agar plates, utilise the streaking method to streak out frozen stock of *E. coli* onto a single plate. Keep plate in the 37^{o}C incubator to grow overnight. Once bacterial colonies have grown, pick a single colony from the LB plate and inoculate with 4ml LB medium + 0.125 µg ampicillin. Each mixture was transferred to a 15ml falcon culture tube, and grown in a 37^{o}C incubator, overnight with shaking at 220rpm. Once grown, 1ml of overnight culture was inoculated with 100ml LB medium and grown to an OD_{600} of ~ 0.4 - 0.6 (mid-log phase), at 37^{o}C with shaking at 220rpm in the incubator. Once the optimal OD_{600} had been reached, the mixture was transferred into a 50ml falcon tube and centrifuged at 2,000 g for 30 min at 4^{o}C. To obtain competent cells, the supernatant was discarded, and the cell pellet was resuspended in 15 ml ice-cold 0.1 M $CaCl_2$, by slight vortexing. This solution was then kept on ice for ~ 1 h. Once incubation was complete, the suspension was centrifuged at 2,000 g at 4^{o}C for 10 min. The supernatant was then aspirated and the pellet re-dissolved in 4 ml of 0.1 M $CaCl_2$ + 15% (v/v) glycerol, by gentle pipetting up and down. 200 µl of each cell mixture was then added to pre-cooled 1.5 ml microcentrifuge tubes, frozen in liquid N_2, and stored as competent cells at -80^{o}C (Nishimura et al., 1990).

- Chemical transformation

100 µl of competent cells were then extracted and added to 1-5 µl plasmid solution. A positive control utilised 5 µl plasmid solution, whilst a negative control substituted this for 5 µl of 1 x TE (pH 8.0) buffer, each solution added to a pre-cooled microcentrifuge tube. Cells were then placed on ice for 30 min. These cells were then heat-shocked in a 42^{o}C water bath

for 1.5 min. The cells were again placed on ice for 2 min. Once complete, 1 ml of LB medium was added to cell mixture and made up in a 15 ml falcon tube. Cell suspension was then incubated at 37ºC for 1 h with shaking at ~220rpm. Once incubation had finished, the streaking technique was utilised to plate 100 µl of cell mixture onto an LB (+ Ampicillin) agar plate. The plate was then incubated at 37ºC until colonies began to appear (Casali, 2010).

7.2.2 Preparation of Plasmid DNA

- *Plasmid Miniprep*

5ml of LB medium was added to 2.5 µl of 50 µg/ml ampicillin to each centrifuge tube and inoculated with a single colony of *E. coli* cells, as mentioned earlier. 1.5ml of saturated overnight *E. coli* was placed into a 1.5ml microcentrifuge tube. The rest of the culture was stored at 4ºC (fridge). Cells were then acquired by centrifugation at 14,000 g for 1 min at RT, and the subsequent supernatant was aspirated. Once again, centrifugation at 14,000 g for 1 min at RT was used to remove any further supernatant. Once the cell pellet had been obtained it was necessary to resuspend it in 100 µl of 50 mM D-Glu, 25 mM Tris·HCl (pH 8.0), 10 mM EDTA, and fully mixed by vortexing the solution. This sample was then incubated at RT for 5 min. The sample was then dissolved in 200 µl of 0.2 M NaOH, 1% (w/v) SDS, and again fully mixed by inverting the tube several times. This sample was then incubated on ice for 5 min. Further, the sample was dissolved in 150 µl of ice-cold 5 M KOAc (pH 4.8), and lastly fully mixed by inverting the tube several times. This sample was then incubated on ice for a final 5 min. Once complete, the solution was centrifuged at 14,000 g for 3 min at 4ºC, and the flocculent material was discarded, whilst the supernatant was transferred to fresh 1.5ml microcentrifuge tubes. Once transferred, the supernatant was added to 0.8ml of EtOH, fully mixed by inverting the tubes several times, and again incubated at RT for a few min. The solution was then centrifuged at 14,000 g for 1 min at RT, and the supernatant discarded. To ensure full dissolution of cell pellet, 1ml of 70% EtOH was added to the sample, fully vortexed and then centrifuged at 14,000 g for 1 min at RT, removing the supernatant when complete. Finally, the cells were centrifuged at 14,000 g for 15 s at RT, and the supernatant was aspirated for the last time. The excess liquid was removed, and the pellet left to dry, by keeping them upright on the bench, at RT for 15 min. The remaining pellet was then re-dissolved in 30 µl of 1 x TE buffer (pH 8.0) with 0.3 mg/ml RNase A and left to fully dissolve in the fridge (4ºC), up to 1 h (Bimboim and Doly, 1979).

7.2.3 Analytical restriction digests

The total mix (Tables 11, 12) was prepared for the single and double digest reactions. The single digest, for pAC595, utilised H_2O, 10 x Buffer, *Spe*I enzyme and BSA. 2.5µl (200 ng) of plasmid was added to two tubes, one for the digest and the other for the control mixture. Once the contents of each tube had been fully mixed, each tube was placed in a water bath (37^{o}C) and heated for 1 h. Once complete, each mix was loaded onto an agarose gel. The single digest, for pAC667, utilised H_2O, 10 x Buffer and *BamH*I enzyme. 2.5µl (200 ng) of plasmid was added to two tubes, one for the digest and the other for the control mixture. The following procedure was repeated as before.

The double digest, for pAC595, utilised H_2O, 10 x Tango buffer, *Xho*I enzyme and *Bsu36*I enzyme. 48.7µl (20 µg) of plasmid was added to two tubes, one for the digest and the other for the control mixture. Once the contents of each tube had been fully mixed, each tube was placed in a water bath (37^{o}C) and heated for 24 h. Once complete, each mix was loaded onto an agarose gel. The double digest, for pAC667, utilised H_2O, 10 x Tango buffer, *Xho*I enzyme and *Bsu36*I enzyme. 36.8µl (20 µg) of plasmid was added to two tubes, one for the digest and the other for the control mixture. The following procedure was repeated as before.

Table 11. The master mix preparation for the single digest of each plasmid.

Reagent	**Volume (µl)**
H_2O	14.5
10 x Buffer	2.0
*Spe*I Enzyme	0.5
BSA	0.5
pAC595 (200 ng)	2.5
Total volume (µl)	20

Reagent	**Volume (µl)**
H_2O	15.0
10 x Buffer	2.0
*BamH*I Enzyme	0.5
pAC667 (200 ng)	2.5
Total volume (µl)	20

Table 12. The master mix preparation for the double digest of each plasmid.

Reagent	**Volume (µl)**	**Volume (µl) for gel loading**
H_2O	35.3	7.06
10 x Tango Buffer	10.0	2.0
*Xho*I Enzyme	4.0	0.8
*Bsu36*I Enzyme	2.0	0.4

pAC595 (20 µg)	48.7	9.74
Total volume (µl)	100	20

Reagent	**Volume (µl)**	**Volume (µl) for gel loading**
H_2O	47.2	9.44
10 x Tango Buffer	10.0	2.0
*Xho*I Enzyme	4.0	0.8
*Bsu36*I Enzyme	2.0	0.4
pAC667 (20 µg)	36.8	7.36
Total volume (µl)	100	20

7.2.4 Ligation

Ligation was used to join the pAC595 fragment with the pAC667 fragment, to form the pAC595R repaired plasmid. A negative control (100ng of pAC595 cut with *SpeI* enzyme), a vector + insert 1:1 M ratio (25ng of pAC667 cut with *BamHI* enzyme) and a vector + insert 1:3 M ratio (75ng of pAC667 cut with *BamHI* enzyme) all took part in this ligation.

Each reaction mixture was composed of 1µl of T4 DNA ligase, 1µl of 10 x T4 DNA ligase buffer, 100ng of vector (pAC595 cut with *SpeI* enzyme) and the appropriate volumes (25ng and 75ng of pAC667 each cut with *BamHI* enzyme) for the latter 2 mixtures respectively. Each solution was made up to 10µl with H_2O. Each solution was added to an appropriate tube, placed in the G-storm machine, and ligated overnight at 18^{o}C for ~18-20 h. Once complete, 5µl of ligation mixture was added to 1ml of 30% (w/v) glycerol solution, to be stored at -80^{o}C, whilst the other 5µl was used in a transformation reaction into competent *E. coli* cells. 5 different mixtures were chemically transformed: negative control, positive control, vector only ligation, vector + insert 1:1 M ratio and vector + insert 1:3 M ratio. The negative control was composed of 5µl of 1 x TE buffer (pH 8.0) with 100µl competent *E. coli* cells, whilst the positive control was composed of 5µl of either pAC595 or pAC667 with 100µl competent cells. The other 3 mixtures were composed of 100µl competent cells with each of their respective plasmid of interest, post ligation mixture. For the negative control, positive control and vector only ligation mixtures, 200µl of each mixture was plated onto a single LB + Ampicillin agar plate and incubated overnight at 37^{o}C. However, for the vector + insert 1:1 M ratio and vector + insert 1:3 M ratio mixtures, 200µl and the rest of solution

(~800µl) each was plated onto a single LB + Ampicillin agar plate and incubated overnight at 37°C, hence 7 plates.

Once bacterial colonies had fully grown it was possible to count all colonies. The plate with the highest colony number was the vector + insert 1:1 M ratio. 24 colonies were picked and used in a Miniprep, to extract plasmid DNA. Once extracted, a single digest was used to provide confirmation of the repair of the *prc1-1* allele.

7.2.5 Agarose Gels

I utilised a 1% (w/v) agarose gel for all plasmid experiments. The gel was prepared by the dissolution of 0.5g of agarose with 50ml of 1 x TAE buffer, fully heated in a microwave. Upon reduction in temperature to ~50°C, 0.5ml of 10 $mgml^{-1}$ of ethidium bromide (to stain plasmid DNA) was added to the agarose solution. Each gel was positioned within a 1 x TAE buffer-submerged tank. Alongside 5µl of gene ruler DNA ladder 1 kb, which was loaded onto the first gel lane, all subsequent samples were loaded into the gel, to detect the plasmid bands with varying sizes (Lee and Kim, 2005).

7.2.6 Yeast culture and sample collection

For the detection and IP of CPY experiments, Y10000 & Y10885 strains were grown on YPD plates. A single colony from each strain was picked and cultivated with ~4ml YPD media. Each small culture was incubated at 30°C and shaken at 220rpm until the required OD_{600} was reached. The appropriate volume of each small culture was added to ~50ml YPD media, incubated at 30°C and grown to a final OD_{600} of ~0.3-0.8 (mid-log phase). It was important to ensure that the OD_{600} was ~0.6-0.7 to ensure a high protein concentration for CPY detection. Cells were then harvested by centrifugation at 3000rpm, 4°C for 2 min and stored at -80°C.

For the Cu^{2+} induction experiment, pAC595R, with pRS423 (-His), pRS423-$P_{Gal1,10}$ (-His) and pRS423-$P_{Gal1,10}$-H338A DCR2 (-His) strains, were grown on SD (-Ura, -Leu) plates. A single colony from each of the three strains was picked and cultivated in ~4ml of synthetic galactose/raffinose (2% (w/v)/1% (w/v)) media. Each small culture per strain was incubated at 30°C and shaken at 220rpm until the required OD_{600} was reached. The appropriate volume of each small culture was added to ~50ml synthetic media over a total of 6 x 50ml flasks per strain, incubated at 30°C and grown to a final OD_{600} of ~0.3-0.8 (mid-log phase). Once the optimal OD_{600} per strain was reached, 5 different Cu^{2+} concentrations were added to each flask. Each flask, excluding flask 1, was then incubated at +15 minutes, +30 minutes, +45

minutes, and +60 minutes, with 50ml of total culture being removed at each time interval and stored on ice. All treated cells were then harvested by centrifugation at 3000rpm, 4°C for 2 minutes and stored at -80°C. The purpose of 5 different concentrations at 4 different time intervals, was to detect whether a correlation was present for rising concentrations of Cu^{2+} induction, and whether this leads to DCR2 overexpression, and subsequent ER stress effects.

7.2.7 Protein extraction for Western blotting analyses

The frozen cells were then warmed to RT and resuspended in 5ml of ice-cold water followed by centrifugation at 4°C. The supernatant was removed from the suspension and the cell pellet was once again resuspended in 1ml of ice-cold water. Each cell suspension was then transferred to a screw-cap tube (2ml) for the lysis buffer step. Centrifugation at 12000rpm, 4°C for 1 min then took place to procure the cell pellet. 100µl of glass beads, followed by 200µl of lysis buffer was added sequentially to each cell pellet. For the IP experiment, 100µl of glass beads, followed by 200µl of optimal lysis buffer (50mM Tris·HCl (pH 7.5 at 4°C), 1mM EDTA, 1% (w/v) SDS) was added sequentially to each cell pellet. Each lysis buffer contains protease inhibitors (PMSF, 2mM & AEBSF, 6mM) and β-mercaptoethanol (5 mM). Homogenisation of each cell pellet took place within a Precellys 24 machine at 6500rpm, 4°C for 10s, for a total of 3 cycles; with each cell pellet being stored on ice between each cycle for 5 min. The final step involved sample centrifugation at 12,000rpm for 10 minutes at 4°C. Each protein lysate was then added to fresh 1.5ml microcentrifuge tubes and frozen at -80°C in liquid N_2 (Kushnirov, 2000; Laadan et al., 2008).

7.2.8 Bicinchoninic Acid (BCA) protein assay

To quantify the extracted protein of each sample, it was necessary to use a bicinchoninic acid assay. BSA standards (0, 62.5, 125, 250, 500, 1000, 2000 $\mu g ml^{-1}$) were prepared by a serial dilution of 1:2 with each diluted (1:10) lysis buffer. All protein lysates were diluted 1:10 with 0.1 M 2-iodoacetamide in 0.1 M Tris·HCl (pH 8.0) and incubated at 37°C for 30 min; to remove any β-mercaptoethanol present in the lysate. 10µl of each solution were sequentially added to a U-bottom 96-well plate. 200µl of standard working solution was added per well and incubated at 60°C for ~30 min. Each sample absorbance was then read at wavelength of 562nm. Subsequent protein concentration calculations were ascertained from the standard curve and used in sample dilutions for SDS-PAGE gels (Smith et al., 1985).

7.2.9 SDS-PAGE gels

I utilised a 9% SDS-PAGE gel with a 1.0mm spacing between the glass plates, on which to run the protein lysates. The gel was divided into stacking (pH 6.8) & separating (pH 8.9) components. The separating gel was polymeric and made from 30% (w/v) acrylamide, 0.8% (w/v) bisacrylamide, 1M Tris·HCl, pH 8.9, H_2O, 10% SDS, 10% APS and TEMED. The stacking gel was also polymeric and made from 30% (w/v) acrylamide, 0.8% (w/v) bisacrylamide, 1M Tris·HCl, pH 6.8, H_2O, 10% SDS, 10% APS and TEMED. The volume was used to cast each type of gel. 50µg of each protein lysate in the CPY detection experiment, 10µg for the Cu^{2+} induction experiment, and both 50 & 10µg of each protein lysate (input) for the IP experiment, were diluted in H_2O to a total volume of 18µl. Before loading, 3.6µl of 6 x SDS-PAGE loading buffer were added to each lysate. Further for the IP, 10µg of each lysate (supernatant) were diluted in H_2O to a total volume of 21µl. These lysates were then boiled (100^oC) for ~5 minutes. Samples were then cooled to RT for a few minutes before being centrifuged at ~12,000g, RT for ~5 min. Each lysate was then loaded onto the gel, with the protein ladder being loaded onto the first lane. Each gel was run for ~1.5 hrs at 130V (Simpson, 2006).

7.2.10 Yeast strain transformation

A single colony was picked and cultivated with 4ml of YPD media. Each small culture was incubated at 30^oC and shaken at 220rpm until the required OD_{600} was reached. Once the optimal OD_{600} had been attained, each small culture was added to ~50ml YPD media, incubated at 30^oC and grown to a final OD_{600} of ~1.0. Cells were then harvested by centrifugation at 3000rpm, 4^oC for 2 min, at which point the cell pellet was preserved on ice whilst the supernatant was discarded. Each cell pellet was then re-suspended in ~88µl of one-step buffer (ratio of 50% (w/v) PEG4000 to 1 M LiOAc was 4:1). Each cell pellet was then added to 1µl of the desired plasmid alongside 12µl of 8.31 mg/ml sheared salmon sperm DNA, with each tube being vortexed at maximum speed for ~10s. The entire cell suspension was then incubated at 42^oC for ~ 30 min, cooled on ice, after which each tube was spun at maximum speed to recover the cell pellet and discard the supernatant. The mixture was then resuspended in 200µl of autoclaved H_2O. The entire mixture was then plated onto a selective SD agar plate. All plates were incubated at 30^oC until colonies were grown (Agatep et al., 1998).

7.2.11 Replica plating

To prevent the possibility of cells, grown on SD plates, possessing a mutation which leads to growth prevention of cells on media containing only non-fermentable carbon sources, it was necessary to replica plate cells from the SD plates onto the PSP2 agar plates.

7.2.12 Semi-dry Electrotransfer

Once each lysate had fully migrated, to appear at the bottom of the gel, each gel was removed from the electrophoresis unit and incubated with semi-dry electrotransfer buffer (0.1M Tris, 0.192M glycine with 5 %(w/v) MeOH) for 15 min. This wash was repeated thrice. After the gel had fully expanded, the stacking gel was removed. One PVDF membrane was cut to the precise dimensions of each expanded gel and incubated in MeOH for 1 min, followed by incubation in the electrotransfer buffer for ~15 min. The final step was to prepare a series of 8 x Whatman 3MM papers, which also were cut to the precise dimensions of each expanded gel and incubated in electrotransfer buffer at 60rpm for ~5 min. It was then necessary to stack each component to form a 'sandwich'. Both the cathode and anode were wetted with a small volume of semi-dry electrotransfer buffer. Upon the anode was stacked 4 x Whatman 3MM papers followed by a PDVF membrane and SDS-PAGE gel, and a further 4 x Whatman 3MM papers. To enable efficient and complete transfer, it was important to remove excess air bubbles between each material in the 'sandwich', with the use of a glass rod which was rolled across each Whatman 3MM paper. The apparatus was then closed to begin electrotransfer. The electrotransfer utilised a constant current (2mA per cm^2), with variable potential, per gel for 1 hr and 15 min. Once complete, each membrane was placed in a TBST + 5%(w/v) milk buffer solution, blocked at 4^oC (cold room), and shaken at 30rpm overnight (Pakula, 2019).

7.2.13 Western blotting & chemiluminescent detection

The selection of antibodies chosen were to detect CPY proteins. Table 7 refers to the choice of antibodies used in this experiment. Each membrane was incubated within 5ml of TBST + 5% (w/v) milk solution on a roller at RT for up to 2 hrs, with the specified primary antibody at a specific dilution (Table 7). Once incubation was complete, each membrane was washed in 50ml of TBST for 5 min at 60rpm, repeated 4 times. Each membrane was then incubated within 5ml of TBST + 5% (w/v) milk solution on a roller at RT for up to 2 h, with the specified secondary antibody at a specific dilution (Table 7). Again, post incubation, each membrane was washed in 50ml of TBST for 5 min at 60rpm, repeated 4 times. Both the ECL2 reagent and the luminol + *p*-coumaric acid (100mM Tris-HCl (pH 8.5) + 0.1%(w/v)

Tween 20, 250mM luminol, 90mM *p*-coumaric acid and 4.35 µl of 30% (w/v) H_2O_2) reagents were possible to use in the chemiluminescent detection of CPY proteins. ECL2 is a very sensitive reagent, to detect low amounts of CPY, and luminol is a less sensitive reagent. 2ml of the chosen chemiluminescent reagent was used and applied to each membrane for 1 min. Each film was exposed to Thermo-Scientific CL – X-Posure X-ray film for three exposure times: 1s, 15s and 1 min (Kurien and Scofield, 2006; Taylor et al., 2013).

7.2.14 Stripping of western blots

Each PVDF membrane was incubated in 50ml of 100mM Tris·HCl (pH 8.5) + 0.1% (w/v) Tween 20 for ~ 5 min. This was then followed by membrane incubation in 50ml of 100mM Tris·HCl (pH 8.5) + 200µM β-mercaptoethanol + 0.1% Tween 20 for ~ 15 min. Once complete, this step was repeated with the same volume at the same incubation time. Next, the PDVF membrane was incubated with 2 x 50ml of TBST and shaken at ~60rpm, RT for 5 min. Further, the PDVF membrane was incubated with 2 x 25ml of 100mM glycine·HCl (pH 2.5) + 0.1% Tween 20 and rolled at ~30rpm, 65^{o}C for 15 min. The final incubation step was 2 x 50ml with TBST, shaken at ~60rpm at RT. Once complete, each membrane was placed in a TBST + 5% (w/v) milk buffer solution, blocked at 4^{o}C (cold room), and shaken at 30rpm overnight. Each membrane could then be re-developed with an alternative selection of antibodies (Kar et al., 2012).

7.2.15 Immunoprecipitation

For both Y10000 & Y10885 strains, 1mg of protein lysate was used per immunoprecipitation. However, a few alterations were needed. Firstly, 2.5% (w/v) SDS in the lysis buffer was a too high concentration, as this would have resulted in denaturation of the IgG protein. Thus, it would need to be diluted by a factor of 25 to reach a tolerable concentration. Secondly, the 5mM β-mercaptoethanol concentration is also intolerable and may cause antibody degradation by breaking of the disulphide bonds in the IgG protein, thus must also be diluted 25 times to reach a tolerable concentration. In IP, all subsequent dilutions were made in a different buffer: 50mM Tris·HCl (pH 7.5 at 4^{o}C), 10mM EDTA (pH 8.0), 0.5% (w/v) sodium deoxycholate, 0.1% (w/v) Triton X-100. Buffer calculations were made and used in the dilution of protein lysates. This dilution established a final SDS concentration of 0.1% and a final β-mercaptoethanol concentration of 0.2mM. A standard protocol for immunoprecipitation was then employed. The amount of Sure Beads protein G magnetic beads added to each sample of diluted lysate was equivalent in all samples used in the IP (100

µl). This type of magnetic bead was used to remove proteins that bind unspecifically to the beads. Once the diluted lysate samples had been incubated with the magnetic beads at ~4^{o}C, a magnetic stand was used to separate the supernatant from the magnetic beads. 1µl of anti-CPY antibody was added to the supernatant and incubated for ~12 h. Once the beads had been washed with first dilution buffer then water, ~30µl of 6 x SDS-PAGE loading buffer (+ β-mercaptoethanol) were added to each immunoprecipitate and denatured by boiling at ~100^{o}C for 5 min. These samples are colloquially known as the pre-immune IP. The following day, a further calculated volume of magnetic beads was added to the supernatant and further incubated at ~4^{o}C for 1.5 h. Once complete, a magnetic stand was again used to separate the supernatant from the magnetic beads. This procured the immunoprecipitate. The remaining beads were once again washed with dilution buffer then water. ~30µl of 6 x SDS-PAGE loading buffer (+ β-mercaptoethanol) were added to each diluted lysis sample and denatured by boiling at ~100^{o}C for 5 min. These samples were then loaded onto SDS gels (DeCaprio and Kohl, 2017).

8.0 Results

8.1 Plasmid Construction

The overarching purpose of this initial experiment, which was utilised as a contingency plan if antibodies against *S. Cerevisiae* CPY were unable to provide strong signals, was to construct pAC595R centromeric plasmids which would encode the increased production and expression of CPY and CPY*. Once formed, these newly made plasmids would be transformed into both WT and mutant *S. Cerevisiae* cells, and protein extracts would be analysed to uncover whether overexpression leads to detection of CPY, in future experiments.

pAC595 & pAC667 plasmids were extracted from *E. coli*, where formerly they were expressed in (section 7.1.2). The pAC595 was singly digested by the *SpeI* restriction endonuclease and the pAC667 was singly digested by the *BamHI* enzyme. The bands at positions ~2500bp & ~5000bp for pAC595 and at positions ~700bp, ~1100bp & ~6200bp for pAC667, correlated well with the expected fragment sizes from this single digest, as can be seen from the agarose gel. 200ng of plasmid digest and 500ng of uncut plasmid were loaded onto this gel.

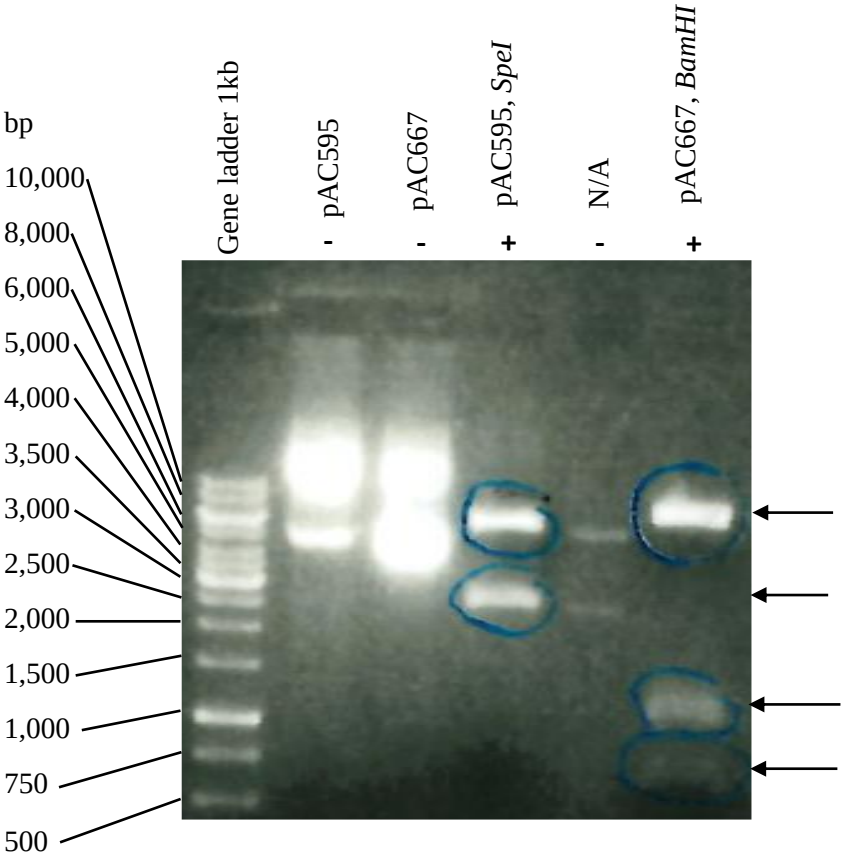

Figure 35. *Agarose gel of the single digest of pAC595 & pAC667 plasmids. Presence of circled bands indicate complete digestion of each plasmid at specific restriction sites. The presence of the endonuclease was confirmed by the +/- symbol.*

Replacement of the 1,580 bp *XhoI* - *Bsu36I* fragment of pAC595 with the 1,580 bp *XhoI* - *Bsu36I* fragment of pAC667 to remove additional point mutations in pAC595 was the motivation to repair the pAC595R.

Thus, both pAC595 and pAC667 plasmids were doubly digested by the *XhoI* - *Bsu36I* restriction endonucleases. The bands at positions ~1600bp & ~6000bp for both pAC595 and pAC667, correlated well with the expected fragment sizes from the double digest, as can be seen from the agarose gel. 20µg of plasmid digest and 200ng of uncut plasmid were loaded onto this gel. Furthermore, this double digest was repeated with the ratio of *XhoI* to *Bsu36I* being increased from equimolar to 2:1, with a total plasmid mixture of 100µl. This elevated concentration was chosen to predict the presence of a more intense band for one plasmid over the other.

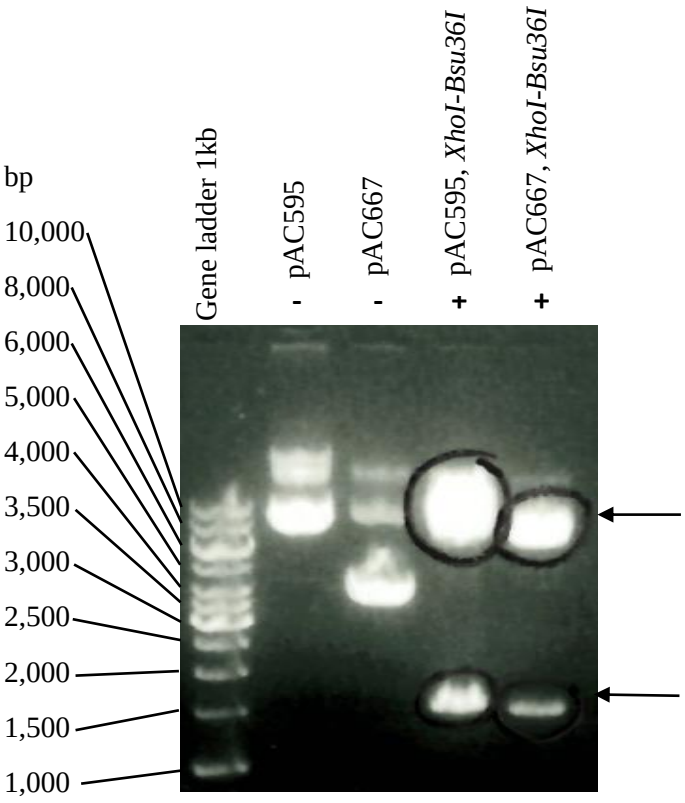

Figure 36. *Agarose gel of the double digest of pAC595 & pAC667 plasmids. Presence of circled bands indicate complete digestion of each plasmid at specific restriction sites. The presence of the endonuclease was confirmed by the +/- symbol.*

An analytical digest was used as confirmation of the repaired pAC595R plasmid. This plasmid was digested by the *HindIII* restriction endonuclease. The bands at positions ~1100bp, ~1900bp & ~5000bp for pAC595R, correlated well with the expected fragment sizes from the single digest, as is evident from the agarose gel.

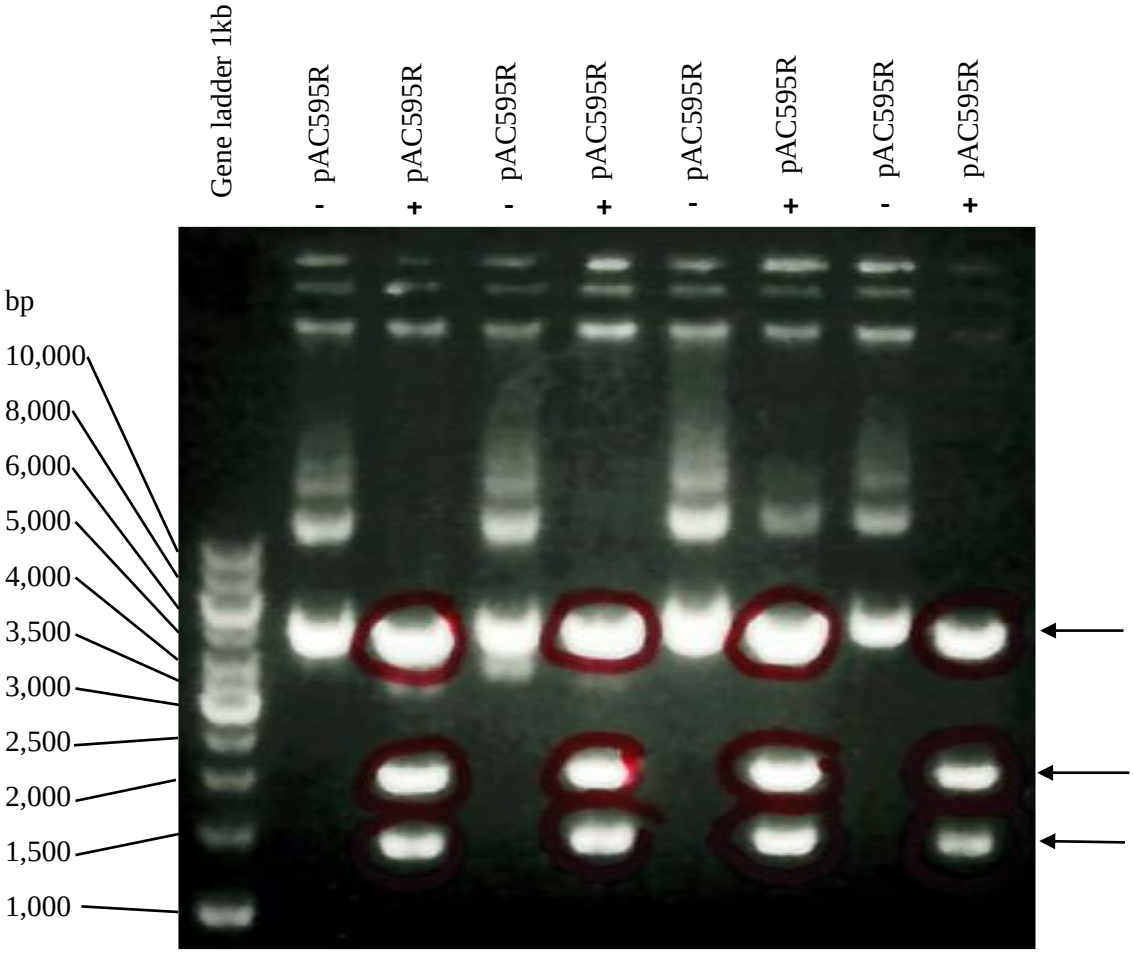

Figure 37. *Agarose gel of the Miniprep analysis using the HindIII restriction enzyme. Presence of circled bands indicate the repair of the prc1-1 allele. The presence of the endonuclease was confirmed by the +/- symbol.*

After single digest, there was an absent band at the expected position of 622 bp. This absent band may have been due to the inability of *SpeI* to cut pAC595 at the 3rd restriction site, or alternatively, the incubation time of 1 hr for the endonuclease to act upon the plasmid may

have been too short to allow full digestion. I repeated this experiment with 20µg of digested plasmid mixture and 500ng of undigested plasmid mixture, with overnight incubation, to test whether the digest reaction time and/or amount of plasmid affected the action of *Spe1* on the 3rd restriction site. The same plasmid volume was used for both pAC595 & pAC667 with the total digest mixture being 50µl and the digest incubation time being extended to ~12 h.

However, from analysis of the agarose gel, there remained an absent band for the expected fragment size at the 3rd restriction site. Therefore, a possible explanation may be due to impurities in either the endonuclease or the chosen reaction buffer.

To ensure validity of results, the double digest was repeated, but yielded virtually identical results. As a result of identical fragment sizes which could be cleaved by the action of both enzymes, the 1,580 bp fragment of pAC595 and the 1,580 bp fragment of pAC667 were able to be substituted by a ligation reaction. Due to the presence of all expected bands from the double digest, all reagents utilised must have been of a high purity and the reaction buffer must have been effective with both enzymes in the digest mixture. Further, the overnight incubation period of 12 h at 37℃, utilised in all double digests, would have significantly aided in complete digest of both plasmids, thus results would have been more accurate than with reduced incubation time. The ligation step was to provide confirmation of the joining of two plasmid fragments, namely the 1580bp fragment of pAC595 to the 1580bp fragment of pAC667. pAC595R is 7,983 bp. Fig. 35 shows three bands per digest lane. The first at ~5,000 bp, the second at ~1,900 bp and the third at ~1,100 bp. These total ~8,000 bp. Thus, there is confidence of the repair of the pAC595R plasmid.

The findings from this initial experiment show successful construction of the pAC595R plasmid. They confirm the substitution of the 1,580 bp fragment of pAC595 with the 1,580 bp fragment of pAC667. Thus, having sequenced the region at the 5' end of the CUP1 promoter, I can be confident in the overexpression of CPY and CPY*, which can now be detected in future experiments.

8.2 Detection of CPY

Once cloning had confirmed overexpression of CPY and CPY*, the reason for this next experiment was to confirm detection of CPY by a monoclonal antibody in a Western Blot. To enable a comparison of band intensity, a negative control, namely the mutant *S. Cerevisiae* cells which lack the *PRC1* gene and thus no signals should be obtained from these proteins, was tested alongside the WT cells, which should detect CPY in a western blot experiment.

The reasoning behind the four different buffers utilised in this experiment, was to compare the amount of CPY extracted. It is known that at a 1% (w/v) SDS concentration, an extraction buffer will denature the CPY protein, thus buffers with different SDS concentrations were tested. Also, at a certain urea concentration, proteins will be denatured, and thus it was important to compare buffers with and without a specified urea concentration. As CPY is a serine protease which can tolerate highly basic environments, buffers with different pH values were also tested to indicate which pH was the optimal for CPY expression.

The purpose of this experiment was to develop an immunoprecipitation technique for CPY, primarily to detect CPY by western blotting of protein extracts from yeast cells. All results collated for this experiment were in the form of western blots, essentially to compare different extraction buffers for their efficiency to extract and/or solubilise CPY. The first set of blots produced were a result of the α-CPY (primary antibody) with the α-Mouse IgG (H+L peroxidase) (secondary antibody) at a diluted concentration of 1:1,000, 1:20,000 respectively, being detected with ECL2. Further, all bands were present for the CPY but all absent for the CPY*, confirming my initial hypothesis that CPY is processed and targeted to the vacuole. The prc1Δ (Y10885) strain served as a specificity control for the α-CPY antibody, in the event of multiple bands on the blot. The molecular weight of each CPY band was consistent at ~59kDa. This correlates well with the predicted molecular weight of 59kDa for mature-CPY, with the pro-sequence cleaved off. Thus, the molecular weight has reduced from 69kDa to 59kDa, due to the transition of p2-CPY to m-CPY form, from the Golgi to the vacuole.

For this film, with 50μg of total CPY protein loaded, 4 blots were present for each buffer type:

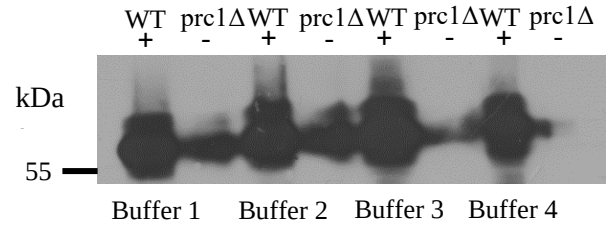

Figure 38. *Western blot data for α-CPY (1:1,000, 1:20,000) with ECL2. Blots are present for the Y10000 (WT) strain but absent for the Y10885 (prc1Δ) strain, across all 4 buffers.*

Table 13. Western blot data for α-CPY (1:1,000, 1:20,000) with ECL2.

Yeast Strain	Strain Type	Buffer	Volume α-CPY
			ECL2
Y10000	WT (+)	1	174000
Y10885	prc1Δ (-)	1	0
Y10000	WT (+)	2	149000
Y10885	prc1Δ (-)	2	0
Y10000	WT (+)	3	263000
Y10885	prc1Δ (-)	3	0
Y10000	WT (+)	4	97400
Y10885	prc1Δ (-)	4	0

Due to the strong intensity of all blots, the second set of blots produced were a result of the same antibodies with the same ECL2 chemiluminescent reagent, but at a greater dilution of 1:5,000/1:50,000 respectively. The same theory as before held for these blots. For this film, with 50µg of total CPY protein loaded, 4 blots were present for each buffer type:

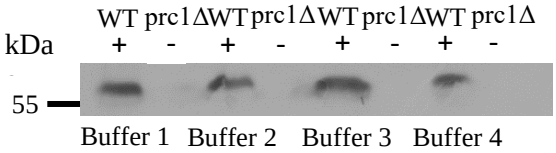

Figure 39. *Western blot data for α-CPY (1:5,000, 1:50,000) with ECL2. Blots are present for the Y10000 (WT) strain but absent for the Y10885 (prc1Δ) strain, across all 4 buffers.*

Table 14. Western blot data for α-CPY (1:5,000, 1:50,000) with ECL2.

Yeast Strain	Strain Type	Buffer	Volume α-CPY
			ECL2
Y10000	WT (+)	1	1520000
Y10885	prc1Δ (-)	1	0
Y10000	WT (+)	2	1810000
Y10885	prc1Δ (-)	2	0
Y10000	WT (+)	3	1910000
Y10885	prc1Δ (-)	3	0
Y10000	WT (+)	4	1450000
Y10885	prc1Δ (-)	4	0

Although the blot intensity volume was now lower, and thus easier to interpret the data, the experiment was repeated once more to acquire a third set of blots produced with the same antibodies at the same dilution, but with the luminol reagent. The same theory as before held for these blots. For this film, with 50µg of total CPY protein loaded, 4 blots were present, across all buffer types:

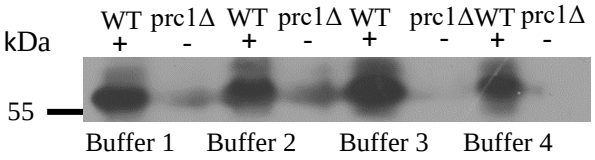

Figure 40. *Western blot data for α-CPY (1:1,000, 1:20,000) with Luminol. Blots are present for the Y10000 (WT) strain but absent for the Y10885 (prc1Δ) strain, across all 4 buffers.*

Table 15. Western blot data for α-CPY (1:1,000, 1:20,000) with Luminol.

Yeast Strain	**Strain Type**	**Buffer**	**Volume α-CPY**
			Luminol
Y10000	WT (+)	1	716000
Y10885	prc1Δ (-)	1	0
Y10000	WT (+)	2	922000
Y10885	prc1Δ (-)	2	0
Y10000	WT (+)	3	1130000
Y10885	prc1Δ (-)	3	0
Y10000	WT (+)	4	607000
Y10885	prc1Δ (-)	4	0

To enable a complete comparison of blot intensity, a loading control, namely β-actin, was utilised in a fourth set of western blots. Identical conditions, as to the first set of blots, were present but with β-actin having replaced α-CPY as the primary antibody. The same theory as before held for these blots. Additionally, there was a complete series of blots present for β-actin across all buffer and strain types. The expected position of β-actin is 43kDa, which correlated well with the blots present at ~43kDa. For this film, with 50µg of total CPY protein loaded, 4 blots were present, across all buffer types:

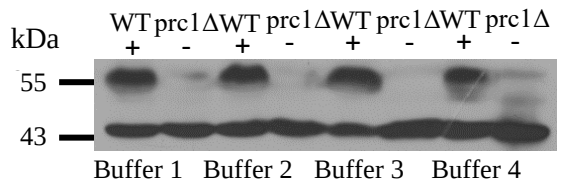

Figure 41. *Western blot data for β-actin (1:1,000, 1:20,000) with Luminol. Blots are present for the Y10000 (WT) strain but absent for the Y10885 (prc1Δ) strain, across all 4 buffers.*

Table 16. Calculated ratios for α-CPY across all CPY detection experiments.

Yeast Strain	**Strain Type**	**Buffer**	**Exposure Time**	**Ratios for α-CPY**		
				1:1,000, 1:20,000 [ECL2]	**1:5,000, 1:50,000 [ECL2]**	**1:1,000, 1:20,000 [Luminol]**
Y10000	WT (+)	1	1s	0.01	0.01	0.01
Y10000	WT (+)	1	15s	0.0104	0.0356	0.0127
Y10000	WT (+)	1	1min	0.0141	0.0763	0.0235
Y10000	WT (+)	2	1s	0.0101	0.0201	0.0108
Y10000	WT (+)	2	15s	0.0102	0.0540	0.0145
Y10000	WT (+)	2	1min	0.0146	0.0544	0.0237
Y10000	WT (+)	3	1s	0.0125	0.0443	0.0157
Y10000	WT (+)	3	15s	0.0100	0.0945	0.0162
Y10000	WT (+)	3	1min	0.0132	0.0931	0.0237
Y10000	WT (+)	4	1s	0.00655	0.00640	0.00580
Y10000	WT (+)	4	15s	0.00564	0.0218	0.00761
Y10000	WT (+)	4	1min	0.00753	0.0280	0.0137

It was then necessary to calculate the appropriate ratios to ascertain the optimal choice of buffer. These ratios were calculated from the blot intensity volume of α-CPY relative to the blot intensity volume of β-actin. Each ratio was then calculated from the ratio of each volume ratio relative to a standard volume ratio. The calculation was for all 3 sets of experiments: α-CPY (1:1,000, 1:20,000) with ECL2, α-CPY (1:5,000, 1:50,000) with ECL2 & α-CPY (1:1,000, 1:20,000) with luminol. Due to the nature of this experiment, only the Y10000 (WT) strain, tested with all 4 extraction buffers, yielded ratios.

Graph 1. Plotted results across all three CPY detection experiments.

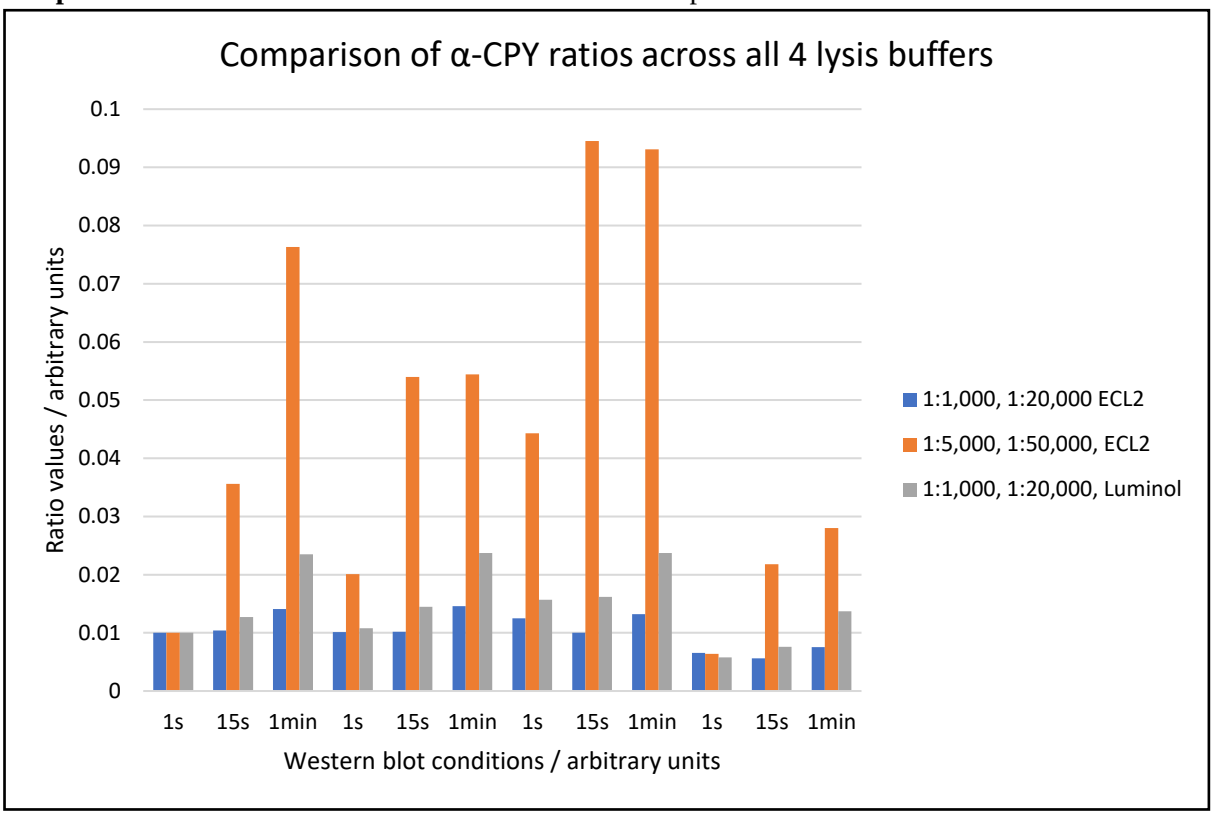

The tabulated results from this experiment show that the optimal detection of CPY, and thus the highest ratio values obtained from the western blot, are present at a 1:5,000 and 1:50,000 dilution of primary and secondary antibodies with ECL2. Furthermore, across all western blot experiments, the results show full detection of CPY with the WT cells but no detection with the mutant cells, thus confirming my initial hypothesis.

8.3 Immunoprecipitation of CPY

Now that CPY detection had been confirmed through western blot analysis, the reasoning behind this immunoprecipitation experiment was to test whether the antibody could detect CPY, in significant quantities, in an immunoprecipitate. Optimising the conditions of the immunoprecipitation would enable more quantitative results which would limit the use of the α-CPY antibody, needed in this experiment.

Once again, all results from these experiments were presented through the quantification of western blot films. The results from such films were to conclusively demonstrate that the α-CPY antibody was able to immunoprecipitate CPY. Unfortunately, due to the use of CPY: Mouse monoclonal, clone [10A5B5], type IgG_1 purchased from Abcam, the blot intensity results were affected and unable to be quantified. Possible reasons for this defect were the purity of this type of antibody sold from this specific company. Although the CPY: Mouse

monoclonal, clone [10A5B5], type IgG_{2a} purchased from Thermo-Scientific Fisher was found in the literature as an identical antibody from a different company, the lack of time for delivery (~5-6 months) and use in the IP of CPY was insufficient for any quantifiable or accurate data. Hence, progress was not achieved as the alternative antibody arrived too late. However, some results from western blot films were obtained from the IP of CPY. Although this experiment was repeated more than a dozen times over a period of 5-6 months, the results from the last set of western blot films indicated that a defect must have been present in the first α-CPY antibody tested. The last set of blots produced were a result of the α-CPY (primary antibody) with the α-Mouse IgG (H+L peroxidase) (secondary antibody) at a diluted concentration of 1:5,000, 1:50,000 respectively, being detected with ECL2. Further, as the input volume was 50µg in the first lane but 10µg in the second, the blot intensity volume was higher in the first lane. Theoretically, the α-CPY antibody should have been able to immunoprecipitate the Y10000 (WT) strain but result in no detection and thus no bands for the Y10885 (prc1Δ) strain. However, in practice, there were no bands present for any of the IP concentrations of the Y10000 strain of CPY, as the antibody couldn't immunoprecipitate CPY (defect). For this film, with 50µg of input, 10µg of input & 10µg of supernatant, three blots were present. However, I believed it was unnecessary to quantify these blots as the critical IP blots were absent. All three blots were detected at ~59kDa, and as stated prior, correlates with the m-CPY present in the vacuole.

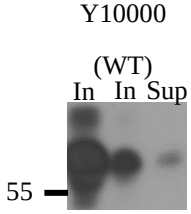

Figure 42: *Western blot data for the IP of CPY. Although blots are present for the Input (50 & 10µg respectively) and Supernatant (10 µg), no bands are present for the IP. WT is detected, whilst mutant type is undetected. Insufficient data to draw any quantitative conclusion on the IP of CPY.*

The results from this experiment are inconclusive to demonstrate that the α-CPY antibody can immunoprecipitate CPY. Analysis of the western blot films failed to produce a signal for CPY at any IP concentration, and thus an alternative methodology would be required.

*8.4 Optimisation of Cu^{2+} induction of expression of CPY**

The purpose of this last experiment was to understand the overexpression of CPY*. As the Cu^{2+}-CUP1 promoter is lethal to expression of CPY*, the CUP1 promoter was substituted by the GAL1,10 promoter, being far more tolerable to CPY* expression levels. Once these new

plasmids were available, they could then be transformed into mutant (Y10885) cells, the proteins extracted, and expression levels monitored in a western blot over the course of ~4 h. This would entail induction of Cu^{2+} ions into the mutant cells, at increasing concentrations across differing time intervals, to ascertain the optimal conditions for CPY* expression.

The results from this final experiment in trying to understand the decay kinetics of CPY* were once again present through quantification of data from western blot films. The purpose was to find induction conditions that produce high levels of CPY*. As there were three different strains, which were tested across five different Cu^{2+} concentrations at four different time intervals, including an untreated sample, data from nine membranes were present per western blot film. The first set of films utilised the α-CPY (primary) antibody and the α-Mouse IgG (H+L peroxidase) (secondary) antibody in a 1:10,000, 1:100,000 dilution respectively, with ECL2. Unlike previous types of experiments, all blots were present for all three strains at all the different Cu^{2+} concentrations and at all the different time intervals. However, theory suggests that degradation of CPY* occurs predominantly in the ER and the p1-CPY* form is converted neither to p2-CPY* nor to m-CPY*. Thus, all blots were present at a molecular weight of ~67-69kDa which correlated well with the predicted molecular weight of p1-CPY* (67kDa). However, for blots present at all different time intervals at 1mM Cu^{2+} concentration only, additional bands were present at ~59kDa which correlates with the m-CPY*. This strange phenomenon may be caused by the excessively high Cu^{2+} concentration of 1mM. Thus, contrary to degradation, CPY*, at a specific Cu^{2+} concentration, may transit across the secretory pathway until it reaches the vacuole at a molecular weight of 59kDa.

Due to the difficulty of obtaining accurate and quantifiable data from western blot films, the first set of experiments yielded quantifiable results for only the 1st strain (pRS423 (-His) (Control)). For this film, at 10μg of total CPY* protein loaded, blots were present at all five Cu^{2+} concentrations and at all four time intervals. For the 1mM Cu^{2+} concentration, blots were present for both the precursor (p1/p2) and mature forms of CPY*. Both ECL2 & Luminol, as viable chemiluminescent reagents, were used to detect degradation kinetics of CPY*.

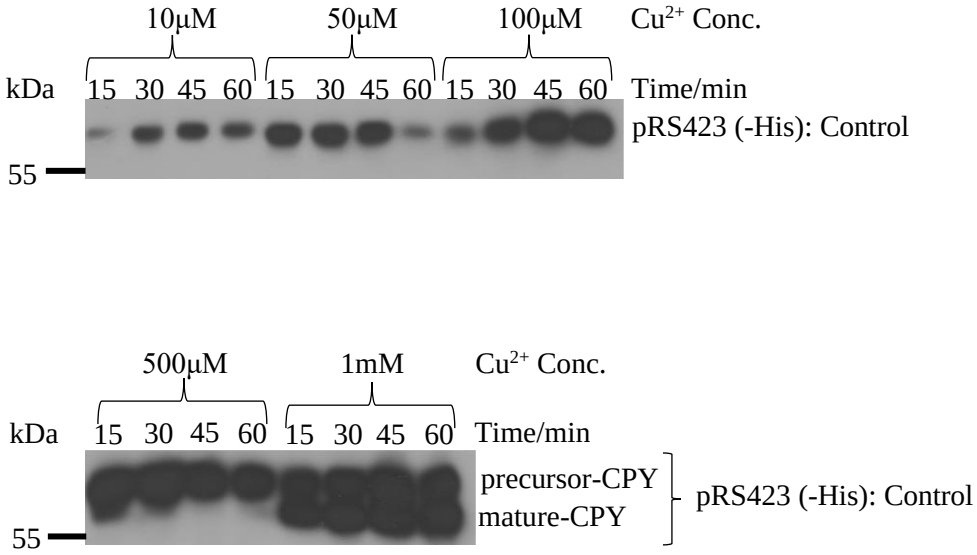

Figure 43: *Western blot data for α-CPY (1:10,000, 1:100,000) with ECL2. Blots are present for the 1st strain at five different Cu^{2+} concentrations and four different time intervals. Further, both the precursor and mature forms of CPY are present at 1mM Cu^{2+} concentration.*

Table 17. Western blot data, with calculated ratios, for α-CPY with ECL2 across a Cu^{2+} induction experiment for the 1st strain.

Cu^{2+} Conc. [µM]	**Time [min]**	**Volume α-CPY**	**Ratio**
		ECL2	**ECL2**
10	15	42400	0.01
10	30	130000	0.0317
10	45	141000	0.0231
10	60	123000	0.0550
50	15	226000	0.0915
50	30	239000	0.0234
50	45	237000	0.0287
50	60	93700	0.0280
100	15	160000	0.0244
100	30	307000	0.0426
100	45	409000	0.0370
100	60	359000	0.0511
500	15	612000	0.0259
500	30	631000	0.0343
500	45	535000	0.0793
500	60	521000	0.0788
1000	15 (p-CPY)	367000	0.0555
1000	15 (m-CPY)	358000	0.0541
1000	30 (p-CPY)	522000	0.183
1000	30 (m-CPY)	282000	0.0989
1000	45 (p-CPY)	292000	0.120
1000	45 (m-CPY)	508000	0.209
1000	60 (p-CPY)	318000	0.302
1000	60 (m-CPY)	503000	0.478

Graph 2. Plotted results across the 1st strain using ECL2.

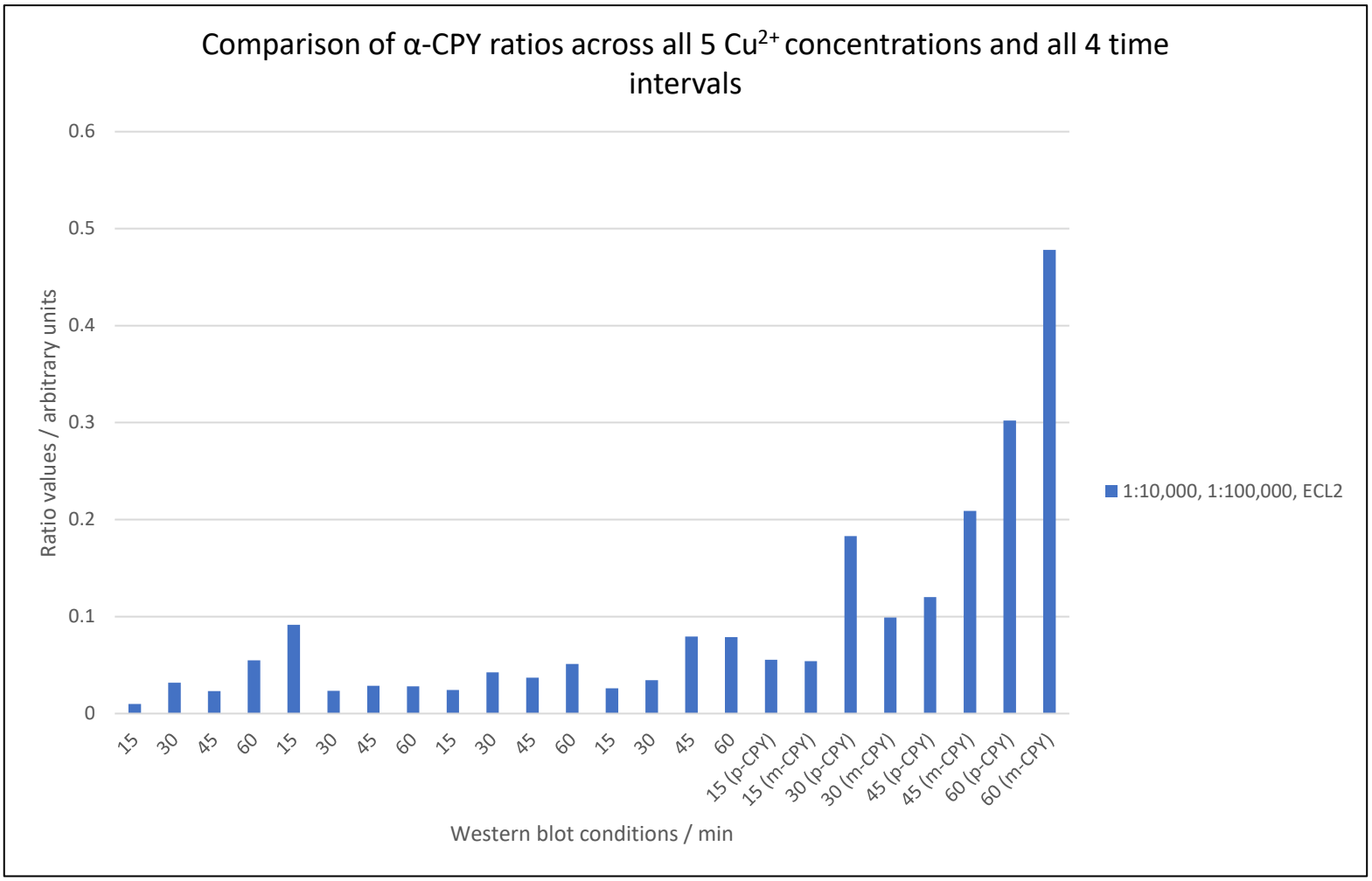

Now turning to Luminol with identical antibody dilutions:

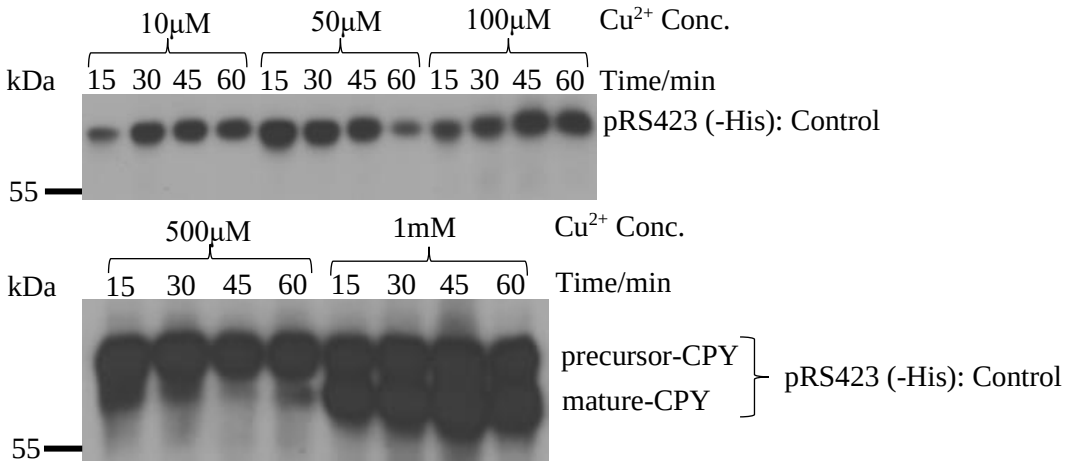

Figure 44: *Western blot data for α-CPY (1:10,000, 1:100,000) with Luminol. Blots are present for the 1st strain at five different Cu^{2+} concentrations and four different time intervals. Further, both the precursor and mature forms of CPY are present at 1mM Cu^{2+} concentration.*

Table 18. Western blot data, with calculated ratios, for α-CPY with Luminol across a Cu^{2+} induction experiment for the 1st strain.

Cu^{2+} Conc. [µM]	**Time [min]**	**Volume α-CPY Luminol**	**Ratio Luminol**
10	15	120000	0.01
10	30	230000	0.0198
10	45	230000	0.0133
10	60	217000	0.0342
50	15	332000	0.0475
50	30	289000	0.00998
50	45	251000	0.0107
50	60	127000	0.0134
100	15	203000	0.0110
100	30	245000	0.0120
100	45	318000	0.0101
100	60	288000	0.0145
500	15	713000	0.0106
500	30	647000	0.0124
500	45	536000	0.0280
500	60	635000	0.0339
1000	15 (p-CPY)	364000	0.0194
1000	15 (m-CPY)	491000	0.0261
1000	30 (p-CPY)	556000	0.0687
1000	30 (m-CPY)	374000	0.0462
1000	45 (p-CPY)	607000	0.0880
1000	45 (m-CPY)	501000	0.0726
1000	60 (p-CPY)	291000	0.0975
1000	60 (m-CPY)	567000	0.190

Graph 3. Plotted results across the 1st strain using Luminol.

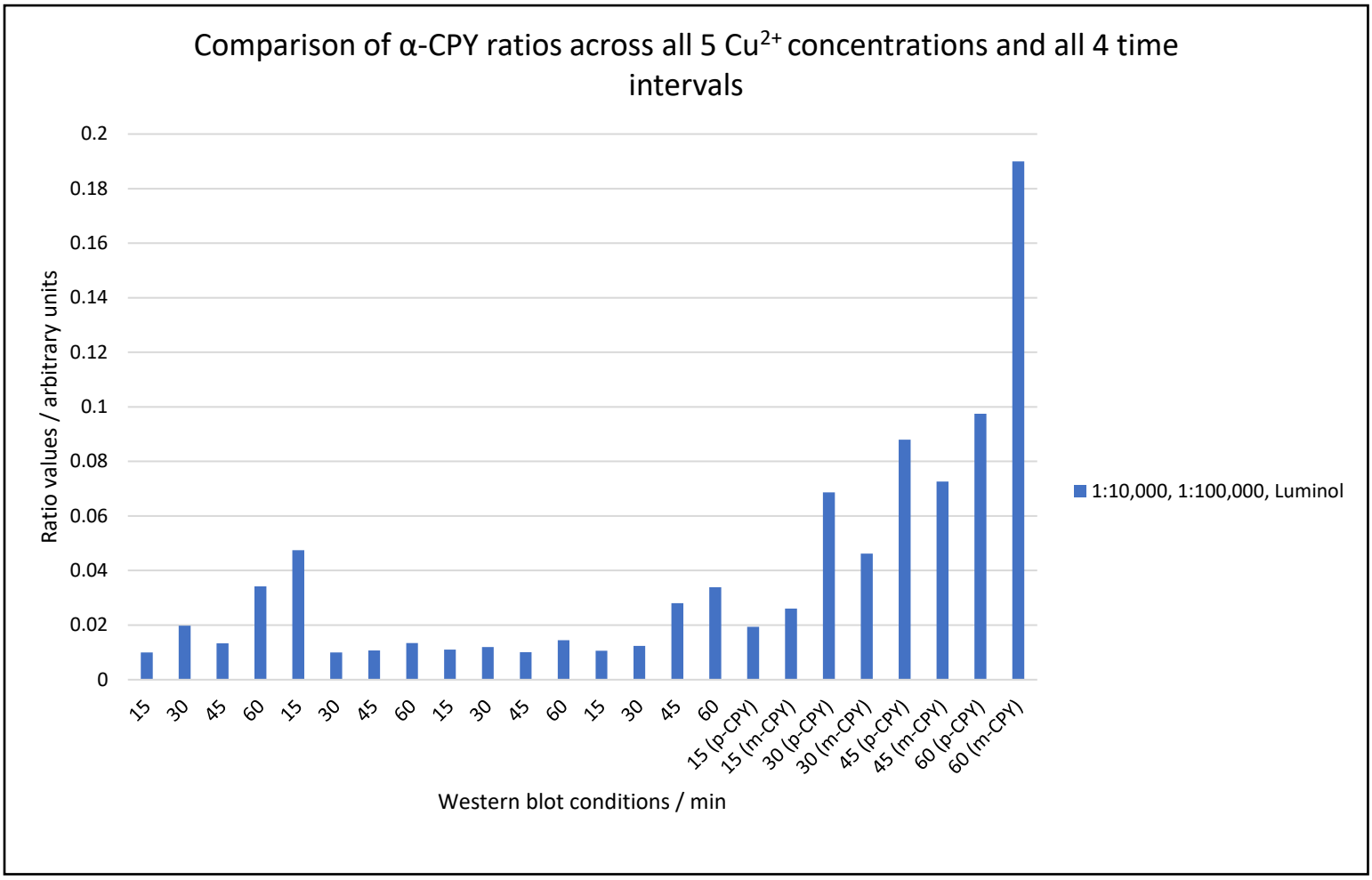

It was necessary to utilise a loading control, namely β-actin, to ensure a complete comparison of blot intensity for the different time intervals at different Cu^{2+} concentrations. The same theory, as with the other blots from the first set of experiments for the control strain, held. However, the β-actin was the substitute for the α-CPY, and thus acted as the primary antibody in these blots. The experiment was repeated with different antibody dilutions, such that there was a lower dilution of both β-actin and α-Mouse IgG to 1:1,000, 1:2,000 respectively. All blots for the β-actin were present across all five Cu^{2+} concentrations at all four time intervals for the control strain, present at ~43kDa, which confirmed well with theory. Further, both the mature and precursor forms of CPY were also present at the 1mM Cu^{2+} concentration. The luminol chemiluminescent reagent was used in all β-actin western blot experiments, as usual.

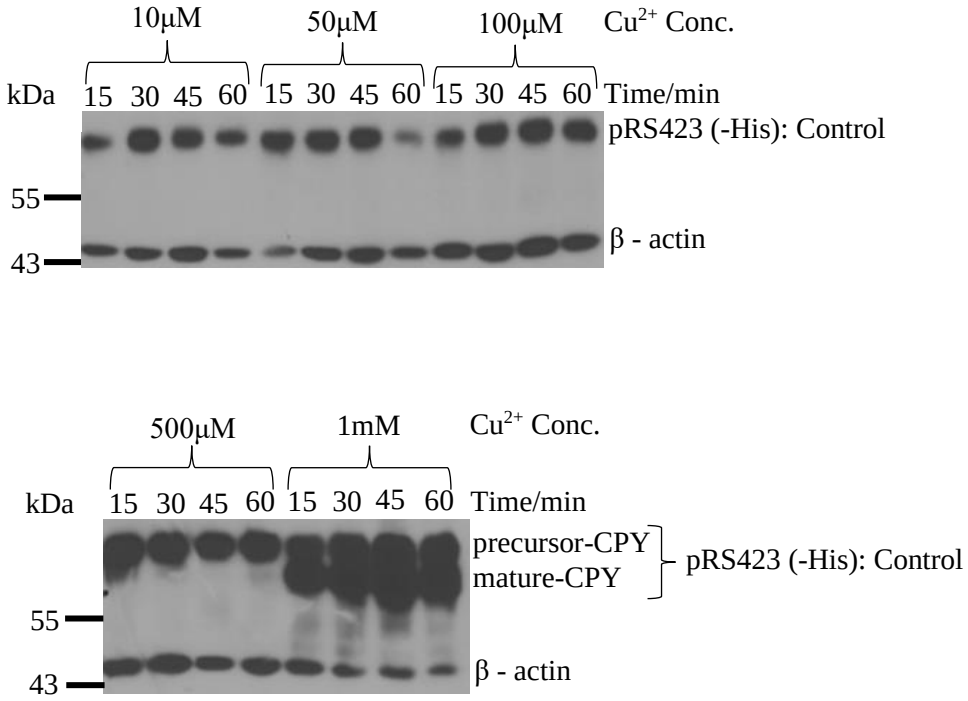

Figure 45: *Western blot data for β-actin (1:1,000, 1:2,000) with Luminol. Blots are present for the 1st strain at five different Cu^{2+} concentrations and four different time intervals. Both the precursor and mature forms of CPY are present at 1mM Cu^{2+} conc.*

Once these results had been quantified, it was necessary to calculate the relevant ratio values of each experiment. The ratio values were calculated from the division of the blot intensity volume of α-CPY to the blot intensity volume of β-actin, for both ECL2 & luminol. Each respective relative ratio was then calculated from the division of each ratio value to a standard ratio value. All relative ratios were calculated for α-CPY (ECL2)/β-actin for 1:10,000, 1:100,000 and for α-CPY (luminol)/β-actin for 1:10,000, 1:100,000.

The second set of results yielded quantifiable results for the 2nd strain (pRS423–$P_{GAL1,\ 10}$ – DCR2– HA (-His)). For this second experiment, for 10µg of total CPY* protein loaded, blots were present at all five Cu^{2+} concentrations and at all four time intervals. For the 1mM Cu^{2+} concentration, blots were present for both the precursor (p1/p2) and mature forms of CPY*.

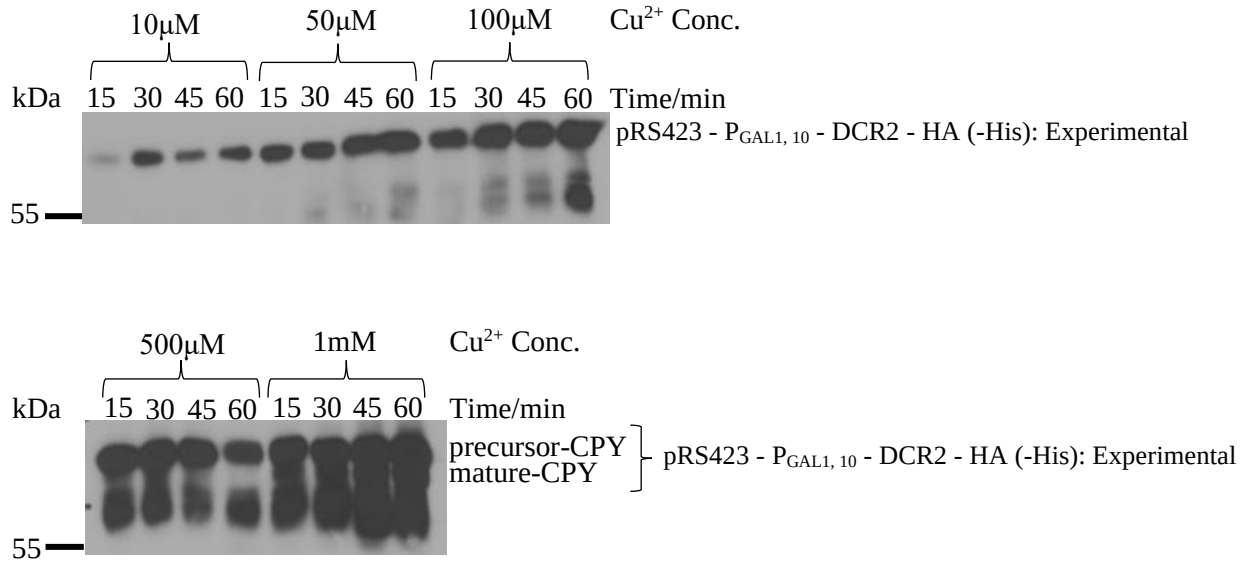

Figure 46: *Western blot data for α-CPY (1:10,000, 1:100,000) with ECL2. Blots are present for the 2nd strain at five different Cu^{2+} concentrations and four different time intervals. Further, both the precursor and mature forms of CPY are present at 1mM Cu^{2+} concentration.*

Table 19. Western blot data, with calculated ratios, for α-CPY with ECL2 of a Cu^{2+} induction experiment for the 2nd strain.

Cu^{2+} Conc. [µM]	Time [min]	Volume α-CPY ECL2	Ratio ECL2
0	0	11600	0.01
10	15	26100	0.0296
10	30	113000	0.112
10	45	69700	0.0929
10	60	102000	0.123
50	15	134000	0.187
50	30	143000	0.134
50	45	186000	0.161
50	60	212000	0.202
100	15	172000	0.205
100	30	247000	0.287
100	45	255000	0.242
100	60	285000	0.501
500	15	322000	0.440
500	30	348000	7.25
500	45	317000	3.88
500	60	232000	0.378
1000	15 (p-CPY)	269000	0.465
1000	15 (m-CPY)	103000	0.177
1000	30 (p-CPY)	251000	2.02
1000	30 (m-CPY)	146000	1.17
1000	45 (p-CPY)	317000	6.21
1000	45 (m-CPY)	95800	1.88
1000	60 (p-CPY)	405000	2.76
1000	60 (m-CPY)	145000	0.987

Graph 4. Plotted results across the 2nd strain using ECL2.

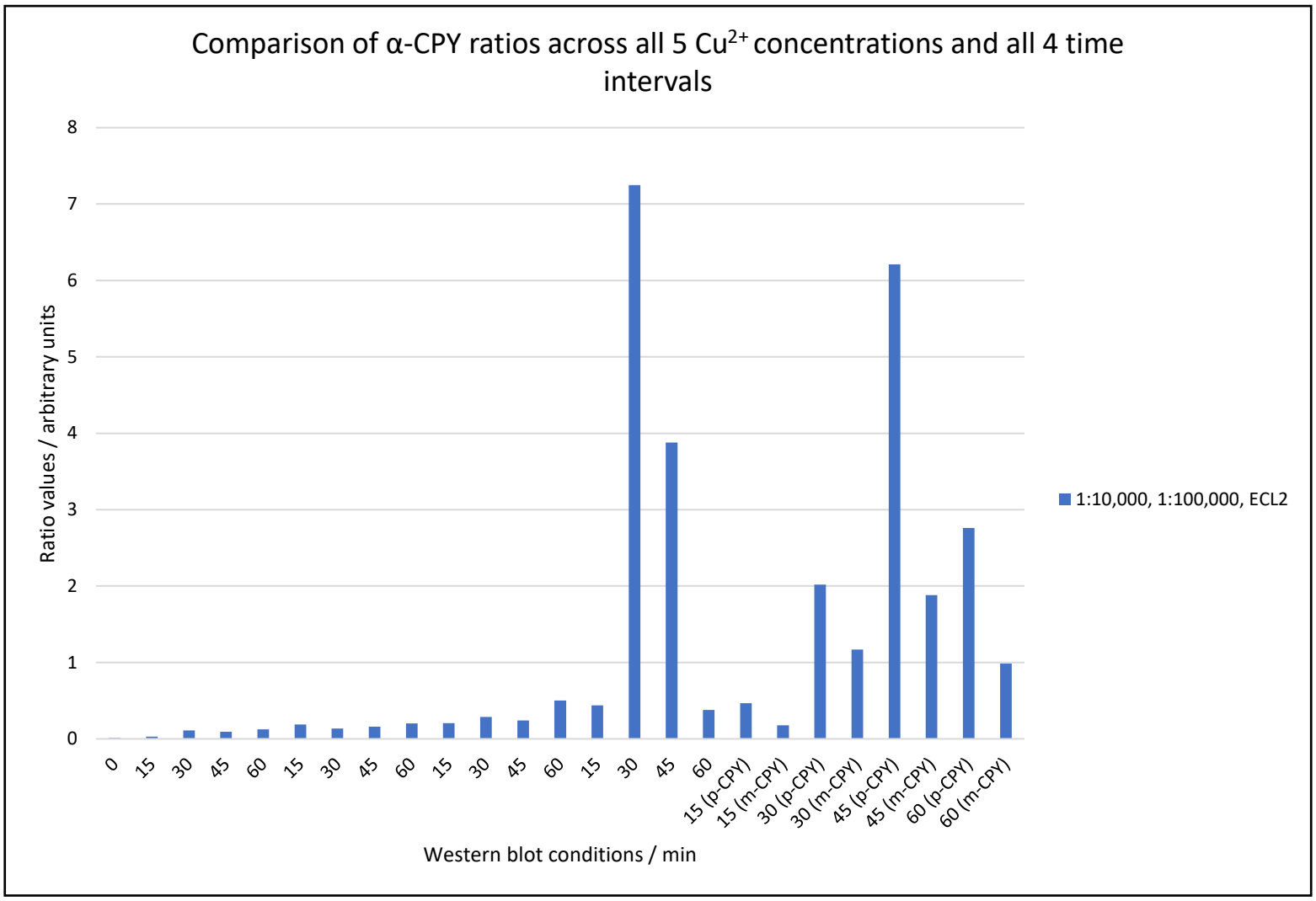

The luminol chemiluminescent reagent was used in all β-actin western blot experiments, as usual.

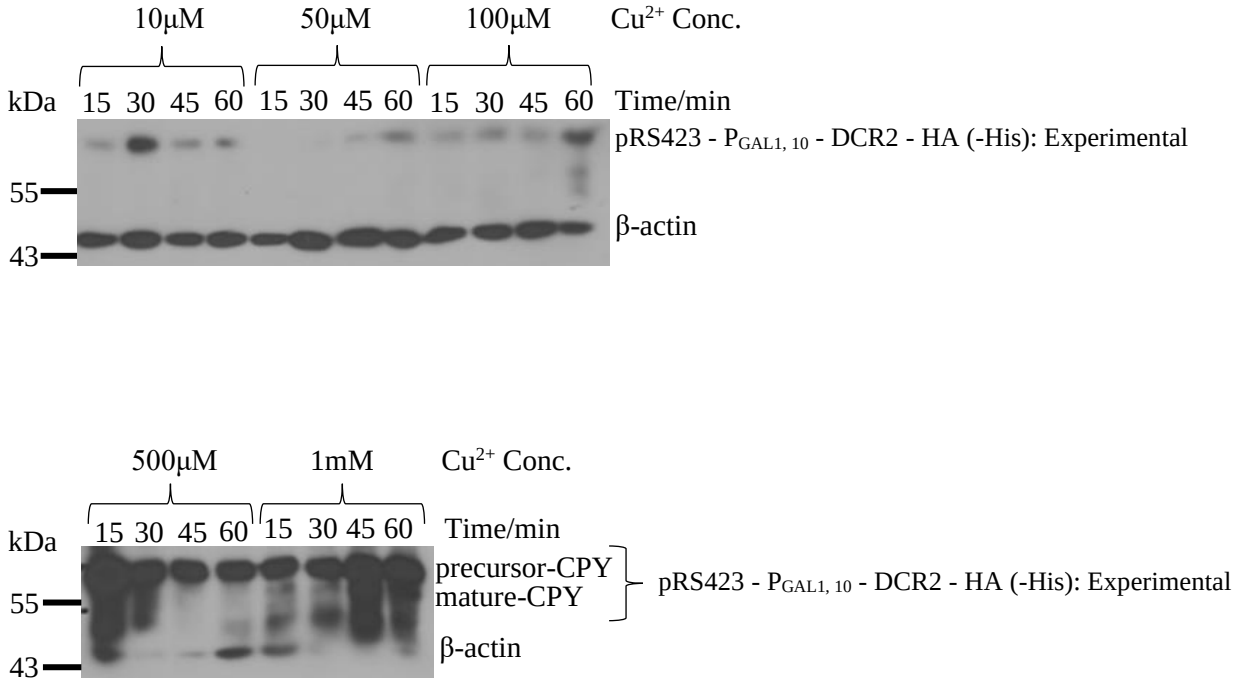

Figure 47: *Western blot data for β-actin (1:1,000, 1:2,000) with Luminol. Blots are present for the 2nd strain at five different Cu^{2+} concentrations and four different time intervals. Further, both the precursor and mature forms of CPY are present at 1mM Cu^{2+} conc.*

The final set of results yielded quantifiable results for the 3rd strain (pRS423–$P_{GAL1,\ 10}$ – H338A-DCR2– HA (-His)). With this film, for 10µg of total CPY* protein loaded, blots were present at all five Cu^{2+} concentrations and at all four time intervals. For the 1mM Cu^{2+} concentration, blots were present for both the precursor (p1/p2) and mature forms of CPY*

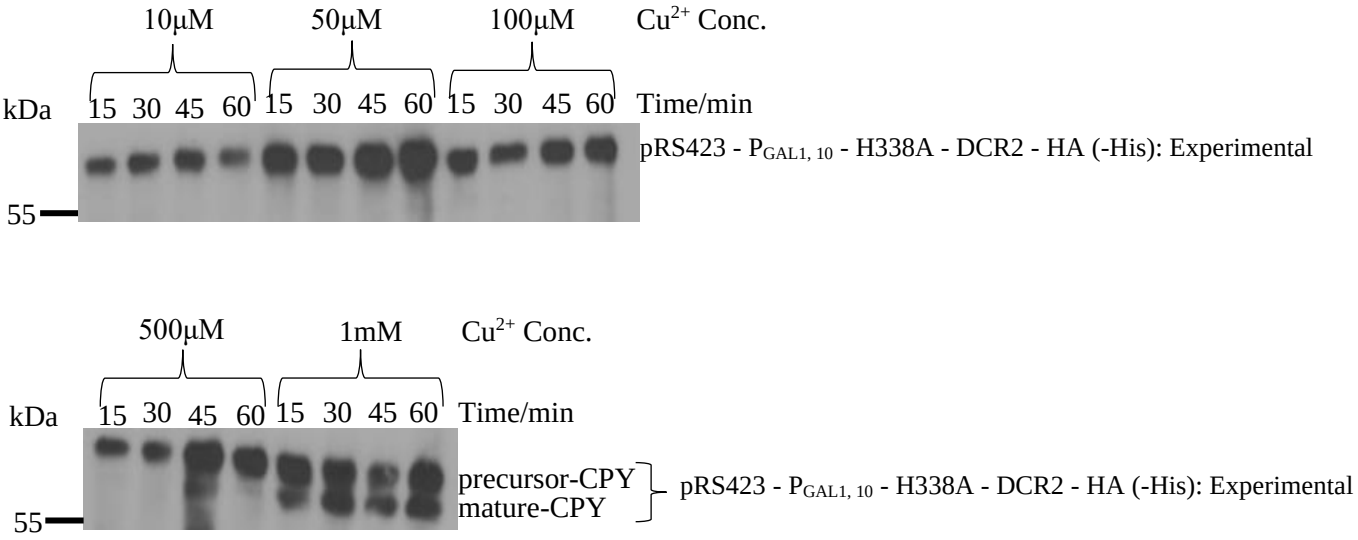

Figure 48: *Western blot data for α-CPY (1:10,000, 1:100,000) with ECL2. Blots are present for the 3rd strain at five different Cu^{2+} concentrations and four different time intervals. Further, both the precursor and mature forms of CPY are present at 1mM Cu^{2+} concentration.*

Table 20. Western blot data, with calculated ratios for α-CPY with ECL2 of a Cu^{2+} induction experiment for the 3rd strain.

Cu^{2+} Conc. [µM]	Time [min]	Volume α-CPY ECL2	Ratio ECL2
10	15	91800	0.01
10	30	115000	0.0604
10	45	127000	0.174
10	60	96300	0.332
50	15	220000	0.0260
50	30	210000	0.0126
50	45	280000	0.0150
50	60	333000	0.0131
100	15	157000	0.00953
100	30	129000	0.00856
100	45	151000	0.00826
100	60	161000	0.00903
500	15	113000	0.00324
500	30	114000	0.00361
500	45	252000	0.00327
500	60	217000	0.00727
1000	15 (p-CPY)	210000	0.00451
1000	15 (m-CPY)	98700	0.00213
1000	30 (p-CPY)	174000	0.00235
1000	30 (m-CPY)	163000	0.00220
1000	45 (p-CPY)	125000	0.00336
1000	45 (m-CPY)	115000	0.00307
1000	60 (p-CPY)	206000	0.00429
1000	60 (m-CPY)	160000	0.00335

Graph 5. Plotted results across the 3rd strain using ECL2.

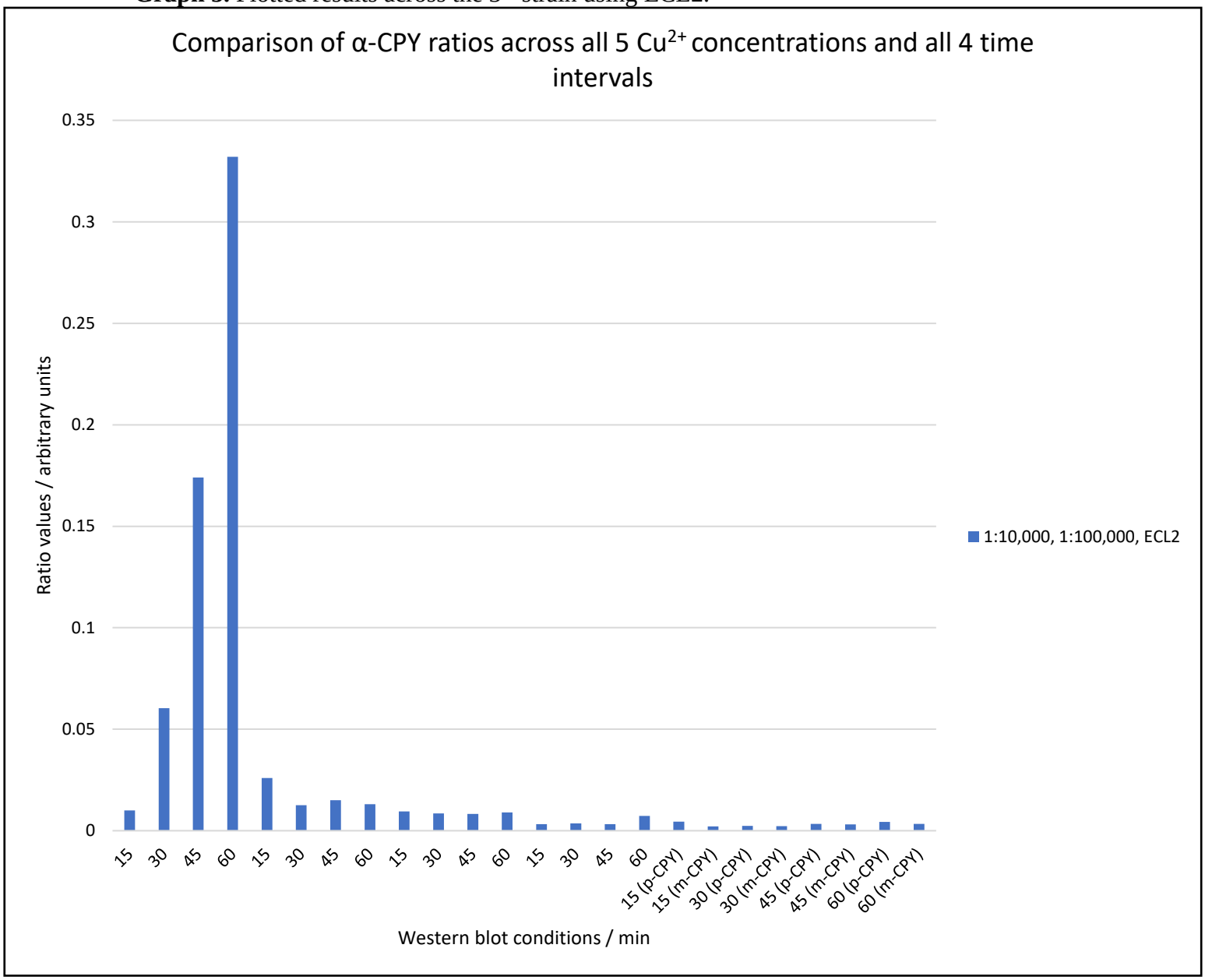

The luminol chemiluminescent reagent was used in all β-actin western blot experiments, as usual.

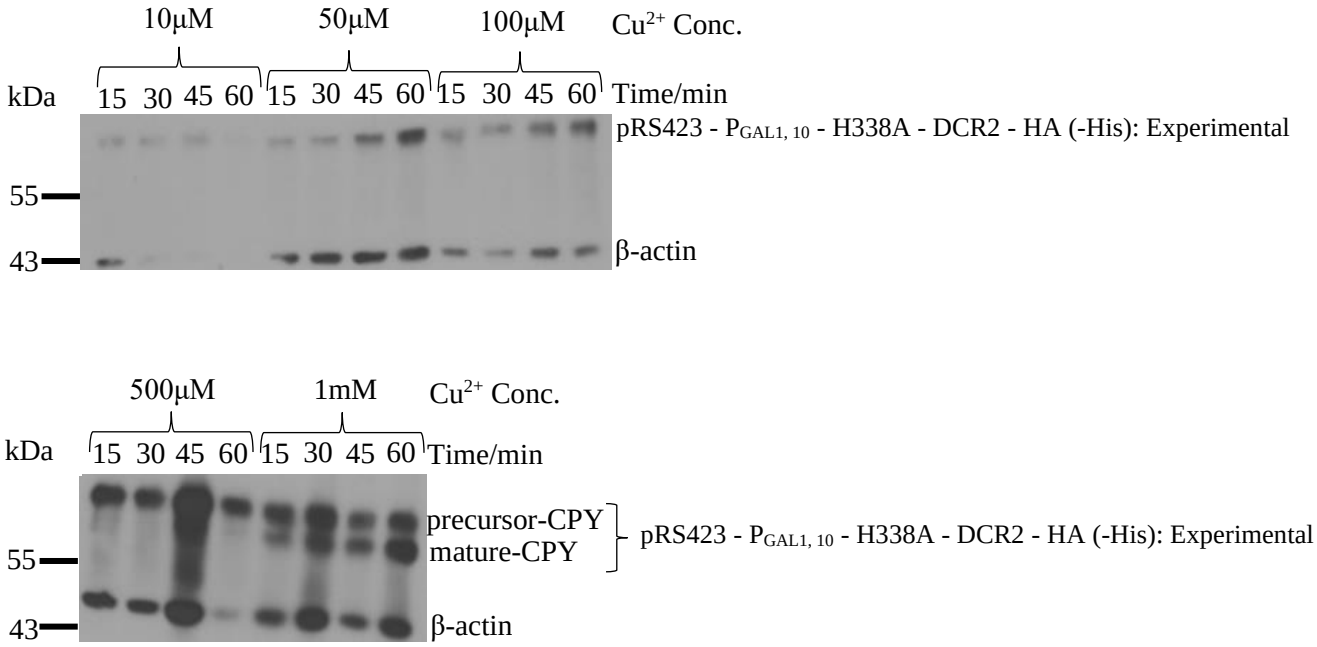

Figure 49: *Western blot data for β-actin (1:1,000, 1:2,000) with Luminol. Blots are present for the 3rd strain at five different Cu^{2+} concentrations and four different time intervals. Further, both the precursor and mature forms of CPY are present at 1mM Cu^{2+} concentration.*

The results from this last experiment show that for the 2nd and 3rd strain at a Cu^{2+} concentration of 1mM, the precursor form (p1) of CPY* has a greater band intensity than the mature form, leading to the idea that DCR2 has the potential for reducing the CPY* transport across the secretory pathway, leading to accumulation of p1-CPY* in the ER, and thus requiring the use of ERAD to remove excess proteins. This agrees well with the role of DCR2 as a dephosphorylating agent, affecting the degradation kinetics of CPY*.

9.0 Discussion

9.1 Detection of CPY

This experiment, shown in Fig. 35, produced quantifiable, accurate results which conclusively demonstrated the presence of bands for CPY and absence of bands for CPY*, thus the Y10000 (WT) strain was detected whilst the Y10885 (prc1Δ) strain was undetected. The results from my initial experiment indicate that 15μg of protein lysate is a sufficient volume for detection of CPY by the α-CPY antibody. Also, the initial band for the Y10000 was found at ~59kDa which proved that the CPY, once synthesised in the ribosome, was expressed in the ER. At the ER, it would have had a higher molecular weight of ~67kDa, but once trafficked through the Golgi to the vacuole, the pro-sequence would have been cleaved and thus the molecular weight would have reduced to ~59kDa, as can be seen from the western blot. This predicts the conversion of the precursor form of CPY to the mature form of CPY, as there is a reduction in molecular weight. These experiments confirm my initial hypothesis that CPY can be synthesised and trafficked across the secretory pathway of the *S. cerevisiae* yeast species. Further, this also confirms my initial hypothesis, that although CPY* is synthesised within the ribosome, it is not trafficked across the secretory pathway. My research indicates the localisation of different forms of CPY at different points along the secretory pathway and can thus be used for comparison with the maturation rates of other proteases present in the ER of *S. Cerevisiae*. This experiment was only repeated once, and fortunately confirmed my hypothesis which was evident from the initial test. The only experimental modification for this repeat experiment was to test the effect of different extraction buffers on CPY expression levels.

Table 21. Composition of all buffers used in the detection of CPY.

Buffer number	Buffer composition
1	50mM Tris·HCl (pH 7.5 at 4^{o}C), 6mM EDTA, 2.5% (w/v) SDS, 8M Urea
2	50mM Tris·HCl (pH 7.5 at 4^{o}C), 1mM EDTA, 1.0% (w/v) SDS, 6M Urea
3	50mM Tris·HCl (pH 7.5 at 4^{o}C), 1mM EDTA, 1.0% (w/v) SDS
4	10mM Tris·HCl (pH 8.0 at 4^{o}C), 1mM EDTA, 1.0% (w/v) SDS

The results from the ratios of α-CPY to β-actin in the Y10000 (WT) strain across all four extraction buffers reveals that the optimal buffer to use is buffer 3. The average highest ratio, across all film exposure times for this buffer, was higher than for the other three buffers,

presumably due to chemical composition and its effect on ensuring a high protein lysate concentration and subsequently a high solubilisation of CPY. Buffer 3 is distinct from the other buffers in composition. I believe that the 50mM Tris·HCl concentration, and the pH at which this compound was buffered (pH 7.5), bears an impact on the effect of this buffer, as the 4th buffer which contains a lower concentration of Tris·HCl at 10mM, has a significantly smaller ratio than with the other 3 buffers. Further, as the SDS concentration is identical for buffers 2,3 & 4, but higher for the 1st buffer, this implies that 2.5% (w/v) SDS concentration for buffer 1 is too high and may lead to increased protein denaturation, thus at a lower ratio compared with other buffers. The same holds for the EDTA concentration, where buffer 1 has a higher concentration at 6mM compared with 1mM for all other buffers. However, the limiting factor in this may be due to the presence of Urea. Urea can denature proteins. Whilst buffers 3 and 4 contain no urea, buffer 1 has 8M urea & buffer 2 has 6M urea. Both the 8M & 6M urea concentration may be too high and result in denaturation of the CPY protein. The absence of urea in buffer 3 may be optimal to ensure limited protein denaturation, and thus be the optimal buffer.

An additional factor which may contribute to the CPY expression level is the calculation and subsequent choice of the OD_{600} value utilised in the CPY protein extraction step. Repeated experiments of the inoculation of both Y10000 (WT) & Y10885 (prc1Δ) with YPD media have shown that the doubling time of the *S. cerevisiae* yeast species was optimised at 1.5 h. To ensure that the optimal OD_{600}, found during the exponential growth phase of the typical yeast cell cycle between ~0.3-0.8 OD_{600}, was reached, I decided to limit the value of the minimum inoculum to 0.02. This enabled a feasible incubation period of between 6.5-7 hours. All the OD_{600} values fell within the optimal range and thus were all valid to have produced accurate and quantifiable ratio results. However, if I were to further optimise this method, I would allow a greater incubation time for the OD_{600} to reach between 0.6-0.7. At this OD_{600}, a higher cell number for both Y10000 & Y10885 would be present, potentially resulting in a higher protein volume per strain. Additionally, the protein concentration measurement with BCA assay could be improved with a longer incubation period of diluted protein lysate sample with 0.1 M 2-iodoacetamide in 0.1M Tris·HCl (pH 8.0). β-mercaptoethanol, present in all extraction buffers at a concentration of 5mM, can reduce disulphide bonds present within the quaternary structure of a protein, and thus cause protein denaturation. However, I firstly set the incubation time of the 1:10 diluted protein lysate sample to be 15 min at 37ºC. I then repeated this step and set the incubation time to be 30

min. An additional portion of time led to a lower protein concentration measurement for both Y10000 & Y10885, implying that a greater incubation time causes more removal of β-mercaptoethanol, and thus leads to lower protein concentrations. If I had additional time, I would repeat this step at a series of different incubation times and test whether there is a positive correlation between increasing incubation time and decreasing protein concentration. Further, as a total of 50μg of protein lysate per strain per extraction buffer was loaded onto the SDS-PAGE gel, all conditions for this were standardised.

During the pre-loading steps in the SDS-PAGE experiment, I utilised a heat block set at 100^{o}C for all experiments. Once I had added the protein lysate samples to appropriate volumes of both deionised H_2O & 6 x SDS-PAGE sample buffer, all samples were boiled at 100^{o}C to ensure complete protein denaturation. If I were permitted additional time, I would repeat this step in the experiment with a range of different temperatures from ~60^{o}C - ~120^{o}C, to test whether the blot intensity volume, and thus CPY expression level, would be affected by this temperature step. Both the semi-dry electrotransfer and most of the western blot methodology to create the quantifiable results is standard. However, due to overdeveloped and strong blot intensity volumes for the α-CPY with ECL2, I repeated the experiment with a greater dilution of the primary and secondary antibodies. Instead of 1:1,000 & 1:20,000 dilution for the primary and secondary antibodies respectively, I redeveloped with 1:5,000 & 1:50,000 dilution respectively. This yielded ~100-fold reduction in blot intensity volume, and thus could be more easily quantified as the image blots were clearer and more distinct. As predicted, the original antibody dilution with luminol yielded ~10-fold reduction in blot intensity volume due to the weaker chemiluminescent effect of luminol over ECL2. The second choice of antibody dilutions resulted in ratios which were more easily comparable across the different strain types and extraction buffers.

Finally, in accordance with the calculated ratios across all 4 extraction buffers, and all 3 western blot experiments, the presence of a single band at ~59kDa instils confidence that the CPY is indeed detectable.

9.2 Immunoprecipitation of CPY

Although this experiment had the potential to produce quantifiable, accurate results for the presence of IP bands for CPY, at varying concentrations, the western blot yielded bands for only the presence of the input (50 & 10µg) and supernatant (10µg) of CPY. I have deduced that a potential cause of this may be due to a defect present in the 'Abcam' antibody. If I had additional time, I would have repeated this experiment with the 'ThermoFisher' antibody, being identical in composition and role, to test whether the IP of CPY bands could be detected. Fortunately, though, the Y10000 (WT) strain was detected whilst the Y10885 (prc1Δ) strain was undetected, confirming my initial hypothesis that CPY is trafficked across the secretory pathway to the vacuole and detected. The results from my first set of western blots for this experiment utilised 50µg of protein lysate for both the input and supernatant initially. This protein lysate volume, which was utilised in the IP of CPY with the α-CPY antibody, was found to be too high and thus the experiment was repeated with a lower protein lysate volume of 10µg. With ECL2, both blots were found to be very intense and thus hard to quantify in their present form. However, m-CPY was found to be present at ~59kDa. Once again, this confirms my initial hypothesis that the newly synthesised CPY is trafficked across the cell pathway until it reaches the vacuole at a molecular weight of 59kDa, post modification. This experiment was repeated multiple times, to gauge whether the α-CPY (Abcam) was able to immunoprecipitate CPY, and thus produce strong, intense bands for the different concentrations of the IP of CPY. However, after much modification, the reality that the 'Abcam' company provided the lab with a defect present in this antibody, was made apparent. Unfortunately, due to limited time, I was unable to test whether the identical antibody from 'ThermoFisher' would be able to immunoprecipitate CPY, and thus result in strong, quantitative bands. Thus, I repeated the experiment a final time with 50µg of protein lysate for the input and 10µg of protein lysate for the supernatant, with an additional lane for 10µg of input, to test the difference in blot intensity volume across the different lanes. Unfortunately, the repeat experiment yielded virtually the same result as for the initial test, but with an additional band for lane 2, which contained 10µg of protein lysate for the input. Sadly, I was unable to acquire sufficient results from this experiment, but still repeated this experiment with slight experimental modifications.

Firstly, the 50mM Tris·HCl (pH 7.5 at 4^{o}C), 1mM EDTA, 0.04% (w/v) SDS extraction buffer was utilised in all IP experiments, as this was found to be the optimum buffer of choice from the CPY detection experiment. The ideal volume of protein lysate required for IP experiments

was ~1mg total protein/IP, therefore it was necessary to procure an optimal OD_{600} value for the cell cultures of both Y10000 (WT) & Y10885 (prc1Δ) strains. After a series of repeats of the inoculation of both Y10000 & Y10885 with YPD media, the optimised doubling time was found to be 1.5 h. To reach the desired optimal OD_{600} value, it was necessary to utilise a feasible and realistic minimum starting OD_{600}, in this case, 0.02. By calculation, the optimal incubation time was found to be 6-6.5 h to reach ~0.65 OD_{600} value. The reason I chose to have four samples per strain, was to maximise the chance of reaching a high OD_{600} value for each strain. With additional time, I would certainly repeat the inoculation step with a longer incubation time to test whether each OD_{600} value could be increased by a single unit, and thus approach ~0.8 OD_{600}. The purpose of ensuring a high OD_{600} value, would be to attain a high cell count, leading to potentially stronger signals which could be accurately quantified from the western blot results. The sample optimisation methods, during protein extraction and protein assay concentration as for the CPY detection, was also utilised in this IP experiment.

Due to the chemical composition of the modified extraction buffer, the concentration of both SDS (1% (w/v)) & β-mercaptoethanol (5mM) were simply too high. The former could denature the antibody, whilst the latter could reduce disulphide bonds and inactivate the antibody. Thus, it was necessary to dilute this extraction buffer with a different buffer: 50 mM Tris·HCl (pH 7.5 at 4^{o}C), 10mM EDTA (pH 8.0), 0.5% (w/v) sodium deoxycholate, 0.1% (w/v) Triton-X 100 (ice-cold). The effect of this buffer on the protein lysates would be to dilute the β-mercaptoethanol concentration. This would avert the negative effect of the high concentration of β-mercaptoethanol on the IgG_1 antibody. To test which dilution factor would be the optimal, I utilised three protein lysate samples per strain at different volumes of 2.5ml, 15ml & 50ml. Further, the appropriate volume of 10g/l SDS would need to have been added to dilute the extraction buffer from 1% (w/v) SDS to 0.1% (w/v) SDS, thus preventing the SDS from affecting the IP of CPY. However, from comparison of the band intensity of western blots from these three diluted protein lysate samples per strain, only the 2.5ml sample produced accurate, quantifiable blots, whilst the other volumes resulted in an absence of bands. A reason for absent bands may have been due to the presence of impurities within the diluted protein lysates which are more likely to occur in larger volumes, such as 15ml or 50ml samples. Due to this phenomenon, I decided to repeat the experiment with only the 2.5ml sample, for both Y10000 & Y10885 strains.

As the different IP concentrations of CPY were unable to be detected, ratios could not be ascertained, and thus the experiment failed to provide meaningful data/insight.

*9.3 Optimisation of Cu^{2+} induction of expression of CPY**

The fundamental purpose of this final experiment was to ascertain whether overexpression of DCR2 plays a role in ER-induced stress, by affecting CPY* degradation. Essentially, the western blot data was used to establish induction conditions that would deliver high levels of CPY* to record the decay curves.

The first strain, which acted as the control, had a complete profile of western blot films for the anti-CPY & anti-mouse IgG (H+L) peroxidase antibodies across a range of dilutions. A single band at ~69kDa was present at each time interval and Cu^{2+} concentration from 10μM – 1mM, suggesting that there is a precursor form of CPY*, possibly p1-CPY*. However, as was evident at only 1mM Cu^{2+} concentration, an additional band was present at each time interval at ~59kDa, which may represent a processed form of CPY*. The presence of this additional band suggests that high expression levels of CPY* can overwhelm the quality control mechanisms in the ER that prevent exit of misfolded proteins from the ER.

Ideally if I had additional time, I would repeat the experiment with incremental Cu^{2+} concentrations from 500μM to 1mM, to discover at which precise concentration the quality control mechanisms in the ER are overwhelmed. This would shed light on the exact Cu^{2+} concentration where the precursor CPY* expression level is at its highest. Fortunately, though, the ratios from the blots were able to be calculated. According to the western blot films, the ratio value, on average, is < 0.05 for most blots from 10μM to 500μM but is > 0.05 for almost all blots at 1mM. Therefore, the observed additional blots are a result of conversion of the precursor CPY* to the mature CPY*.

The second strain, which possessed the DCR2 phosphatase (catalytically active protein), also resulted in a full set of western blot films. However, for the 1 s film exposure time, no additional bands were present at 1mM Cu^{2+} concentration, and thus only the precursor CPY* form was evident. Further, for the 15 s and 1 minute film exposure times, all bands were present at 1mM for the mature CPY*, and thus the 1s film may have led to an anomalous result. An explanation could be that the 1 s film exposure time may have been too short to detect the mature CPY* form. The western blot data is somewhat different to the previous strain. Whilst for the 1s film exposure time the ratio value is < 0.05 for all results from 10μM - 100μM but > 0.05 for all results from 500μM – 1mM, showing similarity to the control strain, the 15 s and 1 min film exposure times reveal a ratio value of > 0.05 for virtually all data points.

After having repeated the western blot experiment for the 2nd strain multiple times, it was difficult to ascertain the true CPY* blot intensity. DCR2 acts as a dephosphorylating agent, by affecting the transport of proteins from the ER to the Golgi, and thus can affect the precursor CPY* expression levels.

The third strain, which possessed the H338A-DCR2 (catalytically inactive protein), also resulted in a full set of western blot films. As with the second strain, DCR2 can inhibit the transport of precursor CPY* from the ER to the Golgi. This would result in the accumulation and build-up of p1-CPY* in the ER, and lead to ER-induced stress.

There was a complete profile of all precursor CPY* (10μM - 500μM) & mature CPY* (1mM) blots present at all-time intervals. Unlike the previous strain, virtually all blots had a ratio value of < 0.05. Therefore, there were the highest precursor CPY* expression levels for this strain, which would result in the maximal amount of ER-induced stress, due to the greatest build-up of p1-CPY* in the ER of *S. cerevisiae*.

10.0 Conclusion

10.1 Summary of findings & Conclusion

This work has shown that there is indeed conversion of the precursor to the mature form of CPY, whilst there remains conversion of the precursor to the mature form of CPY*, only when expression of CPY* is induced with 1mM Cu^{2+} concentration. Further, these experiments have shown that CPY detection is present with different buffers, and thus is certainly in high abundance within the ER. Sadly, due to the lack of time and arrival of the α-CPY antibody (ThermoFisher), it was impossible to draw meaningful data as to whether the α-CPY could immunoprecipitate CPY. From the Cu^{2+} induction experiment, there is evidence of massive expression levels of CPY* which overwhelm the retention mechanism for unfolded proteins in the ER. Thus, there would be accumulation of p1-CPY* within the ER of *S. cerevisiae*, caused by the presence of DCR2 which leads to ER-induced stress.

10.2 Future perspectives

If I had additional time on my project, I would inhibit translation with cycloheximide and then measure its decay rate in both normal cells and cells overexpressing the WT and H338A-DCR2 strain. Further, I would repeat the IP, with the newly arrived α-CPY antibody from ThermoFisher Scientific, and to use either a bridging antibody or to epitope tag CPY*, and pulse-label the cells to measure maturation rates in normal cells, cells overexpressing the WT and cells with the H338A-DCR2 strain. Finally, I would induce my cells with a reducing agent, such as DTT, measure the maturation rates from pulse-labelling of CPY, and wash out the DTT to determine the overall fate of CPY.

11.0 Bibliography

1. Dobson CM. 2003. Protein folding and misfolding. Nature 426:884–890.
2. Shrivastava S. 2017. Protein folding. Introd to Biomol Struct Biophys Basics Biophys 270:33–56.
3. Dill KA. 1990. in Biochemistry Dominant 7133–7155.
4. Lipman DJ, Wilbur WJ. 1991. Modelling neutral and selective evolution of protein folding. Proc R Soc B Biol Sci 245:7–11.
5. Wickner S, Maurizi MR, Gottesman S. 1999. Posttranslational quality control: Folding, refolding, and degrading proteins. Science (80-) 286:1888–1893.
6. Hartl FU. 1996. Molecular chaperones in cellular protein folding. Nature 381:571–580.
7. Makin OS, Atkins E, Sikorski P, Johansson J, Serpell LC. 2005. Molecular basis for amyloid fibril formation and stability. Proc Natl Acad Sci U S A 102:315–320.
8. Aguzzi A, O'Connor T. 2010. Protein aggregation diseases: Pathogenicity and therapeutic perspectives. Nat Rev Drug Discov 9:237–248.
9. O'Brien EP, Brooks BR, Thirumalai D. 2012. Effects of pH on proteins: Predictions for ensemble and single-molecule pulling experiments. J Am Chem Soc 134:979–987.
10. Lins L, Brasseur R. 1995. The hydrophobic effect in protein folding. FASEB J 9:535–540.
11. Calloni G, Zoffoli S, Stefani M, Dobson CM, Chiti F. 2005. Investigating the effects of mutations on protein aggregation in the cell. J Biol Chem 280:10607–10613.
12. Uttara B, Singh A, Zamboni P, Mahajan R. 2009. Oxidative Stress and Neurodegenerative Diseases: A Review of Upstream and Downstream Antioxidant Therapeutic Options. Curr Neuropharmacol 7:65–74.
13. Goldberg AL. 2003. Protein degradation and protection against misfolded or damaged proteins. Nature https://doi.org/10.1038/nature02263.
14. Kostova Z, Wolf DH. 2003. For whom the bell tolls: Protein quality control of the endoplasmic reticulum and the ubiquitin-proteasome connection. EMBO J 22:2309–2317.
15. Meusser B, Hirsch C, Jarosch E, Sommer T. 2005. ERAD: The long road to destruction. Nat Cell Biol 7:766–772.
16. Kikkert M, Doolman R, Dai M, Avner R, Hassink G, Van Voorden S, Thanedar S, Roitelman J, Chau V, Wiertz E. 2004. Human HRD1 Is an E3 Ubiquitin Ligase Involved in Degradation of Proteins from the Endoplasmic Reticulum. J Biol Chem 279:3525–3534.
17. Hirsch C, Ploegh HL. 2000. Intracellular targeting of the proteasome. Trends Cell Biol 10:268–272.
18. Trombetta ES, Parodi AJ. 2003. Quality Control and Protein Folding in the Secretory Pathway. Annu Rev Cell Dev Biol 19:649–676.
19. Pilon M, Schekman R, Römisch K. 1997. Sec61p mediates export of a misfolded secretory protein from the endoplasmic reticulum to the cytosol for degradation. EMBO J 16:4540–4548.
20. Peter E, Candido M. 1997. ER degradation of a misfolded luminal protein by the cytosolic ubiquitin-proteasome pathway. Chemtracts 10:452–457.
21. Makino M, Sahara T, Morita N, Ueno H. 2019. Carboxypeptidase Y activity and maintenance

is modulated by a large helical structure. FEBS Open Bio 9:1337–1343.

22. Jung G, Ueno H, Hayashi R. 1999. Carboxypeptidase Y: Structural basis for protein sorting and catalytic triad. J Biochem 126:1–6.

23. Kato M, Sato Y, Shirai K, Hayashi R, Balny C, Lange R. 2003. The propeptide in the precursor form of carboxypeptidase Y ensures cooperative unfolding and the carbohydrate moiety exerts a protective effect against heat and pressure. Eur J Biochem 270:4587–4593.

24. Stevens T, Esmon B, Schekman R. 1982. Early stages in the yeast secretory pathway are required for transport of carboxypeptidase Y to the vacuole. Cell 30:439–448.

25. Valls LA, Hunter CP, Rothman JH, Stevens TH. 1987. Protein sorting in yeast: The localization determinant of yeast vacuolar carboxypeptidase Y resides in the propeptide. Cell 48:887–897.

26. Valls LA, Winther JR, Stevens TH. 1990. Yeast carboxypeptidase Y vacuolar targeting signal is defined by four propeptide amino acids. J Cell Biol 111:361–368.

27. Jones EW, Zubenko GS, Parker RR. 1982. PEP4 gene function is required for expression of several vacuolar hydrolases in Saccharomyces cerevisiae. Genetics 102:665–677.

28. Hemmings BA, Zubenko GS, Hasilik A, Jones EW. 1981. Mutant defective in processing of an enzyme located in the lysosome-like vacuole of Saccharomyces cerevisiae. Proc Natl Acad Sci U S A 78:435–439.

29. Jones EW. 1991. Three proteolytic systems in the yeast Saccharomyces cerevisiae. J Biol Chem 266:7963–7966.

30. Mechler B, Müller H, Wolf DH. 1987. Maturation of vacuolar (lysosomal) enzymes in yeast: proteinase yscA and proteinase yscB are catalysts of the processing and activation event of carboxypeptidase yscY. EMBO J 6:2157–2163.

31. Germany W. 1982. Vacuolar Proteinases the Yeast. October 25:5–8.

32. Mancini R, Aebi M, Helenius A. 2003. Multiple Endoplasmic Reticulum-associated Pathways Degrade Mutant Yeast Carboxypeptidase Y in Mammalian Cells. J Biol Chem 278:46895–46905.

33. Byrd JC, Tarentino AL, Maley F, Atkinson PH, Trimble RB. 1982. Glycoprotein synthesis in yeast. Identification of Man8GlcNAc2 as an essential intermediate in oligosaccharide processing. J Biol Chem 257:14657–14666.

34. Jakob CA, Burda P, Roth J, Aebi M. 1998. Degradation of misfolded endoplasmic reticulum glycoproteins in saccharomyces cerevisiae is determined by a specific oligosaccharide structure. J Cell Biol 142:1223–1233.

35. Knop M, Hauser N, Wolf DH. 1996. N-Glycosylation affects endoplasmic reticulum degradation of a mutated derivative of carboxypeptidase yscY in yeast. Yeast 12:1229–1238.

36. Mori K, Sant A, Kohno K, Normington K, Gething MJ, Sambrook JF. 1992. A 22bp cis-acting element is necessary and sufficient for the induction of the yeast KAR2 (BiP) gene by unfolded proteins. EMBO J 11:2583–2593.

37. Hitt R, Wolf DH. 2004. Der1p, a protein required for degradation of malfolded soluble proteins of the endoplasmic reticulum: Topology and Der1-like proteins. FEMS Yeast Res 4:721–729.

38. Knop M, Finger A, Braun T, Hellmuth K, Wolf DH. 1996. Der1, a novel protein specifically required for endoplasmic reticulum degradation in yeast. EMBO J 15:753–763.

39. Jungmann J, Reins HA, Schobert C, Jentsch S. 1993. Resistance to cadmium mediated by ubiquitin-dependent proteolysis. Nature 361:369–371.

40. Dunn A, Luz JM, Natalia D, Gamble JA, Freedman RB, Tuite MF. 1995. Protein disulphide isomerase (PDI) is required for the secretion of a native disulphide-bonded protein from Saccharomyces cerevisiae. Biochem Soc Trans 23:4–5.

41. Frand AR, Kaiser CA. 1999. Ero1p oxidizes protein disulfide isomerase in a pathway for disulfide bond formation in the endoplasmic reticulum. Mol Cell 4:469–477.

42. Freedman RB, Hirst TR, Tuite MF. 1994. Protein disulphide isomerase: building bridges in protein folding. Trends Biochem Sci 19:331–336.

43. Braakman I, Helenius J, Helenius A. 1992. Role of ATP and disulphide bonds during protein folding in the endoplasmic reticulum. Nature 356:260–262.

44. LaMantia ML, Lennarz WJ. 1993. The essential function of yeast protein disulfide isomerase does not reside in its isomerase activity. Cell 74:899–908.

45. Tachibana C, Stevens TH. 1992. The yeast EUG1 gene encodes an endoplasmic reticulum protein that is functionally related to protein disulfide isomerase. Mol Cell Biol 12:4601–4611.

46. Tachikawa H, Funahashi W, Takeuchi Y, Nakanishi H, Nishihara R, Katoh S, Gao XD, Mizunaga T, Fujimoto D. 1997. Overproduction of Mpd2p suppresses the lethality of protein disulfide isomerase depletion in a CXXC sequence dependent manner. Biochem Biophys Res Commun 239:710–714.

47. Nishimura A, Morita M, Nishimura Y, Sugino Y. 1990. A rapid and highly efficient method for preparation of competent Escherichia coli cells. Nucleic Acids Res 18:6169.

48. Casali N. 2010. E.coli Plasmid VectorsMethods in molecular biology. http://www.springerlink.com/index/10.1007/978-1-60761-820-1_12%5Cnhttp://www.ncbi.nlm.nih.gov/pubmed/20717785.

49. 1979. ABSTRACT A procedure for extracting plasmid DNA from bacterial cells 1s described . The method 1s simple enough to permit the analysis by gel electrophoresis of 100 or more clones per day yet yields plasmid DNA which is pure enough to be digestible by res 7.

50. Lee Y, Kim VN. 2005. Preparation and analysis of Drosha. Methods Mol Biol 309:17–28.

51. Kushnirov V V. 2000. Rapid and reliable protein extraction from yeast. Yeast 16:857–860.

52. Article R. 2008. Identi cation of an NADH-dependent 5-hydroxymethylfurfural-reducing alcohol dehydrogenase in. Yeast 191–198.

53. Smith PK, Krohn RI, Hermanson GT, Mallia AK, Gartner FH, Provenzano MD, Fujimoto EK, Goeke NM, Olson BJ, Klenk DC. 1985. Measurement of protein using bicinchoninic acid. Anal Biochem 150:76–85.

54. Simpson RJ. 2006. SDS-PAGE of Proteins. Cold Spring Harb Protoc 2006:pdb.prot4313.

55. Agatep R, Kirkpatrick RD, Parchaliuk DL, Woods RA, Gietz RD. 1998. Transformation of Saccharomyces cerevisiae by the lithium acetate/single-stranded carrier DNA/polyethylene glycol protocol. Tech Tips Online 3:133–137.

56. Pakula A. 2019. HHS Public Access. Methods Mol Biol 176:139–148.

57. Kurien BT, Scofield RH. 2006. Western blotting. Methods 38:283–293.

58. Taylor SC, Berkelman T, Yadav G, Hammond M. 2013. A defined methodology for reliable quantification of western blot data. Mol Biotechnol 55:217–226.

59. Kar P, Agnihotri SK, Sharma A, Sachan R, Lal Bhatt M, Sachdev M. 2012. A protocol for stripping and reprobing of Western blots originally developed with colorimetric substrate TMB. Electrophoresis 33:3062–3065.

60. DeCaprio J, Kohl TO. 2017. Immunoprecipitation. Cold Spring Harb Protoc 2017:1003–1008.

61. Guo J, Polymenis M. 2006. Dcr2 targets Ire1 and downregulates the unfolded protein response in Saccharomyces cerevisiae. EMBO reports 7, 1124–1127.

62. Pathak R, Bogomolnaya LM, Guo J, Polymenis M. 2004. Gid8p (Dcr1p) and Dcr2p Function in a Common Pathway To Promote START Completion in Saccharomyces cerevisiae. Eukaryot. Cell 3, 1627-1638.

63. Pathak R, Blank HM, Guo J, Ellis S, Polymenis M. 2007. The Dcr2p phosphatase destabilizes Sic1p in Saccharomyces cerevisiae Biochem. Biophys. Res. Commun. 361, 700-704.